# ADDIS ABABA UNIVERSITY
# COLLEGE OF NATURAL AND COMPUTATIONAL SCIENCES SCHOOL OF EARTH SCINCES

Groundwater Potential Zone Mapping Using GIS and Remote Sensing: a Case of Teji River catchment Southwest Shewa Zone, Ethiopia


By

**WORKINEH TESFAYE**

**(GSR/8128/15)**

Advisor

**Prof. K.V. SURYABHAGAVAN**

Co-advisor

**Dr. TILAHUN AZAGEGN**


**A THESIS SUBMITTED TO**

**SCHOOL OF GRADUATE STUDIES OF ADDIS ABABA UNIVERSITY IN PARTIAL FULFILLMENT OF THE REQUIREMENTS FOR THE DEGREE OF MASTERS OF SCIENCE IN REMOTE SENSING AND GEO-INFORMATICS**

**Addis Ababa, Ethiopia**
**May, 2024**

# ADDIS ABABA UNIVERSITY
# COLLEGE OF NATURAL AND COMPUTATIONAL SCIENCES SCHOOL OF EARTH SCINCES

Groundwater Potential Zone Mapping Using GIS and Remote Sensing: a Case of Teji River catchment Southwest Shewa Zone, Ethiopia


By

**WORKINEH TESFAYE**

**(GSR/8128/15)**

Advisor

**Prof. K.V. SURYABHAGAVAN**

Co-advisor

**Dr. TILAHUN AZAGEGN**


**A THESIS SUBMITTED TO**

**SCHOOL OF GRADUATE STUDIES OF ADDIS ABABA UNIVERSITY IN PARTIAL FULFILLMENT OF THE REQUIREMENTS FOR THE DEGREE OF MASTERS OF SCIENCE IN REMOTE SENSING AND GEO-INFORMATICS**


**Addis Ababa, Ethiopia**

**May, 2024**

# D E C L A R A T I O N

I hereby declare that the dissertation entitled "**Groundwater Potential Zone Mapping Using GIS and Remote Sensing: a Case of Teji River catchment Southwest Shewa Zone, Ethiopia**" has been carried out by me under the supervision of Prof. K. V. Suryabhagavan and co-advisor Dr. Tilahun Azagegn, School of Earth Sciences, Addis Ababa University, Addis Ababa during the year 2023-2024 as a part of Master of Science programme in Remote Sensing and Geoinformatics. I further declare that this work has not been submitted to any other University or Institution for the award of any degree or diploma and that all sources of materials used for the thesis has been dully acknowledged.

Place: Addis Ababa
Date: July 16, 2024

**Workineh Tesfaye**

# C E R T I F I C A T E

This is certified that the dissertation entitled "**Groundwater Potential Zone Mapping Using GIS and Remote Sensing: a Case of Teji River catchment Southwest Shewa Zone, Ethiopia**" is a bona fide work carried out by Workineh Tesfaye under my guidance and supervision. This is the actual work done by Workineh Tesfaye for the partial fulfillment of the award of the Degree of Master of Science in Remote Sensing and Geoinformatics from Addis Ababa University. Addis Ababa.

**Prof. K. V. Suryabhagavan**

School of Earth Sciences
Addis Ababa University
Addis Ababa

# ADDIS ABABA UNIVERSITY

# SCHOOL OF GRADUATE STUDIES

Groundwater Potential Zone Mapping Using GIS and Remote Sensing: a case of Teji River catchment Southwest Shewa Zone, Ethiopia

By
Workineh Tesfaye

College of Natural and Computational Sciences
School of Earth Scinces
Remote Sensing and Geoinformatics

## Approval by Board of Examiners

| | Signature | Date |
|---|---|---|
| Dr. ---------- Chairman, Department Graduate Committee | _____ | _____ |
| Prof. K.V. Suryabhagavan Advisor | _____ | _____ |
| Dr. Tilahun Azagegn Co-advisor | _____ | _____ |
| Dr. Binyam Tesfaw Examiner | _____ | _____ |
| Dr. Behailu Birhanu Examiner | _____ | _____ |

## Table of Contents

## List of Tables

## List of Figures

## List of Acronyms

| | |
|---|---|
| AHP | Analytical Hierarchy Process |
| ASF | Alaska Satellite Facility |
| AUC | Area Under Curve |
| CI | Consistency Index |
| CR | Consistency Ratio |
| DEM | Digital Elevation Model |
| ECDSWC | Ethiopian Construction Design and Supervision Works Corporation |
| ECO | Engineering Corporation of Oromia |
| EO | Earth Observation |
| ERDAS | Earth Resource Data Analysis System |
| ESA | European Space Agency |
| GCP | Ground Control Point |
| GIS | Geographic Information System |
| GPS | Geographic Position Systems |
| GSE | Geological Survey Ethiopia |
| GWI | Groundwater Inventory |
| GWPI | Groundwater Potential Index |
| GWPZ | Ground Water Potential Zone |
| HSG | Hydrological Soil Group |
| IDW | Inverse Distance Weight |
| LiDAR | Light Detection and Ranging |
| LULC | Land Use Land Cover |
| MCDA | Multi Criteria Decision Analysis |
| MCDAM | Multi Criteria Decision Analysis Method |
| MCDM | Multi Criteria Decision Making |
| MSI | Multispectral Instrument |
| NMA | National Metrological Agency |
| NRCS | Natural Resource Conservation Service |
| PWCM | Pairwise Comparison Matrix |
| ROC | Receiver Operating Curve |
| RS | Remote Sensing |
| SRTM | Shuttle Radar Topography Mission |
| TWI | Topographic Wetness Index |
| UNICEF | United Nation Children's Fund |
| USDA | Universal Soil Data Analysis |
| VES | Vertical Electrical Sounding |
| WHO | World Health Organization |
| WLC | Weighted Linear Combination |

**Acknowledgements**

I express my profound gratitude to the Almighty for bestowing upon me health, peace, knowledge, and wisdom, enabling me to complete this thesis work.

I wish to express my deep gratitude to Professor K.V. Suryabhagavan, my esteemed advisor, for his invaluable guidance and unwavering encouragement during the course of this thesis work. His patience, expertise, and friendship have played pivotal role in the successful completion of this endeavor. His adeptness in scientific writing focusing specifically on technical aspects has been particularly illuminating and enriching.

I sincerely thank my co-advisor, Dr. Tilahun Azagegn, for his invaluable guidance and expertise in hydrology and geology, which greatly enhanced the quality of my research title and the overall organization of its contents.

Special thanks are due to my instructors, Dr. Binyam Tesfaw and Dr. Tibebu Kassawmar, as well as all the faculty members of Addis Ababa University, School of Earth Sciences, for their support in imparting knowledge of Hydrology, Geology, Remote Sensing, and GIS.

I am grateful to the Space Science and Geospatial Institute for their financial and material support, enabling me to pursue my postgraduate studies. I also acknowledge the Ethiopian National Meteorological Agency, Ethiopian Geological Survey, Engineering Corporation of Oromia, and Ethiopian Construction Design and Supervision Works Corporation for providing crucial data and resources essential for my research.

Lastly, I extend my heartfelt appreciation to my friends Abel Mesele, Belay Beko and Taye Teshome for their unwavering support and guidance. Additionally, I am thankful to all my colleagues in the Remote Sensing and Geoinformatics stream for their friendship and collaboration.

Groundwater Potential Zone Mapping Using GIS and Remote Sensing: a Case of Teji River catchment Southwest Shewa Zone, Ethiopia
Workineh Tesfaye, MSc Thesis
Addis Ababa University, May 2024


## Abstract

This study identify the groundwater potential zones in the Teji River catchment by using cost-effective and timely remote sensing (RS) and geographic information systems (GIS). Eight thematic maps were employed as the basis for investigation. Primary and secondary data sources were used in this study. The data collected include information on soil texture, drainage density, land-use and land-cover, rainfall, lithology, slope, topographic wetness index, and lineament density. The Analytical hierarchy process (AHP) method in AHP extension used. Weight overlay analysis was utilized to evaluate the groundwater potential zone. According to Saaty's scale of AHP, the weights for each element were assigned based on their significance in relation to groundwater potential. The results of the study indicated that out of total Teji River catchment area of 12.24% (6829.92 ha) has very good potential, 30.88% (17231.64 ha), has good potential, 36.05% (20115.89 ha) has moderate potential, and 20.8% (11611.98 ha) has poor groundwater potential. The study validated the results, indicating that groundwater potential zones can be more accurately identified using GIS and remote sensing approaches. The validation outcomes indicated that approximately 81.25% of the groundwater boreholes classifications aligned accurately with the zoning depicted on the generated groundwater potential map. Further validation utilizing the receiver operating characteristic (ROC) curve gave an AUC of 0.83. Similar methodologies are recommended for delineating groundwater potential zones in data-scarce and challenging terrains. Furthermore, the establishment of purposeful testing wells and field geophysical investigations in potential well-drilling locations is advised to enhance effective groundwater management possibilities.



**Keywords**: AHP, GIS, Groundwater potential, Overlay analysis, RS, Sentinel -2 data

# CHAPTER ONE

# INTRODUCTION

## 1 Background

A vital natural resource, groundwater supplies one-third of freshwater abstractions worldwide and essential to the social and economic advancement of water–scarce places globally (Kordestani et al., 2019; Yilma et al., 2023). Groundwater supplies are to all economic activity, both directly and indirectly. However, a number of variables including geology, chemical weathering, and the effectiveness of recharge, fluctuations in level of groundwater, and various sources of surface pollutants can significantly influence groundwater. On the other hand, surface pollution typically affects surface water (Yildrum, 2021). Because it is closer to the surface, surface water has a lower mineral content, but it also more vulnerable to human activity- related contamination (Chakraborty et al., 2021). Groundwater now more crucial than ever for supplying the demands of business, homes, and agriculture, among other industries (Thapa etal., 2017). The demand for groundwater is increasing in nations like Ethiopia due to fast growing population, urbanization, and economic advancement (Andualem and Demeke, 2019).

An essential component of the hydrological cycle; groundwater is important natural resource on a global scale. Around the world, it sustains wetlands, springs, and surface constancy (Nigussie et al., 2019; Pathak and Dodamani, 2019; Rao et al., 2022). Rain and snow melt that permeates the soil or permeable rocks replenishes groundwater naturally (Hussien et al., 2017). It is essential for many industrial, agricultural, and home requirements across the globe (Abdul-Ganiyu and Prosper, 2021). Nonetheless, the demand for groundwater is sharply rising globally as a result of factors like population growth and urbanization, climate change, droughts, and insufficient rainfall (Assegide et al., 2022).

Modern groundwater exploration relies heavily on a powerful combination: Geographic information systems (GIS) for data analysis and integration, and remote sensing (RS) for gathering crucial information from space. These techniques allow for the quick and simple exploration of the groundwater potential zones in a range of geological situations (Ifediegwu et al., 2019; Kanagaraj et al., 2019; Igwe et al., 2022). Numerous scholars across the world have identified potential groundwater zones using RS and GIS approaches (Allafta et al., 2020; Lawal et al., 2023; Lee et al., 2020; Mallick et al., 2022; Habtemariam and Nanesso ; Sao et al., 2020; Achu et al., 2020; Qadir et al., 2020; Gyeltshen et al., 2020; Ahmed et al., 2022; Barhanu and Hatiye, 2020). Using RS and GIS, groundwater resource exploration and discovery involves a various of factors, comprising lithology, geomorphology, slope, soil type, rainfall, land-use and

land-cover, lineament structure, and patterns of drainage (Hamdani and Baali, 2020; Lentswen and Molwalefhe, 2020). Determining possible groundwater zone is essential to long-term resource management success. Planers, policy makers, and decision-makers can protect groundwater resources from possible effects on quantity and quality with the help of this procedure. The analytical hierarchy process (AHP) approach is one of the most often used techniques for generating multi-criteria decisions making (Aliabad et al., 2018). This method is a groundwater potential zone delineation technique that is simple, uncomplicated, trustworthy, and effective (Igwe et al., 2020, Aju et al., 2023). Using GIS and AHP together makes it easier to transform data in to information that the decision makers can use (Guru et al., 2017).

Therefore, the present study endeavors to identify zones of groundwater potential within the Teji River catchment central, Ethiopia by harnessing the capabilities of the analytical hierarchy process, remote sensing and GIS. Lithology, topographic wetness index (TWI), rainfall, slope, drainage density, soil texture, land-use and land-cover, drainage density, and lineament density were the eight thematic layers that accurately examined to attain a comprehensive knowledge of the landscape's impacts on groundwater occurrence. AHP was subsequently utilized to give weight for each factor depending on its significance in evaluating groundwater probable zone, ultimately guiding to prioritization promising zones for water resource management in the catchment.

### 1.2 Statement of the problem

Water scarcity remains pressing worldwide issue, affecting over 1 billion people worldwide with 67% of rural population in developing nations facing challenges in accessing safe drinking water resources (UNICEF and WHO, 2021). Many rely on potentially unsafe surface water resources, posing health and safety risks (Bain et al., 2014). Groundwater a vital resource for various purposes including domestic, agricultural, industrial, and municipal needs plays a pivotal role in mitigating these challenges. However, the unequal distribution of groundwater across the geographical regions presents significant hydrological challenges, influencing the depth of groundwater in different geological layers.

Despite its importance the exploration of groundwater potential zone in specific regions, such as Teji River catchment in central Ethiopia remains limited. Traditional methods lack the spatial resolution and accuracy required to comprehensively assess groundwater resources. This gap in knowledge underscores the need for advanced techniques like geographic information systems with remote sensing enabling us to provide detailed spatial information on potential groundwater zones mapping. A promising way to close this gap is to combine the use of remote sensing, geographic information systems, and the analytical

hierarch process method. This study intends to assess the groundwater potential zones within Teji River catchment by utilizing the capabilities of these technologies. Eight thematic layers were examined in this through analysis: lithology, rainfall, slope, drainage density, land-use and land-cover, lineament density, soil texture and topographic wetness index were identified to delineate groundwater potential zone mapping and the weights that assign by using AHP to each aspect according to its significance in groundwater potential zone mapping.

The primary objective of this research was mapping groundwater potential zones by combined geographic information systems (GIS) and remote sensing (RS) to collect, manipulate, and display different types of data that ultimately generate thematic maps with the aid of analytical hierarchy process (AHP). The integration of GIS and RS allows for the efficient handling of large datasets and identification of key factors influencing groundwater availability. Additionally, AHP provides structured methodology to weigh and prioritize these factors, enhancing the accuracy and reliability of the potential zones maps.

## 3 Objective of the study

### 1.3.1 General objective

The main objective of this study was to map the groundwater potential zone in a case of Teji River catchment central, Ethiopia using geographic information systems and remote sensing methods.

### 1.3.2 Specific objectives

The specific objectives of the study were listed below:

- To prepare thematic maps of GWPZ factors such as lithology, rainfall, LULC, drainage density, lineament density, soil texture, TWI and slope.
- To integrate different thematic maps to develop and evaluate possible groundwater zones using GIS and remote sensing methods.
- To identify factors that most affects the GWPZ using the analytical hierarchy process (AHP) methods.
- To validate the results of groundwater potential zone mapping using existed groundwater inventory data.

## 1.4 Research questions

- How can lithology, rainfall, LULC, drainage density, lineament density, soil texture, TWI and slope be factors for mapping GWPZ?

- How can different thematic layers be integrated using remote sensing and GIS techniques to develop groundwater potential zone mapping?
- How can the AHP method be used to identify the factors that most affect GWPZ?
- How to validate groundwater potential zone mapping results using existing groundwater inventory data?

### 1.5 Significance of the study

The anticipated outcome of this study is the establishment of a robust groundwater potential zoning framework, serving as a practical tool for facilitating the sustainable utilization, development, and management of groundwater resources within the designated area. Specialists vested in addressing related challenges within the region can leverage this study as a foundational reference point for the intricate delineation of groundwater potential zones and the comprehensive analysis of diverse factors governing groundwater potential. The spatial data generated to map groundwater potential zone with respect to hydrological, hydrogeological, groundwater quality and biophysical characteristics of the study area will enable decision–making agencies, groundwater resource planners and policy makers, stakeholders, and subsequent researchers review and use them for future studies and research work.

### 1.6 Scope of the study

Geographically, the study was restricted Teji River catchment central, Ethiopia. The objective was to assess groundwater potential zone mapping of catchment by employing RS and GIS with AHP techniques. It involves gathering relevant data on lithology, TWI, LULC, slope, rainfall, drainage density, lineament density and soil texture within the catchment. The analysis was conducted using RS and GIS application to generate a groundwater potential zone mapping, indicating zones with very good potential for ground water availability. The scope also includes evaluating the precision and consistency of the mapping with validation of results using ground water inventory data. The finding of the study will enhance understanding and support the wisely management of groundwater resources within the Teji River catchment area.

### 1.7 Limitations of the study

The study faced some limitation, including delays caused by organizations' unwillingness to provide secondary data promptly, constraints in time and resources, and the lack of inventory data for the entire study area and the uneven distribution of existing inventory data points. However, the researcher employs various strategies to mitigate these challenges. Establish clear communication channels with organization to negotiate timely data sharing agreements, seek additional funding or leverage existing resources

efficiently, Furthermore, the researcher employs stringent validation protocols and sensitivity analyses to mitigate potential biases and limitations associated with data quality, thus enhancing the reliability and credibility of the study's findings.

### 1.8 Organization of the thesis

The research comprised five chapters dedicated to mapping groundwater potential zones utilizing Remote Sensing (RS) and Geographic Information System (GIS) techniques. Chapter one introduced the study, covering its background, problem statement, objective, research questions, scope, significance, limitations, and thesis organization. Chapter two provide review of literature pertaining to groundwater potential and recharge zone mapping. Chapter three detailed the materials and methods, data types, software used for preparation of thematic layers, and data processing and analysis techniques. Chapter four presented results and discussions regarding groundwater potential zone mapping, including results validation. Finally, chapter five summarized the study's conclusions and provided recommendations.

# CHAPTER TWO

# LITRATURE REVIEW

## 2.1 Concept of groundwater

Groundwater, the concealed water reserve located below the earth's surface, is a vital natural resource with several key concepts and recent references shedding light on its significance and challenges. Aquifers, geological formations that store and transmit groundwater, are fundamental in this context. Recent research by Scanlon et al. (2012) highlights the critical issue of groundwater depletion in regions like the US High Plains and Central Valley due to excessive irrigation, emphasizing the need for sustainable management. Groundwater contamination is another pressing concern, as pollutants from various human activities can seep into aquifers. Focazio et al. (2021) discuss the issue of groundwater contamination caused by hydraulic fracturing, exploring both its discovery and remediation. Groundwater recharge, the process of replenishing aquifers, plays a pivotal role in groundwater sustainability, as detailed in a study by Scanlon et al. (2012) on global recharge patterns in semiarid and arid regions (Hussein et al., 2017).

Groundwater modeling, a crucial tool for understanding its flow and quality, is examined by Kumar et al. (2022) to provide insights into groundwater management. Effective management strategies are essential to balance extraction and natural recharge, as stressed by Gleeson et al. (2016) in their work on global groundwater volumes and distribution. Groundwater is not immune to climate change, which can alter precipitation patterns and temperatures, as discussed by Taylor et al. (2013) in their research on groundwater and climate change. Monitoring groundwater quality is crucial to ensure safe drinking water, asevidenced by Neumann et al. (2020) in their study on groundwater quality trends in the United States. Lastly, groundwater's impact on ecosystems, by providing base flow to rivers and wetlands, is discussed by (Wendt et al., 2021) in their work on groundwater-surface water interactions in a changing climate. These references collectively underscore the importance of understanding, managing, and protecting groundwater resources in the face of evolving environmental challenges.

## 2.2 Utilizing remote sensing for GWPZ mapping

Remote sensing is a fundamental component in mapping groundwater potential zones. Through the use of satellite imagery and aerial photography, it provides essential data on various land characteristics, including land cover, topography, vegetation, and hydrological features (Al-Shafie et al., 2021). This data is instrumental in identifying areas conducive to groundwater recharge and storage, such as regions with specific vegetative cover or geological formations. Remote sensing data serves as a fundamental input

for subsequent analyses, enabling a comprehensive understanding of the landscape's potential for groundwater availability and replenishment. Furthermore, the role of remote sensing technologies is crucial in improving the precision and efficiency of mapping groundwater potential zones (GWPZ). The incorporation of advanced sensors and platforms, such as hyperspectral and LiDAR data, plays a key role in refining the characterization of land features. For example, LiDAR data aids in creating high-resolution elevation models, providing detailed information about terrain morphology and assisting in the identification of potential areas for groundwater recharge (Kumar et al., 2018). Additionally, hyperspectral data offers insightful composition of land surface, enabling a more detailed in evaluating the factors inducing zone of probable groundwater (Weng et al., 2015). Combination the geospatial technologies enhances the accuracy of GWPZ mapping by capturing intricate details of the landscape.

Numerous studies highlight the role of remote sensing in groundwater potential zone evaluation. Rao et al. (2019) used remote sensing data to analyze changes in LULC, providing insights into their impact on groundwater potential over time. Additionally, Sharma et al. (2020) emphasized the usefulness of aerial photography in identifying surface features indicative of groundwater recharge potential.

### 2.3 Role of Geographic information systems (GIS) in GWPZ mapping

GIS plays a key role to evaluate groundwater potential zone by providing a robust platform for integrating, storing, analyzing, and visualizing geospatial data (Youssef and Pradhan, 2021). It facilitates the creation of maps that incorporate various crucial parameters such as geological structures, hydrogeological features, land-use, and existing wells. Through the overlay and analysis of these diverse data layers, GIS aids in the identification of areas with high potential for groundwater resources as well as areas prone to contamination or over-exploitation.

Furthermore, GIS enables the combination of remote sensing data, enhancing accuracy of groundwater potential zone mapping. By incorporating satellite imagery, GIS allows for a detailed examination of land surface characteristics, vegetation cover, and land-use patterns, which are integral factors in assessing groundwater potential (Kumar et al., 2019). This integration of remote sensing data with GIS not only improves the precision of identifying potential zones but also provides a comprehensive understanding ofthe spatial relationships between various environmental variables.

Moreover, GIS-based groundwater potential mapping offers a valuable tool for decision-makers and water resource planners. The spatial analysis capabilities of GIS allow for the delineation of recharge areas, estimation of groundwater recharge rates, and identification of areas susceptible to pollution, aiding

in sustainable groundwater management (Singh et al., 2020). The interactive and visual nature of GIS platforms facilitates effective communication of complex groundwater information to stakeholders, enhancing decision-making in water resource planning and managing, and aid with its capabilities of mapping.

### 2.4 Application of MCDM in GWPZ mapping

The multi-criteria decision making (MCDM) technique is crucial method for integrating many factors and standards related to groundwater potential. They make it possible for decision-makers to take into account a range of elements, such as precipitation, slope, soil type, land usage, rate of runoff and geological features. MCDM facilitates the process of ranking and prioritizing divert areas depending on suitability for groundwater assessment, hence aiding in the making of decisions related to sustainable groundwater assessment (Al-Adamat et al., 2022).

Additionally, the application of multi criteria decision making (MCDM) in groundwater potential zone mapping allows for a comprehensive evaluation of diverse factors, contributing to a more nuanced understanding of subsurface water availability. The MCDM technique enables the simultaneous consideration of multiple criteria, including but not limited to aquifer properties, groundwater quality, and anthropogenic impacts. This holistic approach enhances the accuracy of groundwater potential assessments by providing decision-makers with a robust framework to weigh and analyze various factors influencing groundwater conditions (Chitsazan et al., 2021).

Furthermore, the versatility of MCDM in groundwater potential mapping is evident in its ability to handle uncertainties and complexities inherent in hydrogeological systems. The technique accommodates the integration of both numerical and descriptive data, allowing for a more thorough exploration of groundwater potential zones. By incorporating stakeholders' preferences and expert knowledge, MCDM contributes to a more inclusive decision-making process, ensuring that the delineated potential zones align with broader goals of sustainable groundwater resource management (Das et al., 2020).

### 2.5 Analytical hierarchy process (AHP)

During the groundwater delineation process in the study area, various thematic maps were produced and integrated using geographic information systems. Prior to integration Saaty’s Analytical Hierarchy process (AHP) (Saaty, 1980) was utilized to assess individual class weights and map scores. A pairwise comparison matrix was prepared for each map, and a nine-point importance scale was employed to assign weights based on relative importance. This process enabled the simultaneous comparison and ranking of

up to nine objects, ensuring the reliability of the results. The consistency ratio (CR) was calculated to evaluate the consistency of judgments mathematically. A CR < 0.1 was deemed acceptable, while CR > 0.1 suggested inconsistences. The unified weight map was generated by logically combining the weights of all input variables, and it was classified to produce the groundwater potential zone map. This map provided an overview of the study area's groundwater prospects. The unified weight map, produced through the logical combination of weights assigned to different thematic layers, played a crucial role in creating the groundwater potential zone map. This integrated approach guaranteed that the final map accurately reflected the combined influence of lithology, lineament density, drainage density, slope, soil texture, land-use and land-cover runoff, and rainfall on groundwater potential zone mapping. The classification of the unified weight map offered visual representation of groundwater prospects in the study area, providing valuable insights for sustainable water resource management and decision-making (Gupta et al., 2019)

### 2.6 Factors affecting groundwater potential and recharge

Groundwater, a hidden treasure beneath our feet, and is essential to maintaining life and providing support for human activities. Its potential and recharge, however, are not uniform across the globe, as they are influenced by a complex interplay of geological, geomorphological, hydrological, and land-use factors. Understanding these factors is essential for effective managing groundwater and making sure the long-term sustainability of such precious resource (Dinka and Abebe, 2021; Girma and Abebe, 2021; Abdi and Abebe, 2022). Among the key factors governing groundwater potential is the geological makeup of the underlying rocks and sediments (Oladunni, 2020; Ouedraogo et al., 2020). Permeable formations, like sand and gravel, allow water to flow freely, facilitating groundwater movement and storage. Conversely, impermeable formations, such as clay, impede water infiltration, hindering groundwater recharge and potential. Geomorphology, the study of landforms and topography, also exerts a significant influence on groundwater dynamics (Oladunni, 2020; Ouedraogo et al., 2020). Areas with steep slopes and high relief often have limited groundwater storage due to rapid water runoff. Conversely, valleys and depressions provide favorable conditions for groundwater accumulation, allowing water to infiltrate and replenish aquifers. Lineaments, surface features that are linear, often show the presence of fractures or faults in the bedrock (Oladunni, 2020; Ouedraogo et al., 2020). These fractures can serve as conduits for groundwater flow, enhancing groundwater potential in areas with abundant lineaments. Soil characteristics, particularly texture and structure, play a crucial role in governing groundwater recharge and infiltration (Oladunni, 2020; Ouedraogo et al., 2020). Sandy soils, with their larger pores, allow water to percolate more readily, promoting groundwater recharge. Clayey soils, on the other hand, impede infiltration and reduce

groundwater recharge. Drainage patterns, including the density and distribution of streams, rivers, and other water bodies, also influence groundwater potential. Areas with well-developed drainage networks may have lower groundwater potential due to rapid water discharge, while areas with limited drainage tend to retain more water, increasing groundwater storage. Land-use practices, ranging from agriculture to urbanization, can significantly impact groundwater recharge and potential. Agricultural activities, such as irrigation and fertilizer application, can alter groundwater quality and quantity. Urbanization, with its increased impervious surfaces, can reduce infiltration and hinder groundwater recharge. Rainfall, the primary source of groundwater recharge, plays a pivotal role in determining groundwater potential areas with abundant and well-distributed rainfall tend to have higher groundwater potential than areas with limited or erratic rainfall. This is because rainfall provides the necessary water input for groundwater replenishment (Oladunni, 2020; Ouedraogo et al., 2020).

### 2.7 Physiography and drainage pattern of Teji River catchment

Teji River catchment, found in the Oromia region in central, Ethiopia, is located within the expansive great rift valley stretching from the Red Sea to Mozambique (Adem and Gebregziabher, 2021). The catchment topography is characterized by a mix of highlands and lowlands, with elevations ranging from 500 to 3,000 m asl (Adem and Gebregziabher, 2023). The highlands dominate the western and southern fringes, while the eastern and northern regions feature lowlands (Gebrehiwot, 2020). These elevation variations significantly impact the catchment's climate, vegetation, and land-use patterns. The drainage system in Teji River catchment is influenced by its physiography (Setegn, 2022). The highlands are drained by a network of rivers and streams that flow into the rift valley lakes, whereas the lowlands rely on intermittent streams converging into the Awash River (Adem and Gebregziabher, 2023). The Awash River, the catchment's primary waterway, serves as a major tributary of the Blue Nile River, supplying essential water resources for irrigation and domestic purposes (Gebrehiwot, 2020). Additionally, the Awash River is a focal point for tourism and sustains diverse wildlife populations (Setegn, 2022). The drainage system plays a crucial role in Teji River catchment's economy and environment (Adem and Gebregziabher, 2021). Rivers and streams not only provide water for irrigation and domestic needs but also support a variety of aquatic life (Gebrehiwot, 2020). Furthermore, the drainage system contributes to climate regulation and helps prevent floods (Setegn, 2022). The soil types in the catchment vary depending on the elevation and topography. The highlands are generally characterized by Nitosols, which is clay-rich well rooted, and well-drained soils (Adem and Gebregziabher, 2021). These soils are suitable for growing a variety of crops, including coffee, maize, and wheat. The lowlands are generally characterized by Luvisols, is soil with a moderate clay percentage that is deep and well-drained

(Adem and Gebregziabher, 2023). These soils are suitable for growing a variety of crops, including sorghum, teff, and chickpeas. The vegetation of Teji river catchment also varies depending on the elevation and topography. The highlands are generally home to a variety of forests and grasslands. The forests are dominated by coniferous trees, such as juniper and cedar. The grasslands are dominated by grasses, such as Poa and Pennisetum (Gebrehiwot, 2020). The lowlands are generally home to a variety of savannas and shrub lands. The savannas are dominated by trees, such as Acacia and Combretum. The shrub lands ar which are deep, well-drained soils with moderate clay content `\ e dominated by shrubs, such as Grewia and Croton (Setegn, 2022).

### 2.8 Geology of Teji River catchment

This geological diversity manifests in a hydrogeological landscape marked by complexities. The Precambrian basement rocks, characterized by limited permeability, function as barriers to groundwater flow, segregating shallower aquifers within volcanic and sedimentary formations from deeper groundwater reserves. The Jurassic-cretaceous volcanic rocks, though suboptimal for extensive aquifer systems, can harbor discrete pockets of groundwater, especially within weathered zones and fractured areas (Abay and Gebrekidan, 2022). The quaternary sediments, endowed with porous and permeable attributes, act as hydrological sponges, adeptly absorbing rainfall and replenishing groundwater resources. Additionally, the catchment's topography significantly influences its hydrogeology. Steep slopes and elevated relief areas experience swift water runoff, constraining infiltration and groundwater recharge. Conversely, valleys and depressions serve as natural catchments, facilitating water accumulation and infiltration, thereby replenishing aquifers (Ayenew and Tadesse, 2014).

### 2.9 Groundwater recharge

The groundwater recharge in Teji river catchment is primarily associated with the quaternary sediments and fractured zones within the Precambrian basement rocks (Gebrehiwot, 2020). Groundwater is a vital water resource in the catchment, utilized for domestic purposes, irrigation, and livestock watering (Gebrehiwot, 2020). Overexploitation of groundwater resources has raised concerns about sustainability, particularly in areas with limited recharge and high demand. The dynamics of groundwater recharge in Teji River catchment are impacted by various elements, such as land-use and land-cover, and geological formations (Adem and Gebregziabher, 2023). Adequate rainfall is crucial for maintaining groundwater recharge, as it provides the necessary water source for infiltration. Land-use practices that promote infiltration, such as preserving vegetation cover and minimizing soil compaction, can enhance recharge rates. Geological formations with high permeability, like fractured rocks and alluvial sediments, facilitate

faster infiltration compared to less permeable formations. Conversely, human activities, such as overexploitation of groundwater resources and land degradation practices like deforestation, can negatively impact groundwater recharge by reducing infiltration rates and storage capacities. Ensuring long-term water security in Teji River catchment and supporting the well-being of its communities hinges on enhancing groundwater recharge (Setegn, 2022). By adopting a comprehensive approach that integrates natural and artificial recharge strategies, Teji River catchment is capable of sustainably managing its groundwater supplies for future generations. Key strategies include: Watershed management: Implementing sustainable land management practices to protect and restore watersheds, which act as natural filters and recharge zones for groundwater. Artificial recharge techniques: Employing techniques like constructing recharge ponds or injecting treated wastewater into aquifers to directly replenish groundwater resources. Water conservation measures: Encouraging water-efficient practices in agriculture, households, and industries to reduce water consumption and minimize groundwater abstraction. Groundwater monitoring programs: Establishing and maintaining a comprehensive groundwater monitoring network to track groundwater levels, quality, and recharge trends.

### 2.10 Previous studies

In the study by Abdi et al. (2022), geospatial techniques were used to identify groundwater potential zone in the drought-prone Feven–Jefer sub-basin of Ethiopia. The researchers incorporated thematic layers, including geology, land-use and land-cover, slope, and rainfall to generate a groundwater potential index (GPI). They classified the sub basin in to four groundwater potential categories: low, moderate, high, and very high. The finding indicated that approximately 84% of the area has moderate groundwater potential, while 14% has high potential. In a similar study Tilahun and Adem (2022) used GIS techniques, integrating thematic layers such as soil, geology land-use and land-cover, and topography to evaluate ground water potential map for Sekota Woreda. This map was validated with well yield data, proving the effectiveness of this technique in identifying groundwater potential zone.

Furthermore, Duguma (2022) employed eight thematic layers: geology, rainfall, slope, land-use and land-cover and drainage density to develop groundwater potential map. The validity of these maps were confirmed using well yield data showcased the effectiveness of multi-criteria decision analysis (MCDA) and remote sensing techniques in identifying groundwater and potential zones in the Guder River basin.

In the research Dhinsa et al. (2022) utilized the Vertical electrical sounding (VES) method to conduct electrical investigations and identify potential borehole sites for groundwater potential extraction. This study aimed to delineate groundwater potential zones by integrating remote sensing, geographic

information systems and 2-D electrical resistivity methods. Similarly, Mulgeta et al. (2021) applied vertical electrical sounding and magnetic methods to evaluate groundwater potential in the Adilo catchment located in the South Nations, Nationalities and Regional government of Ethiopia. The investigation was carried out in the KebataTembaro zone within the Main Ethiopia Rift, collecting data from eight VES point using Schlumberger electrode arrays with a maximum half-current electrode spacing of 500 meters. Additionally, 253 magnetic data points were collected and analyzed.

In the study by Dinka and Abebe (2021), GIS and remote sensing techniques were employed to assess a groundwater potential map using six thematic layers: geology, land-use and land-cover, slope, soil, drainage density, and rain fall. Validation with well yield data demonstrated the efficacy of these techniques in identifying groundwater potential zones in the Jamma River basin.

Abe et al. (2022) assessed groundwater potential zones using multi-criteria decision-making model and geospatial techniques in Lemo woreda and Hossana town of Southern Nation, Nationalities Region. Ground control points (GCP) were gathered from Google earth and data from digital elevation model (DEM) and landsat8 imagery were downloaded. Additionally, secondary data such as soil infiltration, rainfall and lithology were sourced from various governmental institutions key groundwater controlling factors including lithology, geomorphology, slope, LULC, rainfall, and lineament density were identified. The analytical hierarchy process was employed to compute weights for these parameters by comparing eight different factors.

Kabeto et al. (2022) utilized remote sensing and geographic information systems techniques to evaluate the groundwater potential in the study area. This approach proved to be fast, accurate, and feasible. Key parameters influencing groundwater potential and recharge zones were derived from operational land imager 8, digital elevation model, soil data, lithological data, and rainfall data were used. Additionally, borehole data were used to validate the results of the study.
Gebrie et al. (2021) this paper aimed to delineate the groundwater potential zones using GIS and remote sensing. Multi-criteria decision analysis method was used to develop the groundwater potential prospect zones by integrating different groundwater contributing thematic layers.

Yilma et al. (2023) have made the notable contribution to groundwater exploration methodology using RS and GIS techniques, underscoring their potentiality in water resource assessment. Their study successfully applied methodologies such as analytical hierarchy process and weighted linear combination (WLC), similar to the approach taken in this study. Furthermore, they emphasized the integration of high resolution optical microwave data and GPS information demonstrating the robustness the combined

technologies. The validation process, yielding an accuracy of 92.64%, highlights the consistency and reliability of these methods across diverse geographical context; incorporating insights from these researchers enhance the current study and establish a coherent narrative on the effectiveness of RS, GIS, and associated methodologies in groundwater resource assessment.

Additionally Mathewos et al. (2024) carried out research with the aid of the analytical hierarchical approach; as a result, fourteen groundwater parameters were regarded as being related to each theme layer and consistency checks were carried out prior to overlay analysis. Based on weighted overlay analysis, the obtained result showed areas with different zones of groundwater potential in the river catchment system such as low (2.65%), moderate (79.24%), high (18.11%), and very high (0.001%). The removal of the map and thoughtful analysis that followed showed that, in some areas of the catchment along the perennial Wabe River, the most significant groundwater potential zones were interpreted as being geology and land-use and land-cover with some highly productive aquifers in favorable geological areas and some catchment broken and weather-beaten.

Girma and Abebe (2022) the groundwater potential map was created by researchers using seven thematic layers: geology, land-use and land-cover, slope, soil, drainage density, rainfall, and lineament density. The significance of GIS and remote sensing techniques in mapping the study areas groundwater potential demonstrated by validation using well yield data, which offered important insights for groundwater research and development.

# CHAPTER THREE

# MATERIAL AND METHODS

## 3.1 Description of the study area

The Teji River catchment extends across the southwestern part of the Oromia region in central Ethiopia. The catchment lies approximately found on the distance of 60 km from Addis Ababa, and passes through the districts of Sadden Sodo, Becho, Elu, Kersa Malima, and Tole, covering total area of 55,800 ha (Figure 3.1). Geographically the catchment lies between latitudes 8°24'0"−8°42'0"N and longitudes 38°8'0"−38°24'0"E. The catchment ranges from 2080−3568 m elevation.

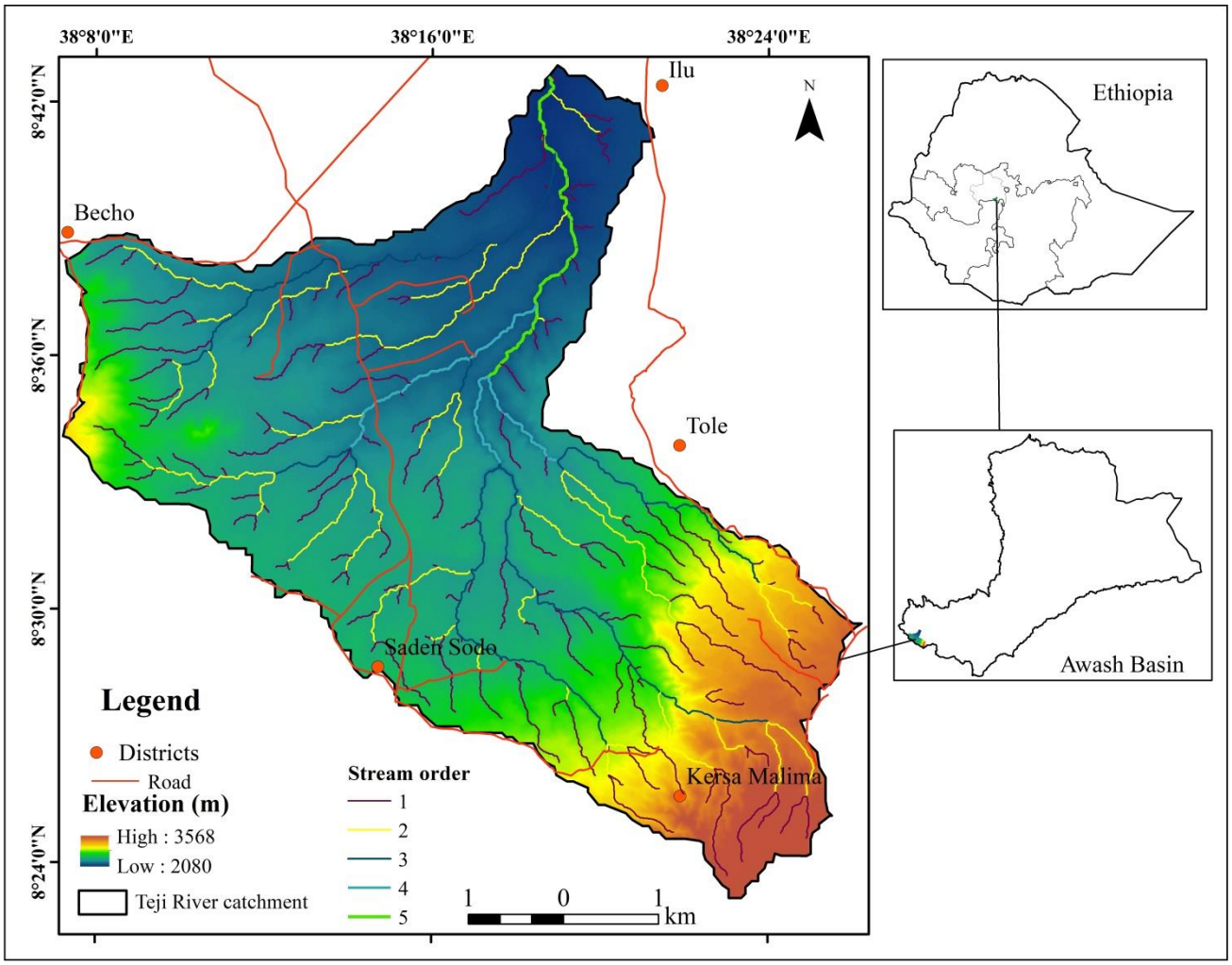


**Figure 3.1** Location map of the study area

### 3.1.1 Rainfall and temperature

July is the wettest month, experiencing an average rainfall of 250 mm (National Meteorological Agency of Ethiopia, 2023). In contrast, February is the driest month, with only 20 mm of rainfall on average (World Meteorological Organization, 2022). Rainfall remains relatively steady year-round, although there is slight reduction during the dry season from November to February (United Nations Food and Agriculture Organization, 2021). Figure 3.2 illustrates the average annual rainfall in the Teji River catchment area. April is the warmest month, with an average temperature of 19.5 °C (Intergovernmental Panel on Climate Change, 2022). Conversely, July is the coolest month averaging 13.5 °C (Ethiopian Meteorological Society, 2023). Overall, temperatures are moderate throughout the year, with minor fluctuations between the wet and dry seasons (World Bank Group, Climate Change Knowledge Portal, 2023).

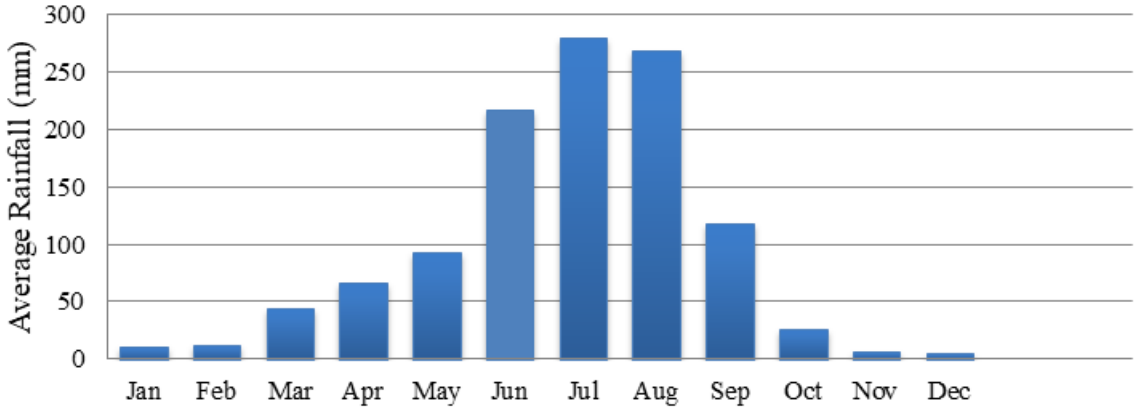


**Figure 3.2** Average monthly rainfall (1992−2022)

## 3.2 Methodology

The study conducted an assessment of factors weights and parameters scores to delineate potential ground water zones in the study area taking in to account its specific characteristics. Factors such as rainfall, hydrology, topographic wetness index, land-use and land-cover**,** slope, drainage density, lineament density, and lithology were identified based on their influence on groundwater potential zones, drawing on insights from previous research (Seifu et al., 2022; Desta et al., 2022; Teshome et al., 2020). The geological aspect was further categorized in to distinct units and lineaments, while the soil factor received attention with a focus on hydrological soil class and soil moisture components. Recognizing that these factors exert varying degrees of influence on ground water potential, a weight evaluation approach was devised using a pair-wise comparison matrix within the analytical hierarchy process (AHP) model

(Saaty,1980). Subsequently, a map overlay analysis was employed to generate the final groundwater potential zone map for the study area. The accuracy of the map was then validated with existing ground water inventory data. A comprehensive overview of the methodology is visually represented in (Fig. 3.3)

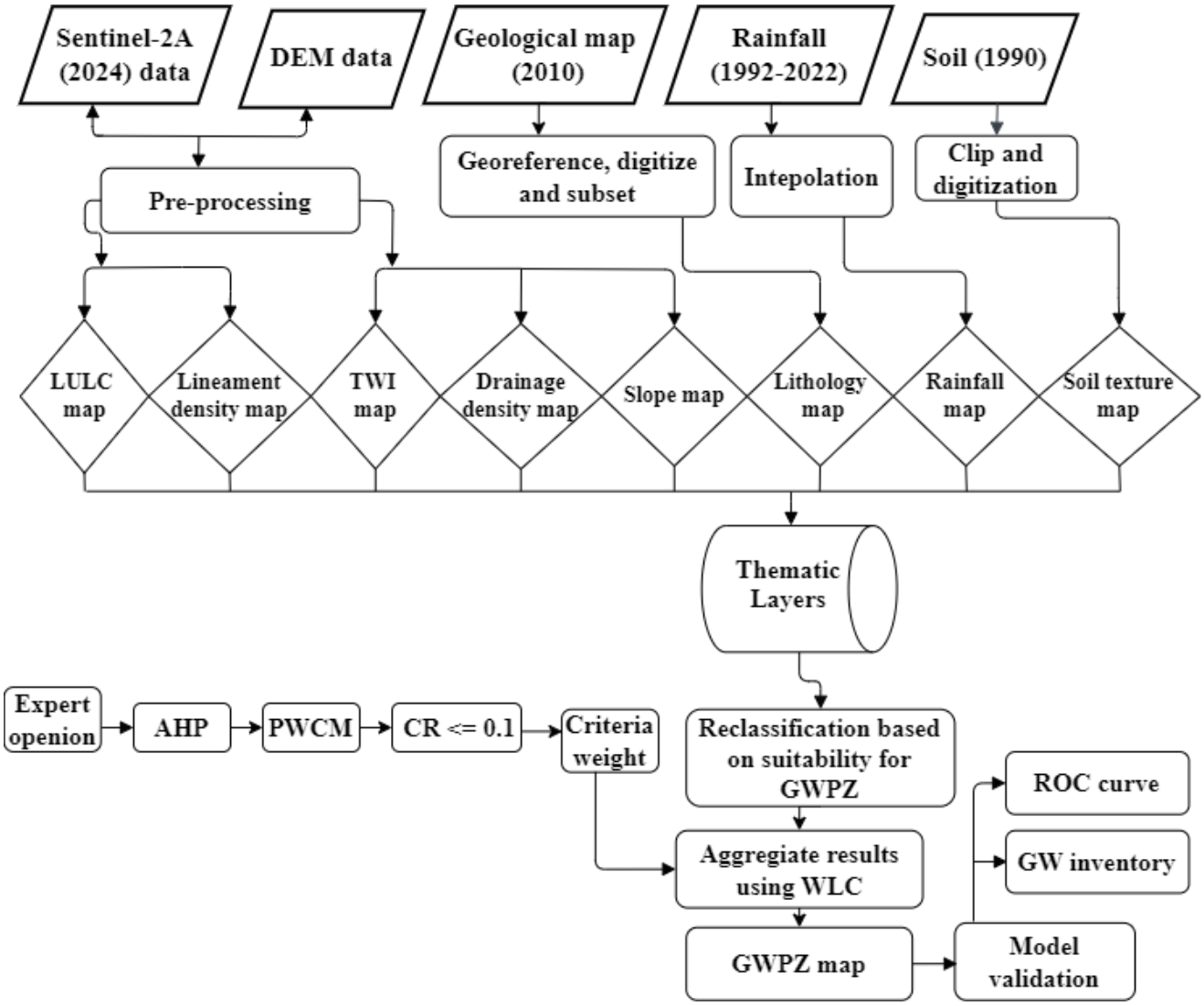


**Figure 3.3** Methodology adopted for the study

### 3.2.1 Data and software

Both primary and secondary data were collected and organized for the study. Primary data include high spatial resolution data Earth Observation (EO) data; freely available from various open sources, and freely downloadable sentinel 2A (MSI) data from the European Space Agency (ESA) (https://www.esa.int/) were employed for satellite based data acquisition used for mapping LULC and lineament density. The catchment's land-use and land-cover (LULC) analysis conducted on ERDAS imagine 2015 software was employed for satellite data processing, including atmospheric correction, radiometric correction, and layer

stacking, mosaicking, and coordinate transformation. Supervised maximum likelihood image classification algorithm was employed for LULC classification of the catchment. Sentinel 2A imagery for 2024 year offers sophisticated insight in to the spatial distribution and dynamics of land futures during the period. Sentinel 2A, equipped with multi spectral sensors, provides high resolution imagery enabling detailed land-use and land-cover classification. Shuttle radar topographic mission (SRTM) data with 12.5 m spatial resolution, freely downloadable from the ASF website (https://ask.alaska.edu/), served as the foundation for extracting hydrologic and geologic parameters, including drainage patterns, slope gradient and topographic wetness index (reflecting soil moisture levels). Following the sequential filling of sinks to establish flow direction, flow accumulation, stream order, stream features and snap pour points were derived within the catchment. Secondary data such as ground water inventory data, encompassing boreholes, hand-dug wells, shallow wells, springs, and pumping tests, were obtained from The Engineering Corporation of Oromia (ECO) office and (Ethiopian Construction Design and Supervision Corporation (ECDSWCo). Long term annual rainfall data from 1992−2022, spanning 30 years, was taken from the National Metrological Agency (NMA) to generate rain fall distribution of the study area. Soil data were also collected from (ECO) office to map soil texture within the study area. Geological data from Ethiopian Geological Survey were utilized to produce lithological map of the Teji River catchment. Finally, the GIS-based output was validated using groundwater inventory data. ArcGIS 10.8 software was utilized for analysis, interpretation and mapping of thematic layers, ERDAS imagine was employed for LULC analysis and classification, lineament were extracted using PCI Geomatica Banff 2020 software. The extracted lineaments were also exported in shape file format and analyzed on ArcGIS to prepare lineament density map. The ROC and AUC for validating the GWPZ map for the study area were calculated using RStudio software in ROC package. The summary of data and software used for the study was prepared in Tables (3.1 and 3.2)

**Table 3.1** Data used

| Data | Sources | Function of data |
|---|---|---|
| Long term annual rain fall from (1992-2022) | National Metrological Agency | Areal rain fall map preparation |
| SRTM (DEM) 12.5 m spatial resolution | ASF webhttps://asf.alaska.edu/ | To produce drainage density, TWI and slope maps |
| Existing wells/springs, Borehole | ECO and ECDSWCo | For validation of GWPZ map |
| Geology data | Geological Survey of Ethiopia | Geology maps |
| Soil data | ECO | Soil texture map |
| Sentinel 2A (MSI) | European Space Agency (ESA) (https://www.esa.int/) | LULC and lineament density map |

**Table 3.2** Software used for the study

| Software | Version | Function |
|---|---|---|
| ArcGIS | 10.8 | Data management, Spatial analysis, Geo-processing Mapping, layout and visualization. |
| IDRISI Selva | 17.0 | Weight calculation and pairwise comparison. |
| ERDAS Imagine | 2015 | Layer stacking and mosaicking, image preprocessing, image enhancement. |
| ArcHydro | 10.8 | Drainage network extraction and DEM analysis |
| GPS | Garmin | Used to locate specific location of well, spring and borehole and LULC classes. |
| Google earth pro | version 7.3 | Used for collecting ground control points to validate the LULC map. |
| RStudio | 2024.04.1 | Statistical calculation of ROC and AUC for validation |
| PCI Geomatica Banff | 2020 | To generate lineament density map |

### 3.3 Preparation of thematic layer maps

Thematic layers provide important insights in the variables affecting groundwater recharge, storage, and outflow, making them indispensable instruments for groundwater evaluation. The groundwater potential zone mapping overall goal was supported by the preparation of each factor map; to make these maps suitable for mapping the groundwater potential zone, controlling factors, and computing each of theme maps using AHP pairwise comparison to assess the groundwater potential zone, the digital vector layers and prepared input layers were transformed and resampled to raster layers with 10 m cell size.

#### 3.3.1 Rainfall

The rainfall data gathered from the National Meteorological Agency covering a period of 30 years (1992−2022) from eleven stations in the study area, including Busa, Bantuliben, Asgori Tulubolo, Arbuchulule, Welenkomi, Ameyagindo, Chitu, Dilela, Teji, and Guranda Meta, offers valuable insights into groundwater recharge potential and temporal variability. Through spatial analysis techniques in ArcGIS 10.8, the rainfall data underwent interpolation using the Inverse Distance Weighting (IDW) method to generate detailed rainfall map of the catchment.

#### 3.3.2 Drainage density

In evaluating groundwater potential zone of a region, one crucial parameter is drainage density, as highlighted by Manap et al. (2011). According to their findings there exists an inverse relationship between infiltration rates and drainage density. In simple terms regions with higher subsurface water infiltration tend to exhibit lower drainage density (Agarwal and Garg, 2016; Yadav et al., 2020; Kumar

and Singh, 2021). This relationship implies that areas with low drainage density experience low runoff and more water infiltration, thereby, potentially enhancing groundwater resources (Bhunia, 2020; Barua et al., 2021). Drainage density often computed from digital elevation model, serves to delineate regions with high ground water discharge potential and assess the impact of surface drainage on ground reservoirs. It is strongly correlated with groundwater recharge; hence, areas characterized by high drainage density typically exhibit low ground water recharge potential (Verma and Patel, 2021). The drainage density is calculated using equation (1)

$$Dd = \left(\frac{L \times n}{A}\right) \quad (1)$$

where, L is the accumulate length in km, n is the stream order, and A is the study area's surface in $Km^2$.

### 3.3.3 Slope

Slope data obtained from digital elevation models identifies areas with high runoff potential and assess the impact of topography on recharge rates. The significance of topography in determining the features of the land surface cannot be overstated. It offers vital information about the geological geodynamic processes that shape the land at regional scale, which has substantial impact on surface runoff and infiltration rates, as well as the direction of groundwater flow. For instance steep slopes tend to lead to less recharge because water from precipitation quickly runs off down the slope during rainfall, leaving insufficient time for the water penetrate and recharge the ground water systems (Akhtar et al., 2020). In contrast, the presence of flat slope in the region may result in increased infiltration compared to a steep slope. Therefore, the study area was classified in to four distinct slope classes for classification purposes, ranging from flat to very steep, based on their percentage gradient. The flatter slopes were assigned a higher weight because they are more likely to retain precipitation and promote the replenishment of groundwater resources (Tolche, 2021). In contrast, steeper slopes were assigned lower weight. This classification method helps in identifying zones where the ground water potential is likely to be higher or lower based on slope characteristics.

### 3.3.4 Lineament density

Geological lineaments referred to surface expression of underlying geological structure such as faults and fractures, which may exhibit either noticeable displacement or significant fracture displacement**.** Lineament characterized by their straight alignments in satellite imagery. These lineaments contribute to the development secondary porosity and permeability, which are crucial for groundwater flow (Choudhary et al., 2022). In this research, lineaments were automatically extracted from sentinel 2A using PCI Banff Geomatica 2020 software and exported as shape file format or polyline. The resulting lineament density

map was generated in ArcGIS 10.8 software spatial analysis tools in arc toolbox and extracted line density. To analyze lineament density data of the catchment, it was categorized in to four categories namely poor, moderate, good and very good. These categories were defined based on specific ranges of lineament density values. The formula for calculating lineament density was given with equation (2).

$$Ld = \sum_{i=1}^{n} \left(\frac{li}{A}\right) \quad (2)$$

where Ld is lineament density, Σli is total length of all lineaments in (km) and A is total area of the catchment in ($km^2$).

### 3.3.5 Soil texture

The Natural Resource Conservation Service (NRCS) categorizes soils into four Hydrological Soil Groups (HSG) based on their runoff potential, as established by Schoener (2019). These four groups are A, B C, and D, with A having the least runoff potential and D the most. The USDA's Universal Soil Data Analysis delineates the properties of these classes based on the relative proportions of sand, silt, and clay in the soil, as determined by standard soil texture analysis methods. Group A consists of sand, loamy sand, or sandy loam soils, which have low runoff potential and high infiltration rates, even when fully saturated. They are made up of deep, well-drained sands or gravels and exhibit a high rate of water transmission. Group B includes silt loam or loam soils, which have moderate infiltration rates when fully saturated and consist of moderately deep, moderately well-drained soils with moderately fine to moderately coarse textures. Group C soils are sandy clay loams, which have low infiltration rates when fully saturated and consist of soils with a layer that impedes the downward movement of water and soils with moderately fine to fine structure. Group D soils are clay loam, silty clay loam, sandy clay, silty clay, or clay, and have the highest runoff potential. They have very low infiltration rates when fully saturated and consist of clay soils with a high swelling potential. Soils with a permanent high water table, a clay pan or clay layer at or near the surface, and shallow soils covering nearly impervious material are characteristics of Group D. Table 3.3 soil texture water capacity and its infiltration rate.

**Table 3.3** Soil texture with water capacity and infiltration rate

| Soil texture type | Effective water capacity (mm) | Infiltration rate (mm/hr.) | HSG |
|---|---|---|---|
| Clay | 2.032 | 0.5 | D |
| Clay loam | 3.556 | 2.3 | D |
| Sandy clay loam | 3.556 | 4.3 | C |
| Loam | 4.826 | 13.2 | B |

Source**:** (Berhanu et al., 2013)

### 3.3.6 Topographic wetness index

Topographic Wetness Index (TWI) serves as a tool for assessing the influence of topography on hydrological processes, particularly in estimating the potential for groundwater infiltration (Mokarram et al., 2015). TWI calculations are commonly derived using the "TOPMODEL," a hydrological model designed to simulate water fluxes within a watershed. Equations (3, 4, 5, 6, and 7) provided below were employed to estimate the TWI of the catchment using the ArcGIS spatial analyst tool and calculating water values using map algebra.

$$\text{Rasterslope} = \left(\frac{\text{Raterslope}\times 1.570796}{90}\right) \quad (3)$$

$$(\text{SlopeTan} = \text{Con}(\text{Rasterslope} > 0, \text{Tan}(\text{Rasterslope}), 0.001) \quad (4)$$

$$\text{FlowAcc2} = (\text{FlowAcc} + 1) \times \text{Cell size}(10) \quad (5)$$

$$\text{TWI} = \ln\left(\frac{\text{FlowAcc2}}{\text{RasterslopeTan}}\right) \quad (6)$$

$$\text{TWI} = \ln\left(\frac{\alpha}{\tan\beta}\right) \quad (7)$$

where α is Upslope contributing area; β is Topographic gradient (slope)

### 3.3.7 Lithology description

The Teji River catchment, situated within the main Ethiopian rift, exhibits distinctive lithological characteristics marked by extensively faulted rift floors and escarpments, which have arisen primarily from volcanic activity. Ethiopian encompasses a diverse array of geological Eras and Periods evident through the presence of various relics such as metamorphic basement rocks, sedimentary deposits, and volcanic formations. Both plateau and rift regions prominently define the Ethiopian landscape, particularly the land mass, where volcanic processes have exerted a significant influence on the geological terrain. Within Teji River catchment, the lithological formation present a multifaceted a composition shaped by volcanic eruption and tectonic forces. These formations contributed to the intricate geological framework of the region. As (GSE, 2010) and geology of Akaki Beseka index map sheet NC 37-14, the catchment's lithological formations encompass distinct lithological units, including the Pre- rift unit tarmaber–megezez formation (E3tm), inductive of early geological process. Additionally, Syn-rift units comprising welded pyroclastic flows (Nwp) and welded to partially welded pyroclastic flows (Npp), denote the dynamic tectonic activity and volcanic phenomena experienced within the area. Main-rift unit comprise gash megal rhyolites (Ngr). Furthermore, quaternary surficial deposit such as alluvium (Qus), further enrich the lithological diversity of the Teji River catchment. Encompassing this geological configuration, the landscape of the catchment mirrors a sophisticated interplay among volcanic activity, tectonic shifts, and

sedimentary processes. This underscores its importance within the broader geological framework of Ethiopia.

**A. Trmaber-megeze formation (E3tm)**

The term tarmaber megezez formation refers to a geological formation comprising younger shield volcanoes that originated during the Pliocene to Miocene epochs. The tarmaber megezez formation (E3tm) is present in southern and western part of the study area. Fresh samples exhibit a dark grey hue, while weathered specimens tend to display reddish-brown coloration. Comprised of fine grained volcanic rock, this units consists primary of plagioclase, pyroxene, and opaque minerals.

**B. Welded pyroclastic flows (Nwp)**

The exposure of this unit is primarily found in the southern part of the Teji River catchment, covering a relatively small area. In fresh samples, it appears light to dark-grey, while weathered specimens exhibit hues ranging from reddish to yellow to pink. This unit is characterized by fine-grained, densely welded rock containing vitrophyric fiamme and lithic fragments, interspersed with rhyolitic lava flows interlayered with ash and unwelded tuffs. Microscopic analysis reveals composition comprising (35%, 40%, 20%, and 5%) of K-feldspar, quartz, plagioclase and hornblende respectively exhibiting a vitreous surface, as documented by Geological Survey of Ethiopia.

**C. Welded to partially welded pyroclastic flows (Npp)**

The occurrence of welded to partially welded pyroclastic flows (Npp) unit is situated along the southern, southeastern, and eastern peripheries of the catchment's territory. In its fresh state, the unit exhibits shades ranging from light to dark-grey, while weathered samples showcase hues transitioning from reddish to yellow to pink. This unit is characterized by fine-grained, densely welded rock containing vitrophyric fiamme and lithic fragments, accompanied by associated rhyolitic lava flows interspersed with ash and unwelded tuffs. Microscopic examination reveals a composition comprising 35% K-feldspar (sanidine), 40% quartz, 20% plagioclase, and 5% hornblende, displaying a vitreous texture.

**D. Gash megal rhyolites (Ngr)**

This lithological unit is common in the southern and southeaster catchment areas, appearing light gray to pink and primarily composed of alkali, quartz, and mica. It forms small domes and broad gently sloping hills. Some sections show alternating fine ash and unwelded tuffs. Its composition is 45% feldspar, 35% quartz and 20% muscovite with rhyolite texture.

**E. Alluvium (Qus)**

The exposure of the alluvium (Qus) unit is predominantly located in the central northern and northeastern sectors of the study area. This unit contributes to the formation of flat-lying topography and marshy

regions. Comprising loose sediment, the alluvium exhibits shades ranging from brown to grey and contains sand, silt, and clay interspersed with various clasts. These clasts encompass boulders composed of basalt, rhyolite, and scoria. Additionally, the presence of thick black, brown, and reddish-brown soils within this unit is not uncommon. This map was processed by georeferencing, digitizing, and clipping to fit the catchment's boundaries. The digitized shape file was then converted into raster format, a standard for GIS analysis and modeling. To ensure spatial consistency and accuracy, the raster data was projected onto the Adindan−UTM−Zone 37 coordinate system using ArcGIS conversion tools. Geological units within the catchment were classified based on lithological characteristics and geological formations, with a detailed table compiled to document the attributes of each unit.

### 3.3.8 Land-use and land-cover (LULC)

Land-use and land-cover (LULC) data, extracted from Sentinel-2A (MSI) imagery at 10-meter resolution, is instrumental in analyzing the influence of land use land cover on groundwater recharge and discharge dynamics. This data offers insights into surface water presence, soil moisture levels, infiltration rates, and groundwater distribution. The classification system for LULC involves four primary categories: settlements, cropland, vegetation and wetlands. To generate the LULC map, Sentinel-2A data's three bands (4, 3, and 2) red, green and blue were processed using radiometric techniques including image stacking, mosaicking, and enhancement. A supervised maximum likelihood classification algorithm was employed using ERDAS IMAGINE 2015. The sentinel 2A (MSI) image was accused from Copernicus hub on 2024-02-07 with image code TPDK. Following Mukherjee and Singh's (2020) the land-use land-over (LULC) data should consider additional characteristics such as infiltration properties, water retention capabilities, and treatment requirements. Eighty total referenced or sample data points were taken. The accuracy of the classification was verified, yielding an overall accuracy of 95% with a kappa coefficient of 0.93. The accuracy assessment of LULC and Kappa coefficient for Teji River catchment presented in Table 3.4.

**Table 3.4** Accuracy assessment of LULC for Teji River catchment

| Classes | Reference totals | Classified totals | Number correct | Producers accuracy | Users accuracy | Class name | Kappa |
|---|---|---|---|---|---|---|---|
| Settlement | 20 | 20 | 19 | 95.00% | 95.00% | Settlement | 0.93 |
| Cropland | 22 | 20 | 20 | 90.91% | 100.00% | Cropland | 1.00 |
| Vegetation | 19 | 20 | 18 | 94.74% | 90.00% | Vegetation | 0.87 |
| Wetland | 19 | 20 | 19 | 100.00% | 95.00% | Wetland | 0.93 |
| Totals | 80 | 80 | 76 | | | | |
| Overall classification accuracy | | 95% | | | | Kappa statics | 0.93 |

### 3.4 Analytical hierarchy process

The analytical hierarchy process (AHP) is a theory of measurement by pairwise comparison and depend on the decision of experts to derive priority scales. The comparison was made on a scale of numbers 1–9 which shows how many times a layer is important than the other (Saaty, 1980). If the matrix formed is equal to bij, aij = wi/wj, where w is the weight of each parameters, i, j=1….n of every positive numbers entry to everywhere and satisfy the reciprocal properties, bnij = i/bij which is called reciprocal matrices. Table 3.5 details of Saaty's scale of relative importance.

**Table 3.5** Saaty's scale of intensity relative importance

| Scale | 1 | 2 | 3 | 4 | 5 | 6 | 7 | 8 | 9 |
|---|---|---|---|---|---|---|---|---|---|
| Importance | Equal importance | Weak or slight | Moderate importance | Moderate plus | Strong importance | Strong plus | Very strong | Very very strong | Extremely importance |

Source: (Saaty, 1980)

#### 3.4.1 Weight evaluation and normalization

The analytical hierarchy process (AHP) was used to determine the cumulative weights of the main criteria for mapping of GWPZ. Eight factors were classified and weighted using AHP, with Saaty's scale for normalization (Saaty, 1980). Pairwise comparison matrices were produced for the thematic layers and their class, and weights were normalized using the Eigen vector approach. The consistency ratio (CR) was calculated to evaluate the normalized weights, following Saaty's method, using Equations (8, 9, and 10)

$$A_1\begin{bmatrix} ai11 & a12\cdots & a1n \\ \vdots & \ddots & \vdots \\ a21 & a22\cdots & a2n \\ \vdots & \vdots & \vdots \\ an1\cdots & an2\cdots & ann \end{bmatrix}, \text{aij} = \frac{\text{aij}}{\sum \text{aij}} \text{ for i, j} = 1,2 \ldots \text{n} \quad (8)$$

The Eigen value and Eigen vector calculated as:

$$\text{w} = \begin{bmatrix} \text{W1} \\ \text{W2} \\ \vdots \\ \text{Wn} \end{bmatrix} \text{ and Wi} = \frac{\sum_1^{\text{n}} \text{aij}}{\text{n}} \text{ for all n} = 1,2..\text{n and W}' = \begin{bmatrix} \text{W1}' \\ \text{W2}' \\ \vdots \\ \text{Wn}' \end{bmatrix} \quad (9)$$

$$\lambda\text{max} = \left(\frac{\text{w}'}{\text{w1}} + \frac{\text{w}'}{\text{w2}} + \frac{\text{w}'}{\text{wn}}\right) \quad (10)$$

where W is eigenvector, $W_i$ is eigenvalue of criterion i, and, λmax is average Eigenvalue of the pair wise comparison matrix.

The matrices exhibit a property a property of called consistency ratio. If CR exceeds 0.1, then the matrix needs re-evaluation. Table 3.6 presents Saaty's Random Index (RI).

**Table 3.6** Random Index (RI) developed by Saaty (1980)

| N | 1 | 2 | 3 | 4 | 5 | 6 | 7 | 8 | 9 | 10 |
|---|---|---|---|---|---|---|---|---|---|---|
| RI | 0 | 0 | 0.58 | 0.9 | 1.12 | 1.24 | 1.32 | 1.41 | 1.45 | 1.49 |

### 3.4.2 Assessment of weight

In the weight assessment process the relative importance of the thematic layers (including rainfall, lineament density, drainage density, soil texture, LULC, TWI, lithology, and slope was determined based on their significance of groundwater potential zone mapping. This determination was made through the collective judgment of researchers or experts with relevant experiences in similar study (Mathewos et al., 2024). Comparing the importance of two layer maps helps identify which one has greater influence on groundwater occurrences. Table 3.7 represents the pairwise comparison matrix generated through the AHP process, while Table 3.8 shows the normalized weights derived from this matrix.

**Table 3.7** Pair-wise comparison matrix of thematic layers with AHP

| Factors | LI | RF | LULC | ST | DD | TWI | LD | SL |
|---|---|---|---|---|---|---|---|---|
| LI | 1 | 2.00 | 3.00 | 5.00 | 6.00 | 4.00 | 6.00 | 7.00 |
| RF | 0.50 | 1 | 2.00 | 3.00 | 5.00 | 5.00 | 6.00 | 7.00 |
| LULC | 0.33 | 0.50 | 1 | 0.50 | 2.00 | 4.00 | 2.00 | 3.00 |
| ST | 0.20 | 0.33 | 2.00 | 1 | 2.00 | 2.00 | 2.00 | 3.00 |
| DD | 0.17 | 0.20 | 0.50 | 0.50 | 1 | 2.00 | 3.00 | 4.00 |
| TWI | 0.25 | 0.20 | 0.25 | 0.50 | 0.50 | 1 | 3.00 | 4.00 |
| LD | 0.17 | 0.17 | 0.50 | 0.50 | 0.33 | 0.33 | 1 | 4.00 |
| SL | 0.14 | 0.14 | 0.33 | 0.33 | 0.25 | 0.25 | 0.25 | 1 |
| Sum | 2.76 | 4.54 | 9.58 | 11.33 | 17.08 | 18.58 | 23.25 | 33.00 |

where LD is Lineament density, DD is Drainage density, TWI is Topographic wetness index, LULC is Land use -land cover, RF is Rainfall, SL is Slope, LI is Lithology, ST is Soil texture

**Table 3.8** Normalized weight of the matrix

| Factors | LI | RF | LULC | ST | DD | TWI | LD | SL | Criteria weight | Criteria weight (%) |
|---|---|---|---|---|---|---|---|---|---|---|
| LI | 0.363 | 0.441 | 0.313 | 0.441 | 0.351 | 0.215 | 0.258 | 0.212 | 0.320 | 32 |
| RF | 0.181 | 0.221 | 0.209 | 0.265 | 0.293 | 0.269 | 0.258 | 0.212 | 0.238 | 23.8 |
| LULC | 0.120 | 0.111 | 0.104 | 0.044 | 0.117 | 0.215 | 0.086 | 0.091 | 0.111 | 11.1 |
| ST | 0.073 | 0.073 | 0.209 | 0.088 | 0.117 | 0.107 | 0.086 | 0.091 | 0.105 | 10.5 |
| DD | 0.060 | 0.044 | 0.052 | 0.044 | 0.059 | 0.107 | 0.129 | 0.121 | 0.077 | 7.7 |
| TWI | 0.091 | 0.044 | 0.026 | 0.044 | 0.029 | 0.054 | 0.129 | 0.121 | 0.067 | 6.7 |
| LD | 0.060 | 0.037 | 0.052 | 0.044 | 0.019 | 0.018 | 0.043 | 0.121 | 0.049 | 4.9 |
| SL | 0.051 | 0.031 | 0.035 | 0.029 | 0.015 | 0.013 | 0.011 | 0.031 | 0.027 | 2.7 |
| Sum | 1.00 | 1.00 | 1.00 | 1.00 | 1.00 | 1.00 | 1.00 | 1.00 | 1.00 | 100 |

### 3.4.3 Normalized Principal Eigen vectors

To assess the weights in Table 3.9 computed the normalized principal Eigen vector value (λmax) using (Eq. 12) and derived the consistency ratio formula Eq. 11. This involved multiplying each criterion's weight (lithology = 0.32) by its corresponding value from pairwise comparison matrix (example lithology 2.76). (Table 3.5). The resulting value were summed to obtain the consistency vector (λmax = 8.84) shown in (Table 3.7) for calculating the consistency index the consistency ration, indicating the acceptability of the reciprocal of matrix, was computed.

$$CR = \frac{CI}{RI} \tag{11}$$

where CI is consistency index and RI is random consistency index

$$CI = \frac{\lambda max - n}{n-1} \tag{12}$$

where *n* is number of factors (8) and $\lambda$ is average value of the consistency vector. Lambda max equals to column sum multiplied by Eigen vector. For 8 by 8 matrixes the RI is 1.41. Equations (11, 12) CR is calculated as:

2.76×0.32+4.54×0.238+9.58×0.111+11.33×0.105+17.08×0.077+18.58×0.067+23.25×0.049+33.00×0.027 = 8.9

**Table 3.9** Normalized Principal Eigen vector

| Factors | Normalized principal Eigen vector |
|---|---|
| LI | 0.894 |
| RF | 1.082 |
| LULC | 1.064 |
| ST | 1.196 |
| DD | 1.317 |
| TWI | 1.250 |
| LD | 1.147 |
| SL | 0.891 |
| λmax | 8.84 |

The consistency index (CI) was calculated using Eq.12, yielding value of CI = 0.12. Subsequently, the consistency ratio (CR) was determined using Eq. 11, resulting in a CR of 0.08, which is below the threshold of 0.1 validating the assigned weights for further analysis. After verifying all criteria, the groundwater potential zone map (GWPZM) was generated using Eq.13

GWPZ =LI×0.32+RRF×23.8+RLULC×11.1+RST×10.5+RDD×7.7+RTWI×6.7+RLD×4.9+RSL×2.7 (13)

where, RRF is Reclassified Rainfall, RLI is Reclassified Lithology, RLULC is Reclassified Land-use and Land-cover, RDD is Reclassified Drainage Density, RTWI is Reclassified Topographic Wetness Index, RLD is Reclassified Lineament Density, RST is Reclassified Soil Texture and RSL is Reclassified Slope.

### 3.5 Model validation for GWPZ map

The evaluation of the accuracy of the generated groundwater prospects was carried out through a rigorous cross-validation process, which entailed comparing them with both on-site observations of established groundwater resources data obtained at specific locations. This comprehensive approach was designed to ensure the reliability and precision of the identified groundwater potential zones by comparing the generated prospects with field-derived datasets.

Field observations provided valuable insights into the actual presence and characteristics of groundwater resources, while inventory data contributed detailed subsurface information crucial for validation. The integration of diverse data sources and methodologies in the cross-validation process further enhanced the overall accuracy of the groundwater prospect zone mapping. This comprehensive approach effectively minimized uncertainties, providing a thorough and dependable evaluation of the identified groundwater potential zones. Moreover, the groundwater inventory data for boreholes, hand-dug wells, and springs, along with supplementary yields, underwent a meticulous comparison with the indicated prospective groundwater potential zones. The potential water yields were utilized to categorize the data, and the precision of the potential groundwater zones was assessed in conjunction with the entire dataset. This evaluation methodology aligns with the principles outlined by Opoku et al. (2024), allowing for a comprehensive assessment of the identified groundwater potential zones based on both the overall dataset and water level data obtained from drilled wells within the entire validation set. Equation (14) used for model validation.

$$\text{Accuracy} = \frac{\text{Total number of agreement data}}{\text{Total number of validation data}} \times 100 \quad (14)$$

# CHAPTER FOUR

# RESULTS AND DISCUSSION

## 4.1 Results

### 4.1.1 Rainfall

The interpolated rainfall data reveals remarkable spatial disparities in rainfall distribution across the catchment area. The south western part experiences very good rainfall distribution 11.26 % (6, 280.67 ha), followed by the southern and western regions with good rainfall coverage 18.90% (10, 547.15 ha). The north western, central and south eastern part exhibits relatively moderate rainfall having 41.77 % (23, 308.18 ha). The north eastern areas receives notably lowest rainfall coverage with 28.07% (15662.56 ha). This distribution pattern underscores the influence of topographical features, particularly the steep slope gradient in the southwestern and western highland regions. The high rainfall in these areas significantly impacts groundwater recharge potential downstream, particularly in the central and eastern parts of the study area. The topography not only dictates the amount of rainfall received but also affects infiltration rates, thus shaping groundwater potential zones across the landscape. Table 4.1 and Figures 4.1, and 4.2 depict the factors and rank of rainfall for GWPZ map for the catchment.

**Table 4.1** Rainfall classes and its suitability rank for GWPZ mapping

| Factors | Rainfall (mm) | Area (ha) | Area (%) | GWPZ | Suitability rank |
|---|---|---|---|---|---|
| Rainfall | 2140−2220 | 15,662.56 | 28.07 | Poor | 1 |
| | 2230−2280 | 23,308.18 | 41.77 | Moderate | 2 |
| | 2290−2350 | 10,547.15 | 18.90 | Good | 3 |
| | 2360−2430 | 6,280.67 | 11.26 | Very good | 4 |

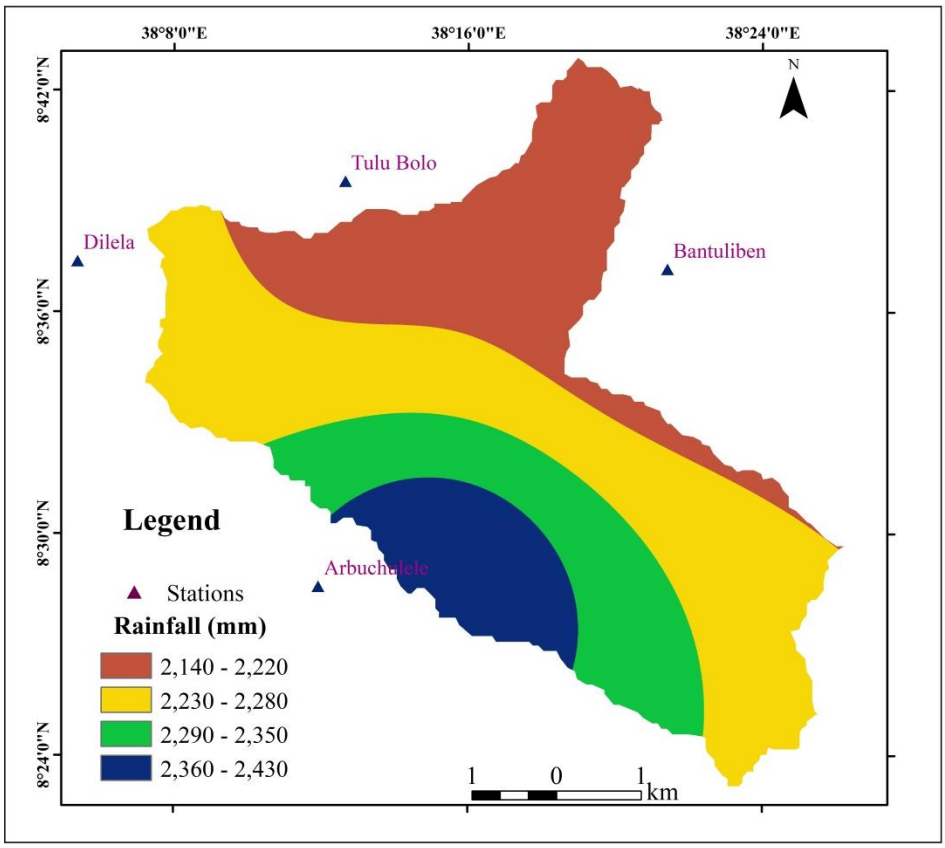


**Figure 4.1** Rainfall map

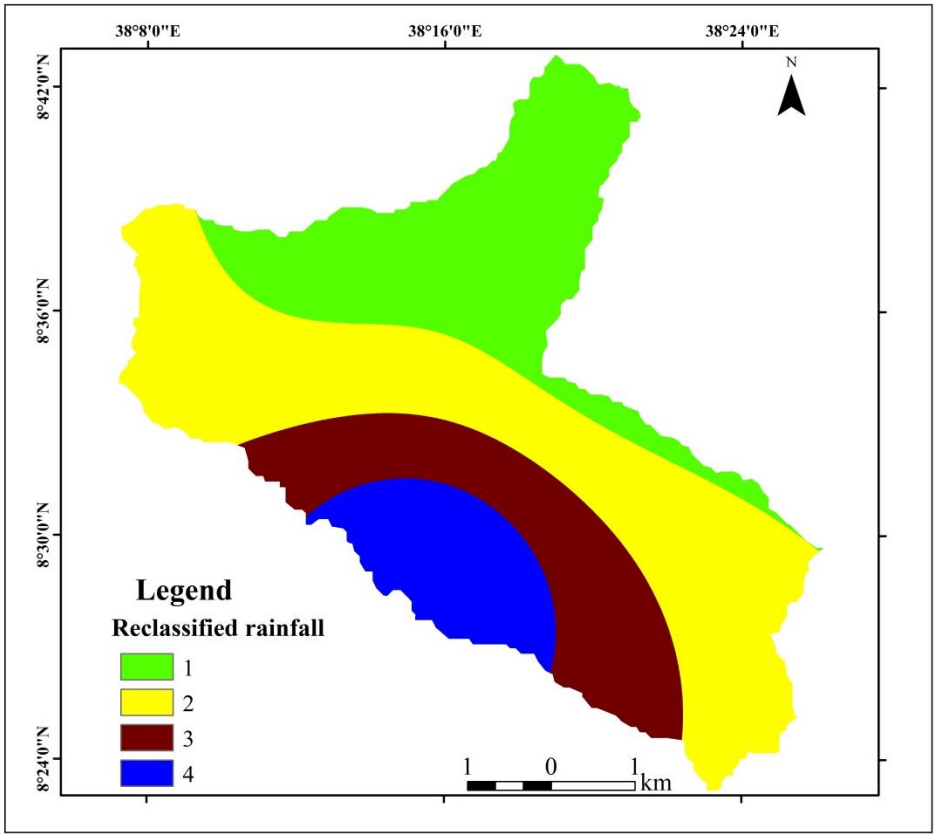


**Figure 4.2** Reclassified rainfall map

### 4.1.2 Drainage density

The river catchment exhibits a combination of parallel and dendritic drainage patterns. Some of the streams in the river catchments are perennial. Drainage density in the region differed from 1.58 to 6.33 km/ $km^2$ and was reclassified into four subclasses. Higher drainage density values were recorded in the eastern part of the catchment. Poor to moderate drainage density value were noted in south eastern and western part of the catchment. In general, the catchment has good drainage density, which was governed by the flow direction of the Teji Rivers, flowing nearly towards the west direction. Higher drainage density implies a greater abundance of streams and rivers, which in turn facilitates a well-connected network of watercourses. This leads to increased surface runoff and diminished soil infiltration capacity. Consequently, areas with higher drainage density exhibit reduced groundwater potential due to decreased recharge. Conversely, regions characterized by low drainage density values are allocated higher weights. The drainage density of the study area classification as per GWPZ mapping is presented in Table 4.2 and Figures (4.3, and 4.4) drainage density and reclassified drainage density map in Teji River catchment respectively.

**Table 4.2** Drainage density classes and its suitability for GWPZ mapping

| Factors | Dd (km/$km^2$) | Area (ha) | Area (%) | GWPZ | Suitability rank |
|---|---|---|---|---|---|
| Drainage density | 4.76–6 .33 | 2,862.14 | 5.13 | Poor | 1 |
| | 3.18−4.75 | 15,497.78 | 27.78 | Moderate | 2 |
| | 1.59−3.17 | 18,679.35 | 33.48 | Good | 3 |
| | 0−1.58 | 18,783.79 | 33.67 | Very good | 4 |

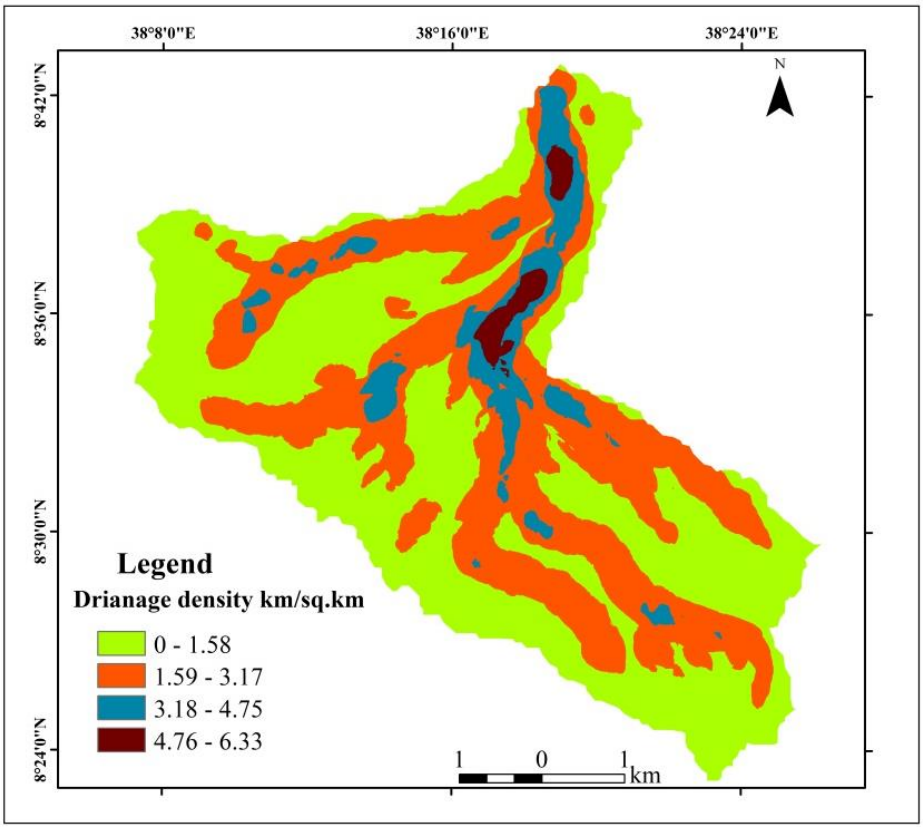


**Figure 4.3** Drainage density map

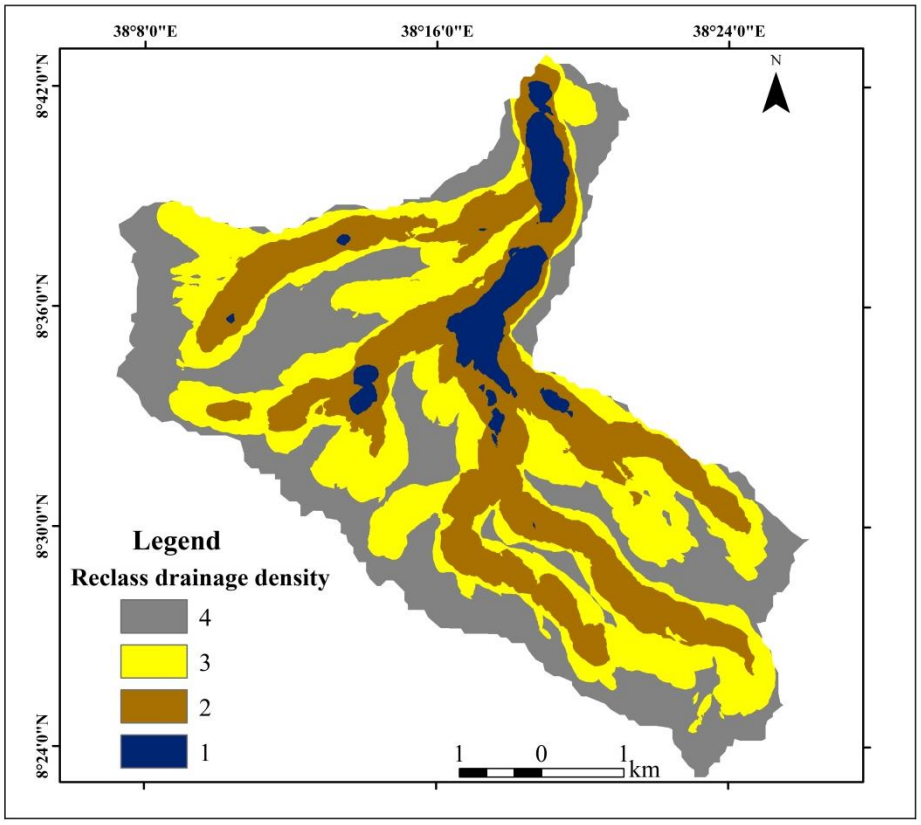


**Figure 4.4** Reclassified drainage density map

### 4.1.3 Slope

The slope of the river catchment ranges from 0° to 48°, with a significant part of the area exhibiting flat to gentle slopes (0°–4.71°). The slope of the terrain was categorized into four classes, with higher weights assigned to flat and gentle slope categories, while lesser weights were allocated to steep and very steep slope subclasses. Very steep 2723.55 ha, steep 6.646.16 ha, gentile 17507.56 ha and Flat 28768.04 ha or 5.10%, 11.92%, 31.42% and 56.56% respectively as detailed in Table 4.3. In regions with steep slopes, water runoff occurs more rapidly, leading to reduced infiltration and subsequently lower groundwater recharge rates. Figure 4.5 and 4.6 shows the slope map and reclassified slope map respectively.

**Table 4.3** Slope classes and its suitability rank for GWPZ mapping

| Factor | Slope (degree) | Area (ha) | Area (%) | GWPZ | Suitability rank |
|---|---|---|---|---|---|
| Slope | Very steep (18.6–48) | 2,723.55 | 5.10 | Poor | 1 |
| | Steep (10.3–18.5) | 6,646.16 | 11.92 | Moderate | 2 |
| | Gentle (4.72–10.2) | 17,507.56 | 31.42 | Good | 3 |
| | Flat (0–4.71) | 28,768.04 | 51.56 | Very good | 4 |

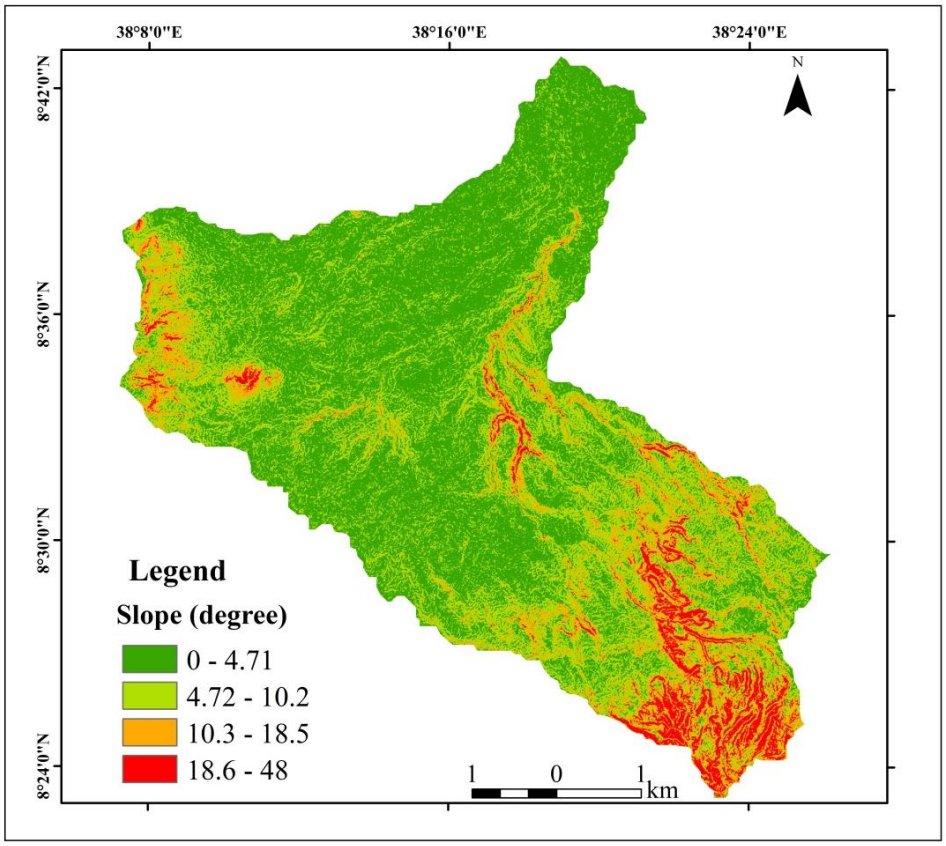


**Figure 4.5** Slope map

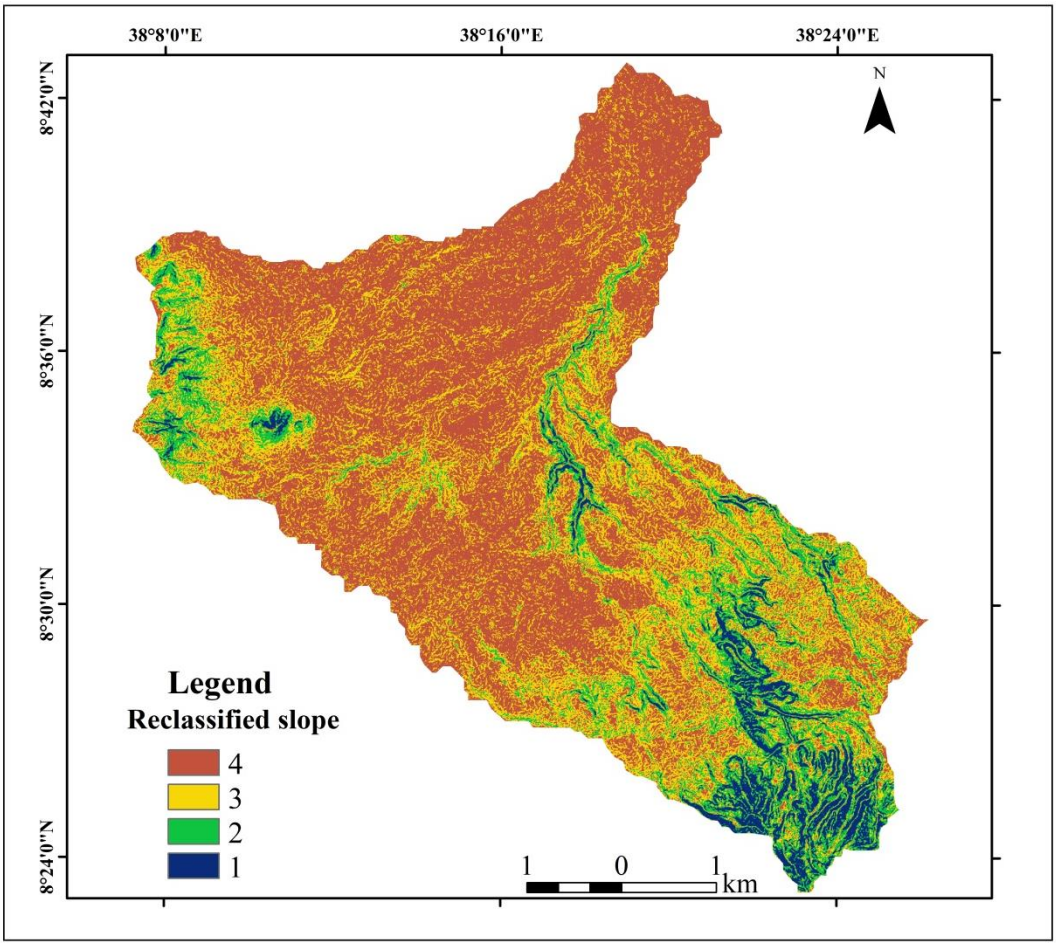


**Figure 4.6** Reclassified slope map

### 4.1.4 Lineament density

The lineament density within the study area ranges from 0–3.9 km/km², as illustrated in Figure 4.7. Upon careful analysis of these values, the lineament density was reclassified into four distinct categories, with higher weights assigned to greater lineament densities and lower weights to lower densities, as outlined in Table 4.4. Areas exhibiting higher lineament densities correspond to increased secondary porosity, indicating an area with significant groundwater potential. Notably, the majority of high-density lineaments are situated proximal to the perennial Teji River. This region is characterized by well-defined normal faults and fractures, facilitating secondary porosity conducive to groundwater recharge within the tract. Figure 4.8 shows the reclassified lineament density map.

**Table 4.4** Lineament density classes and its suitability for GWPZ mapping

| Factors | LD in km/km$^2$ | Area (ha) | Area (%) | GWPZ | Suitability rank |
|---|---|---|---|---|---|
| Lineament density | 0–0.9 | 12532.88 | 22.46 | Poor | 1 |
| | 1–1.9 | 18869.52 | 33.82 | Moderate | 2 |
| | 2–2.9 | 17022.69 | 30.51 | Good | 3 |
| | 3–3.9 | 7397.97 | 13.26 | Very good | 4 |

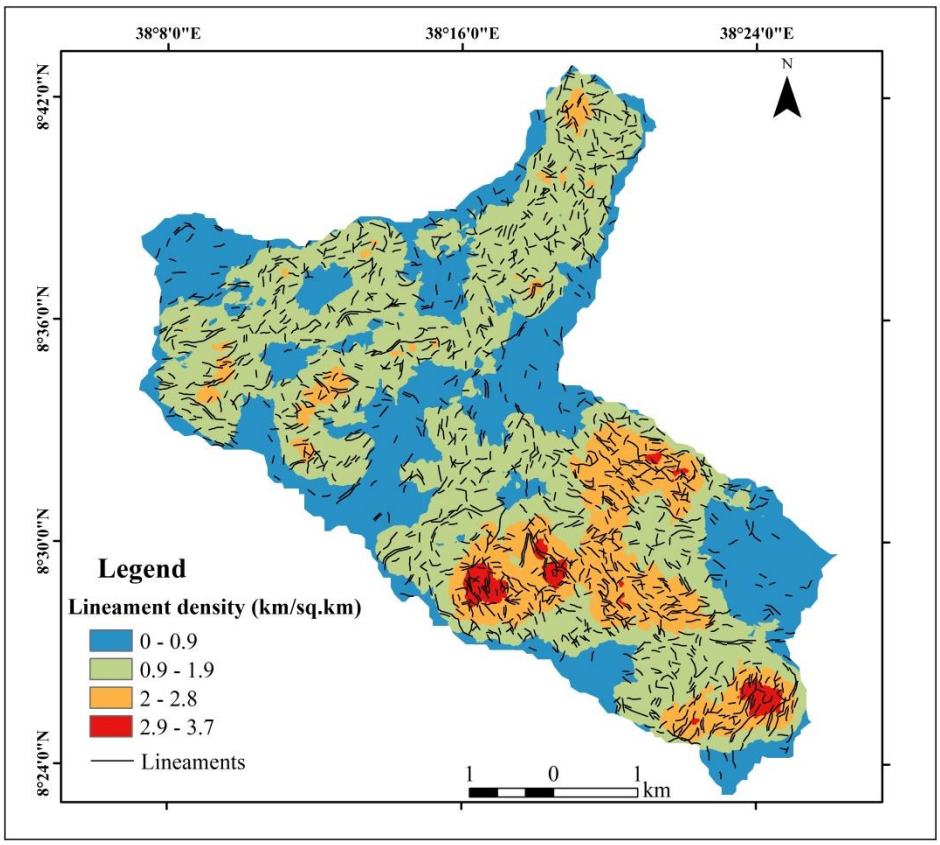


**Figure 4.7** Lineament density map

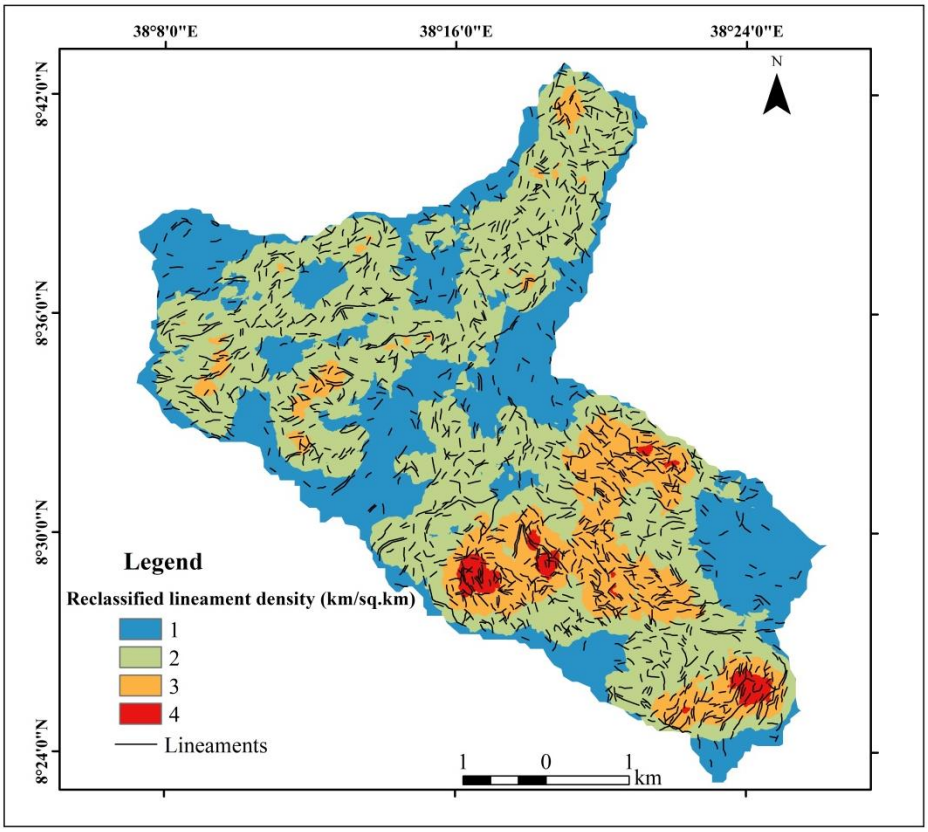


**Figure 4.8** Reclassified lineament density map

### 4.1.5 Lithology

Lithology affects groundwater and regulates the aquifer's permeability and porosity because of its conductivity and penetrability. The tarmaber megezez formation was categorized as having highly favorable groundwater potential due to its fractured and weathered condition and ranked as most suitable. Conversely, the gash megal rhyolites were assigned a very low rank due to its fine grain, consolidated and it's unfractured. Welded pyroclastic flows and partially welded pyroclastic flows both assigned a moderate ranking for groundwater potential. Additionally, the alluvium was ranked favorably due to its loose sedimentary nature and varied composition. Nonetheless, its immediate groundwater availability may be hindered compared to more porous volcanic formations. Detailed descriptions of the lithology map and its reclassified version for the study area are presented in Figures (4.9, 4.10). Furthermore, Table 4.5 provides a comprehensive classification of the lithological factors considered for mapping groundwater potential zones.

**Table 4.5** Lithology classes and its rank for GWPZ mapping

| Factors | Lithological unit | Area (ha) | Area (%) | GWPZ | Suitability rank |
|---|---|---|---|---|---|
| Lithology | Gash megal rhyolites (Ngr) | 11952.03 | 21.42 | Poor | 1 |
| | WPF(Nwp) and WPWPF (Npp) | 20586.52 | 36.90 | Moderate | 2 |
| | Alluvium (Qus) | 14004.12 | 25.10 | Good | 3 |
| | Tarmaber megezez (E3t) | 9101.37 | 16.31 | Very good | 4 |

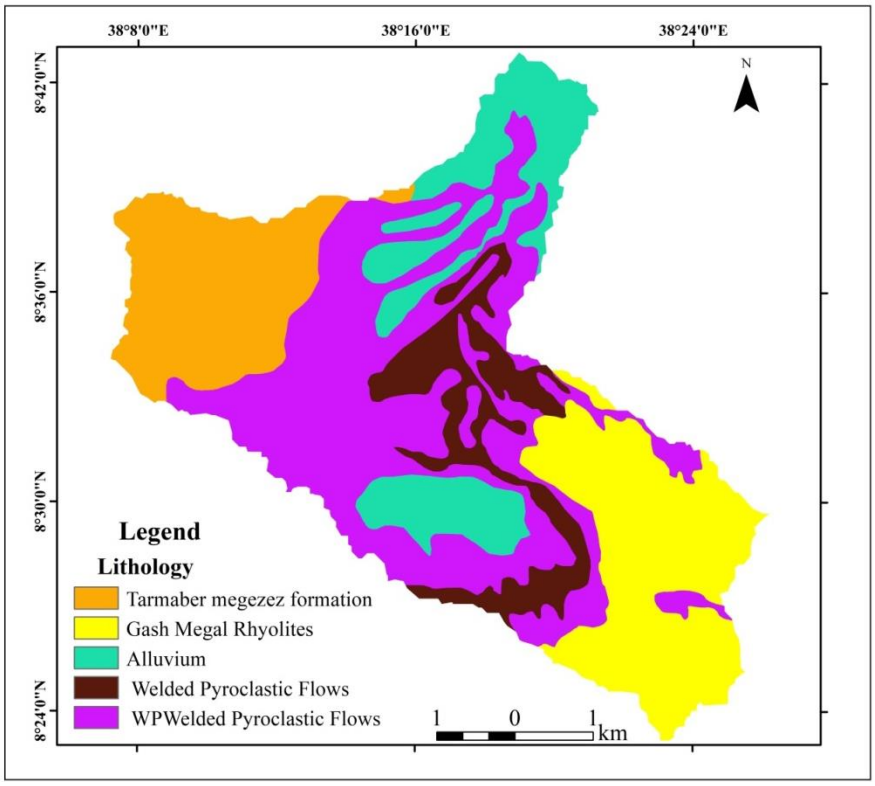


**Figure 4.9** Lithology map

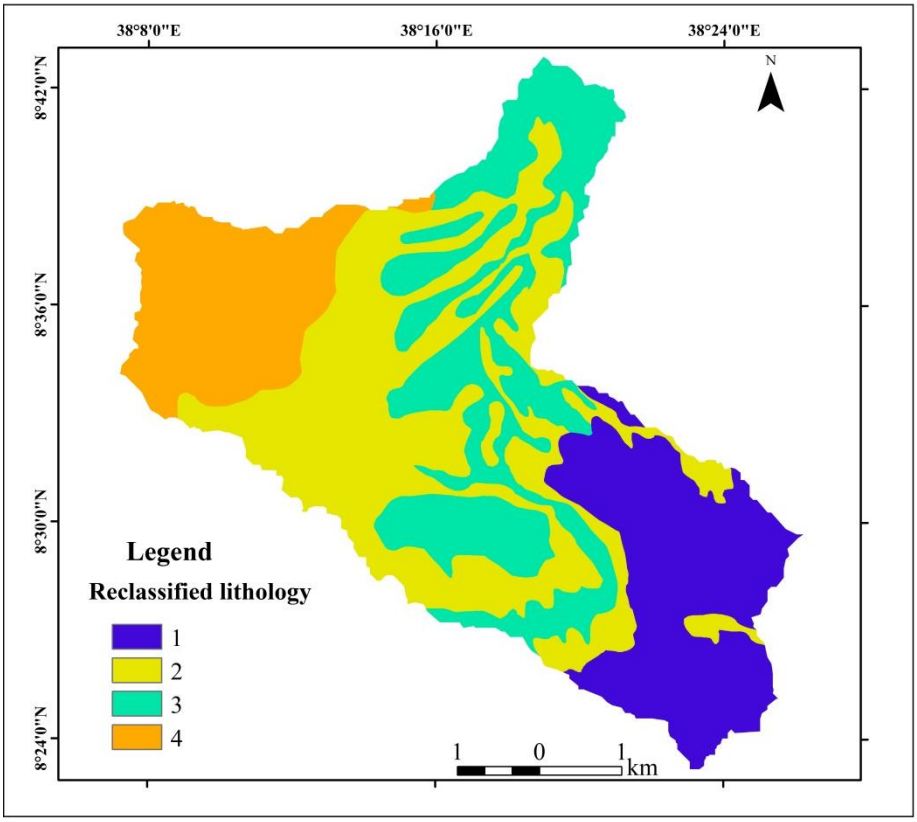


**Figure 4.10** Reclassified lithology map

### 4.1.6 Soil texture

Loam soil texture covers 8.98% (5003.23 ha) out of total area and located in southern, western and eastern parts of the catchment. Sandy clay loam covers 9.22% (5145.04 ha) of the study area. It is located in western and southeastern of the catchment's boundary. Clay soil covers 45.45% (25354.18 ha) of the catchment. This type of soil texture is located in northeastern, western and southern of the catchment. Clay loam covers 36.36% (20135.48 ha) of the total area of the catchment. It is located in southwestern, central, eastern, and southern part of the catchment. Table 4.6 describes the factors of soil texture for ground water potential zone mapping. Figures (4.11 and 4.12) indicate the soil texture and reclassified soil texture map.

**Table 4.6** Soil texture classes and its rank for GWPZ mapping

| Factors | Soil class | HSG | Area (ha) | Area (%) | GWPZ | Suitability rank |
|---|---|---|---|---|---|---|
| Soil texture | Clay | D | 25354.18 | 45.45 | Poor | 1 |
| | Sandy clay loam | C | 5145.04 | 9.22 | Moderate | 2 |
| | Clay loam | D | 20135.48 | 36.36 | Good | 3 |
| | Loam | B | 5003.23 | 8.98 | Very good | 4 |

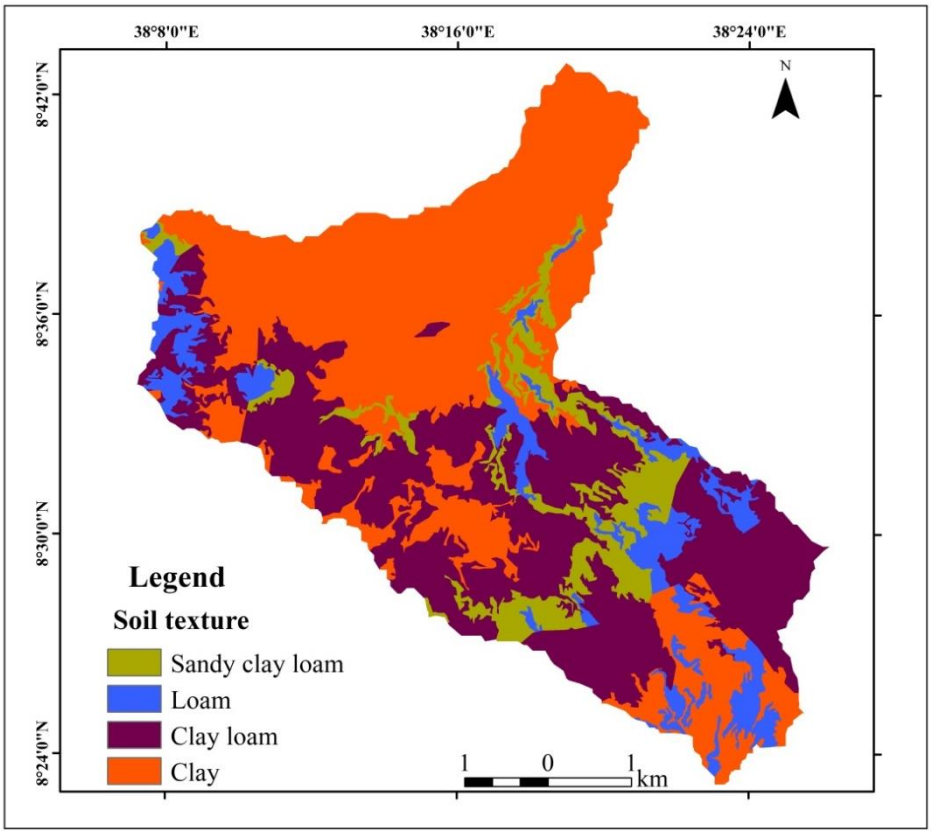


**Figure 4.11** Soil texture map

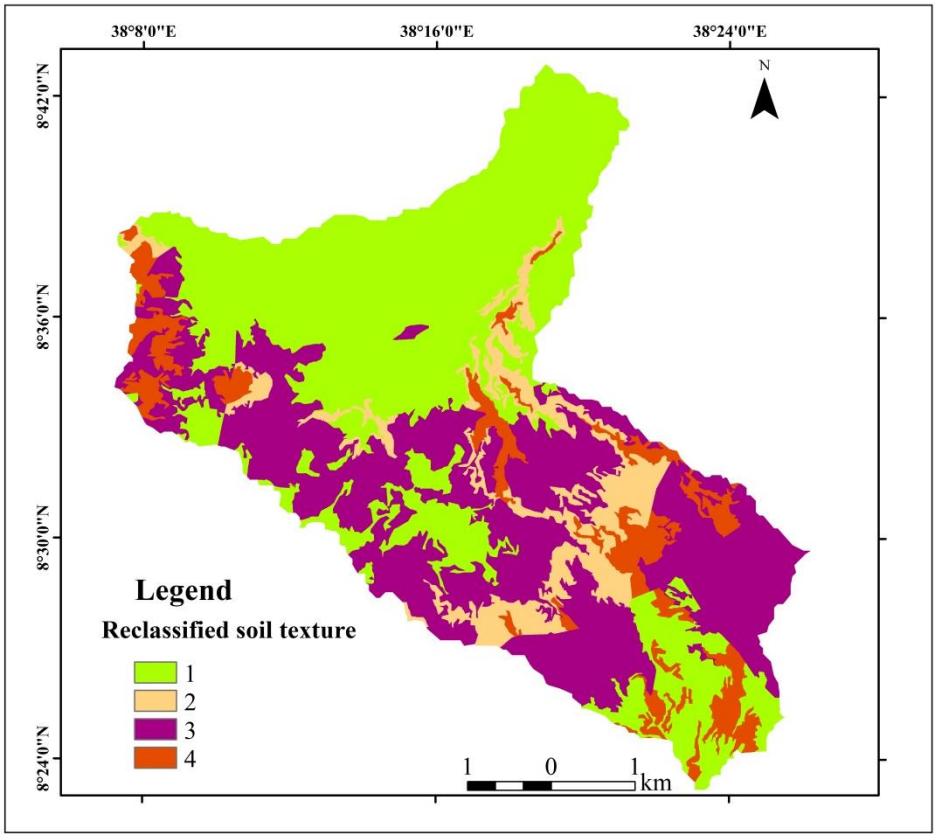


**Figure 4.12** Reclassified soil texture map

### 4.1.7 Topographic wetness index

The TWI of the study area varied from 2.29−24.3. The values were reclassified into four categories. Table 4.7 shows the details of TWI classification for GWPZ mapping. The high weights have been assigned for high TWI and vice versa, indicating a positive correlation. Greater emphasis placed on high TWI values and lesser emphasis on low TWI values. Higher TWI values correspond to areas with abundant moisture content and significant potential for aquifer replenishment. Conversely, lower TWI values indicate regions with limited moisture and reduced potential for groundwater recharge. Figures (4.13 and 4.14) describe the topographic wetness index and reclassified TWI of the catchment map.

**Table 4.7** Topographic wetness index and its suitability rank for GWPZ mapping

| Factors | TWI classes | Area (ha) | Area (%) | GWPZ | Suitability rank |
|---|---|---|---|---|---|
| TWI | 2.29–5.83 | 25854.93 | 46.34 | Poor | 1 |
| | 5.84–8.07 | 20124.24 | 36.06 | Moderate | 2 |
| | 8.08–11.5 | 7773.23 | 13.93 | Good | 3 |
| | 11.6–24.3 | 1892.91 | 3.40 | Very good | 4 |

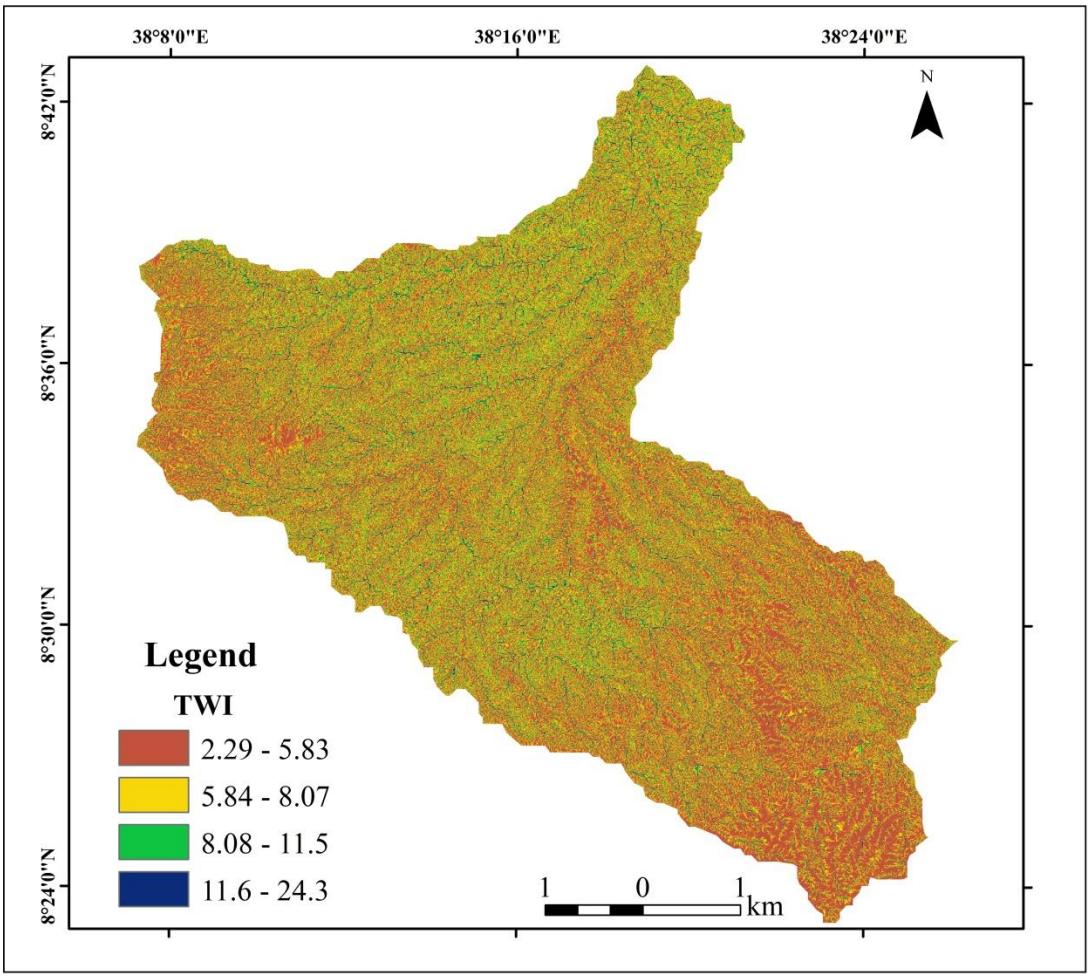


**Figure 4.13** Topographic wetness index map

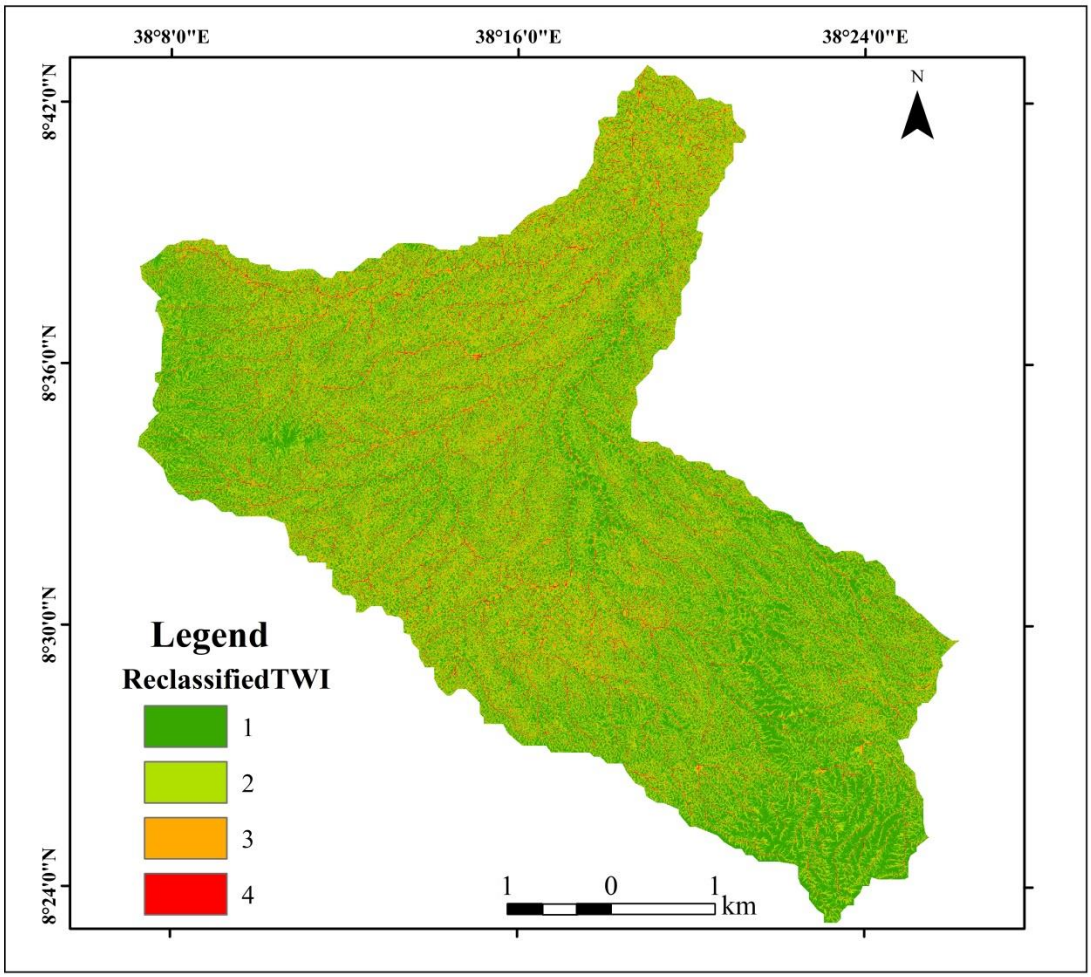


**Figure 4.14** Reclassified Topographic wetness index map

### 4.1.8 Land-use and land-cover (LULC)

The land-use and land-cover classification, illustrated in Figure 4.15, indicates that the primary land-use and land-cover in the study area consists mainly cropland with 80.41% (44870.84 ha) of the total area. Smaller extents of settlement cover 2.62% (1464.05 ha), wetland 3.16% (1762.49 ha) and vegetation covers 13.84% (7724.93 ha). Each LULC subclass is attributed different weights based on its impact on groundwater infiltration rates. Vegetation and wetland, known for their high infiltration capacity and minimal runoff, are assigned the highest weights. Settlement areas, due to their tendency for high runoff and limited infiltration, receive lower weights. Cropland areas, exhibiting favorable infiltration characteristics, are associated with higher weights. Figure 4.16 indicates the reclassified LULC map. Table 4.8 summarizes the factors considered in the LULC classification and their corresponding suitability ranks for evaluating groundwater potential zone (GWPZ).

**Table 4.8** LULC classes and its rank for GWPZ mapping

| Factors | LULC classes | GWPZ | Area (ha) | Area (%) | Suitability rank |
|---|---|---|---|---|---|
| LULC | Settlement | Poor | 1464.05 | 2.62 | 2 |
| | Cropland | Good | 44870.84 | 80.41 | 3 |
| | Vegetation | Very good | 7724.93 | 13.84 | 4 |
| | Wetland | Very good | 1762.49 | 3.16 | 4 |

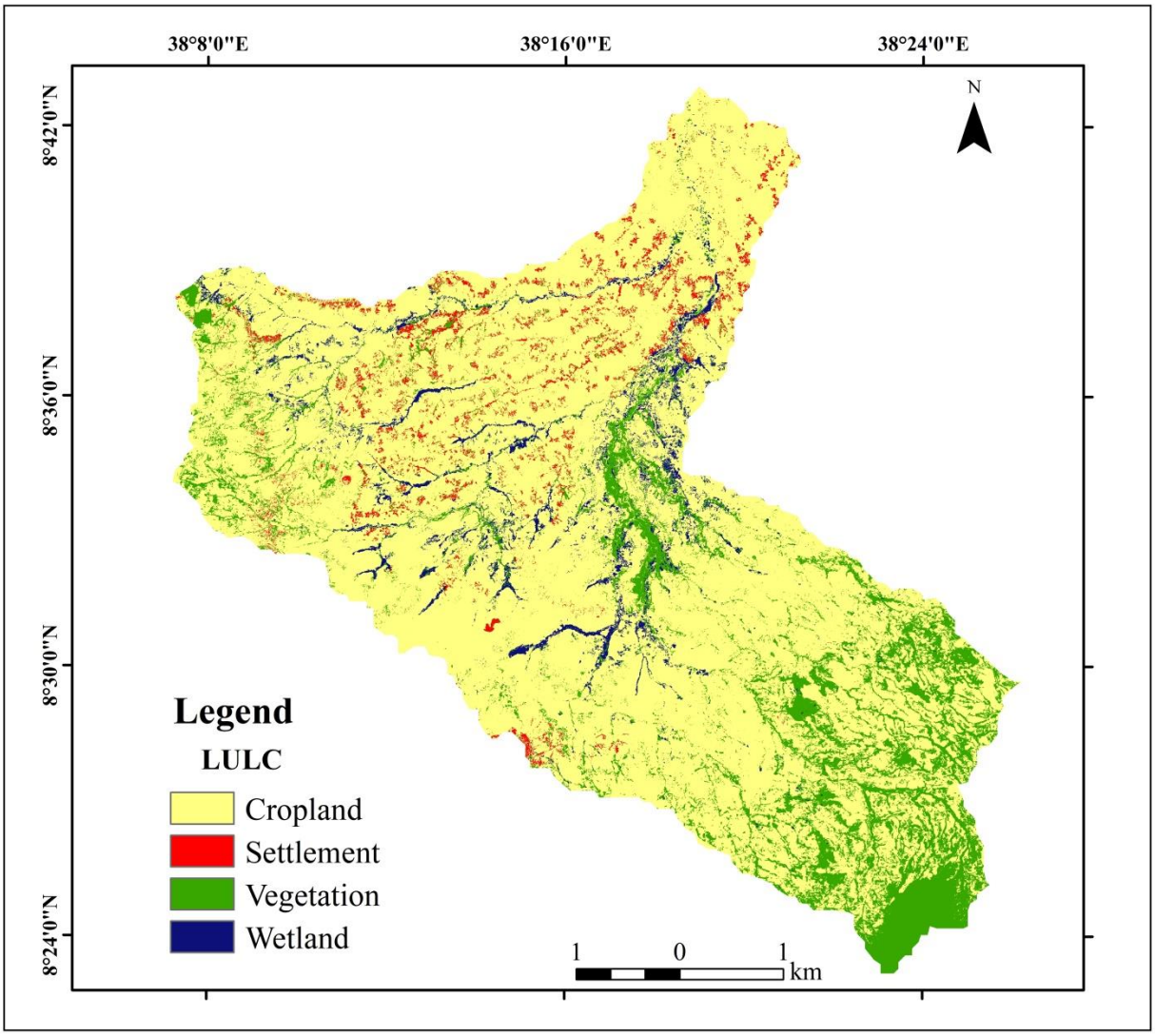


**Figure 4.15** Land-use and land-cover map

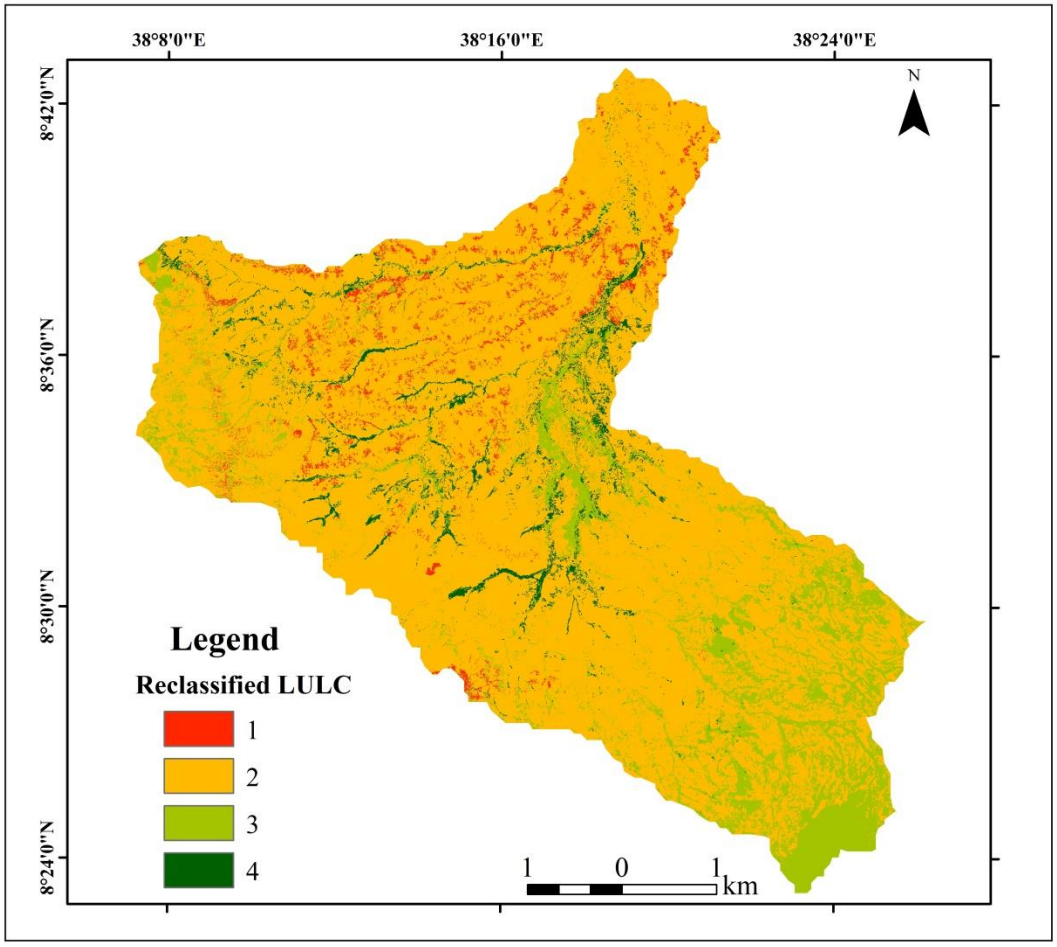


**Figure 4.16** Reclassified land-use and land-cover map

### 4.1.9 Groundwater potential zone mapping

The GWP zone map of the Teji River catchment classified in four classes: very good, good, moderate and poor category with 12.24%, 30.88%, 36.05% and 20.8% respectively. The very good groundwater potential zone has (6829.92 ha) areal coverage, it is located in northern central and southern parts of the catchment. Good GWPZ class is found in western, southwestern, eastern and central of the catchment's boundary with areal coverage of (17231.04 ha). The zone of moderate GWPZ is found in northern, eastern and north eastern parts of the study area with areal coverage (20115.89 ha). The poor GWPZ class is found in eastern, southern, western and south eastern of the catchments having areal coverage of (11611.98 ha). Among the parameter considered, lithology and rainfall were found to be the most significant with lithology having highest weight due to impact on groundwater potential zones Jhariya et al. (2021). Table 4.9 presents relative weight of GWPZ of each thematic layer and its corresponding classes. Figure 4.17 provides further details on the GWPZ final overlay result map and the GWPZ area coverage with percentage respectively. Finally, Table 4.10 displays the final overlay results of the

thematic layers for groundwater potential zone mapping.

**Table 4.9** Relative weights of thematic layer classes

| Factors | Category (class) | GWPZ | Rank | Weight |
|---|---|---|---|---|
| Rainfall | 2140−2220 | Poor | 1 | 23.8 |
| | 2230−2280 | Moderate | 2 | |
| | 2290−2350 | Good | 3 | |
| | 2360−2430 | Very good | 4 | |
| LULC | Settlement | Moderate | 2 | 11.1 |
| | Cropland | Good | 3 | |
| | Vegetation | Very good | 4 | |
| | Wetland | Very good | 4 | |
| Lithology | Gash megal rhyolites (Ngr) | Poor | 1 | 32 |
| | WPF(Nwp) and WPWPF (Npp) | Moderate | 3 | |
| | Alluvium (Qus) | Good | 3 | |
| | Tarmaber megezez formation (E3t) | Very good | 4 | |
| Soil texture | Clay | Poor | 1 | 10.5 |
| | Clay loam | Moderate | 2 | |
| | Sandy clay loam | Good | 3 | |
| | Loam | Very good | 4 | |
| Drainage density | 4.76–6 .33 | Poor | 1 | 7.7 |
| | 3.18−4.75 | Moderate | 2 | |
| | 1.59−3.17 | Good | 3 | |
| | 0−1.58 | Very good | 4 | |
| Lineament density | 0–0.9 | Poor | 1 | 4.9 |
| | 1–1.9 | Moderate | 2 | |
| | 2–2.9 | Good | 3 | |
| | 3–3.9 | Very good | 4 | |
| TWI | 2.29–5.83 | Poor | 1 | 6.7 |
| | 5.84–8.07 | Moderate | 2 | |
| | 8.08–11.5 | Good | 3 | |
| | 11.6–24.3 | Very good | 4 | |
| Slope | Very steep (18.6–48 ) | Poor | 1 | 2.7 |
| | Steep (10.3–18.5) | Moderate | 2 | |
| | Gentle (4.72–10.2) | Good | 3 | |
| | Flat (0–4.71) | Very good | 4 | |

**Table 4.10** Groundwater potential zones classes with area coverage

| GWPZ classes | Area (ha) | Area (%) | Suitability rank |
|---|---|---|---|
| Poor | 11611.98 | 20.8 | 1 |
| Moderate | 20115.89 | 36.05 | 2 |
| Good | 17231.04 | 30.88 | 3 |
| Very good | 6829.92 | 12.24 | 4 |
| Total | 55,800 | 100 | |

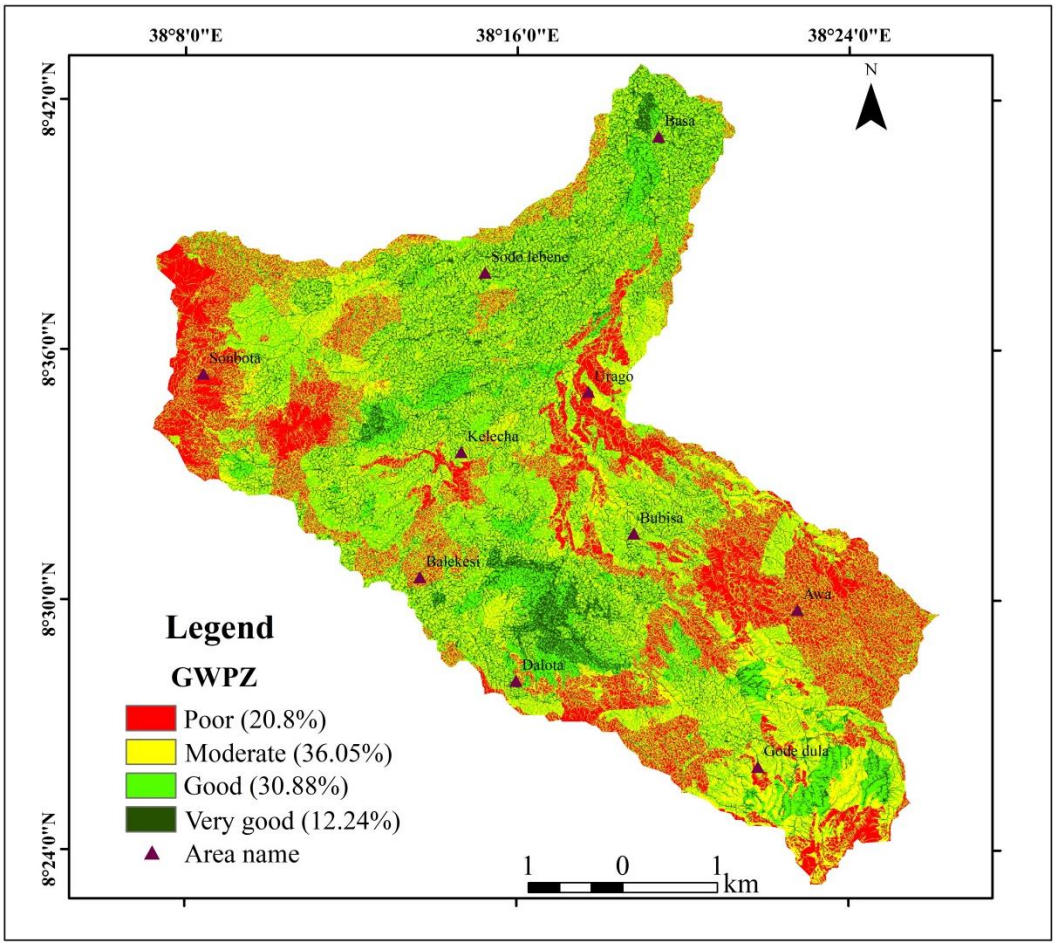


**Figure 4.17** Groundwater potential zone map

## 4.2 Validation of groundwater potential zones (GWPZs)

In scientific research, validating a model is a crucial stage. Several studies used borehole and spring data to verify the correctness of the groundwater potential zone mapping (Mukherjee and Singh, 2020).The final GWPZ map includes field data from 16 existing water points. The boreholes yield points are located in poor, moderate, good, and very good groundwater potentiality zones with percentage of 25%, 31.25%, 12.5%, and 31.25% respectively. Table 4.11 shows inventory points overlaid with the groundwater potential zones.

**Table 4.11** Inventory water points in GWPZ

| GWPZ classes | Rank | Points overlaid on the GWPZ | Percent (%) |
|---|---|---|---|
| Poor | 1 | 4 | 25 |
| Moderate | 2 | 5 | 31.25 |
| Good | 3 | 2 | 12.5 |
| Very good | 4 | 5 | 31.25 |

The precision assessment of the generated groundwater potential zone map involved rigorous cross-validation process against groundwater inventory data, as depicted in Figure 4.18. This validation

procedure was comprehensive, incorporating data from 16 strategically located groundwater wells distributed across the study area. These wells were selected to ensure representation of diverse geological characteristics, variations in land-use and land-cover types, and disparities in topographical features. Categorization of the wells was based on their borehole yield in liter per second, which was classified in to four distinct classes: (0–1l/s), (1–3 l/s), (3–6l/s), and (6–10 l/s) boreholes yields. This study utilized groundwater inventory data comprising yields from boreholes  out of the total 16 inventory data, 31.25% falls within the very good potential groundwater zone, 12.5% within the good groundwater zone, 31.25% within the moderate  yields water points surveyed, 5 with very good yield (6-10 l/s) are situated in the very good groundwater potential zones. Conversely, 4 boreholes located in a poor potential zone (<1 l/s).

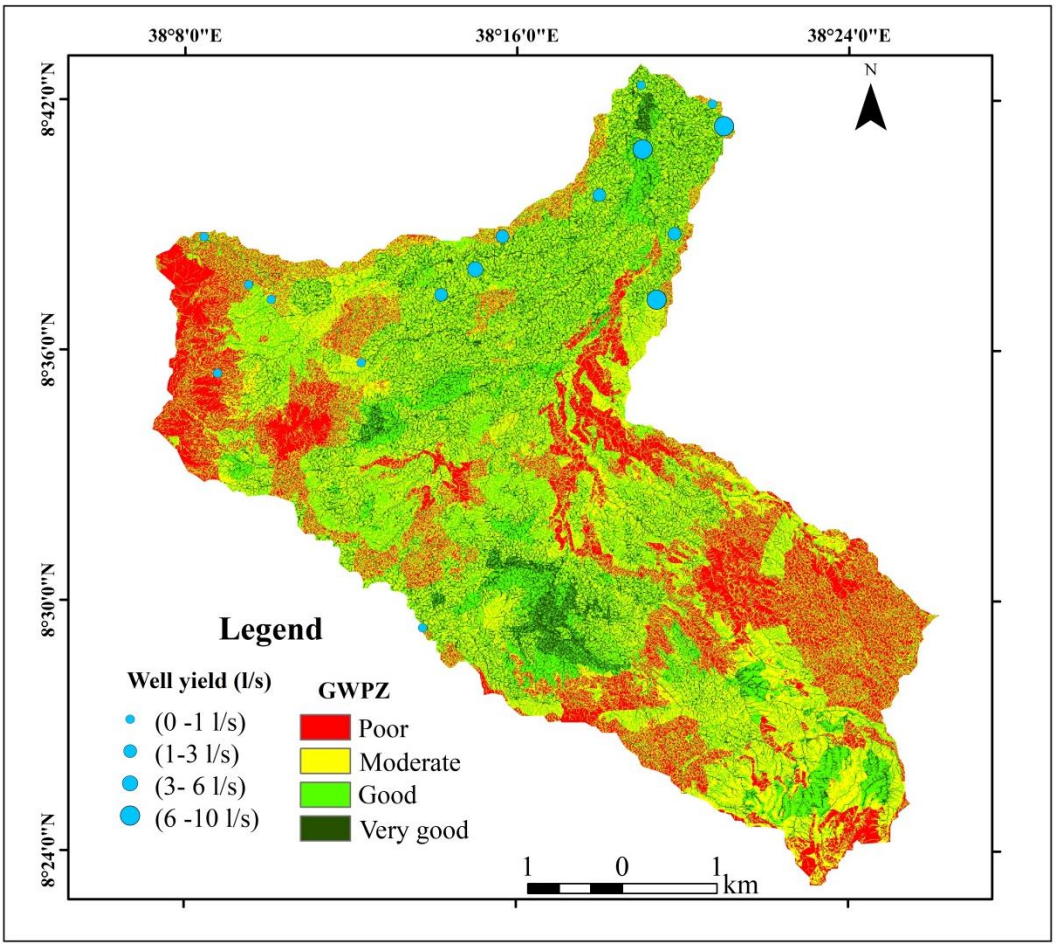


**Figure 4.18** Validation of GWPZ map using boreholes yield data

For the comparative analysis, the locations of the groundwater wells, categorized by boreholes data, were superimposed onto the groundwater potential map, as shown in Figure 4.19. The validation outcomes revealed a high degree of alignment, with approximately 81.25% of the groundwater wells' classifications accurately corresponding to the zoning depicted on the generated groundwater potential map. This

indicated strong correlation underscores the reliability and effectiveness of the GIS-based methodology employed in delineating groundwater potential zones within the study area. The groundwater potential zone of Teji river catchment was also evaluated using receiver operating characteristics (ROC) analysis, specifically by calculating the area under the curve (AUC), a common technique for measuring model accuracy (Prasad et al., 2020). In ROC analysis the AUC value indicates the model's accuracy, with an AUC of 1 representing perfect accuracy. The ROC curve graphically represents specificity (false positive) on the X-axis and sensitivity (true positive) on the Y-axis. An AUC values greater than 0.7, is considered to demonstrate acceptable discrimination and satisfactory model performance (Iqbal et al., 2024). The groundwater inventory data (water table depth) from the ECDSWC was indicates very good model performance, failing with the range of 0.8−0.9 (0.83) or 83% which present in Figure 4.19. Therefore, the model demonstrates accuracy in delineating the GWPZ of the study area.

**Table 4.12** Groundwater potential zone map validation with boreholes data.

| S/N | Well site | Easting | Northing | Depth (m) | Yield(l/s) | Location on GWPZ map | Validation remark |
|---|---|---|---|---|---|---|---|
| 1 | Keta | 424813 | 962331 | 24 | 0 | Very good | Disagree |
| 2 | Migerdi Weserbi | 427961 | 961480 | 24 | 0 | Poor | Agree |
| 3 | Mendi Tuffisa 2 | 407460 | 953526 | 36 | 0 | Poor | Agree |
| 4 | Sankale-Dawo | 414991 | 971562 | 42 | 1 | Very good | Disagree |
| 5 | Tole Belakesi | 415254 | 939047 | 47 | 0 | Poor | Agree |
| 6 | Mendi Tuffisa 1 | 408475 | 952876 | 50 | 0 | Moderate | Disagree |
| 7 | Kilinto | 412826 | 949736 | 50 | 0 | Poor | Agree |
| 8 | Tajab-Dawo | 411878 | 965587 | 56 | 3.5 | Very good | Agree |
| 9 | Maru Sambo | 402350 | 951544 | 60 | 0.18 | Moderate | Agree |
| 10 | Kata Ensilale | 422468 | 966195 | 60 | 2 | Moderate | Agree |
| 11 | Bogi Gefere | 410362 | 964468 | 69.75 | 1 | Moderate | Agree |
| 12 | Areda Leka | 424000 | 952736 | 112 | 10 | Very good | Agree |
| 13 | Tole Megridi | 429000 | 960500 | 128 | 6.2 | Very good | Agree |
| 14 | Basa | 427126 | 971361 | 308 | 9.2 | Good | Agree |
| 15 | Kursiti Arada | 426873 | 970945 | 402 | 2.21 | Moderate | Agree |
| 16 | Senbero | 426362 | 969316 | 420 | 2.34 | Good | Agree |

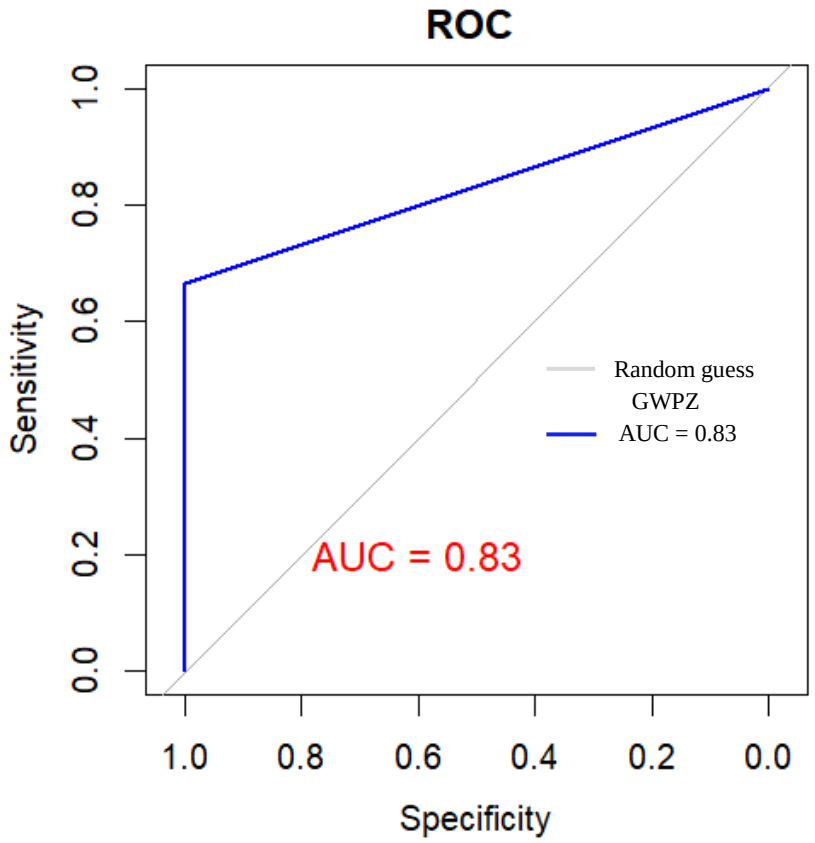


**Figure 4.19** Receiver operating curve (ROC)

### 4.3 Discussion

The groundwater potential zone map within the Teji River catchment area revealed distinct zones with varying suitability for groundwater extraction and management. Notably, a very good potential zone, encompassing 12.24% (6829.92 ha) out of the total area, was identified in the western regions. The zones of very good groundwater potentiality are controlled by diverse factors such as areas of highest annual rainfall, with the presence of tarmaber megezez formation lithology group, vegetation and wetland area of LULC classes, flat nature of the slope class, loam soil texture type, maximum topographic wetness index value, low drainage density and high lineament density of the catchment system (Bhowmick et al., 2023). Additionally, a substantial good groundwater potential zone covering 30.88% (17231.04 ha) was observed in southwestern, western and eastern parts of the study area. This zone was prevailed with the existence of good rainfall area, covered with areas of alluvium lithology group, area with cropland of LULC class, a gentle slope class, clay loam soil texture type, areas of good lineament density and good drainage density (Badamasi et al., 2016). Moderate groundwater potential zone of the study area covering 36.05% (20115.89 ha) primarily concentrated in the northern, eastern, south eastern and western part parts of the

catchment. This zone was experienced with moderate annual rainfall, the existence of settlement land use land cover type, welded to partially welded pyroclastic flows lithology group, sandy clay loam soil texture, moderate topographic wetness index value, moderate lineament density and high drainage density. Moreover, the eastern and southern regions of the catchment displayed characteristics of poor groundwater potential 20.8% (11611.98 ha) of the total area. These findings also align with other researchers conducted in different temporal and spatial scale (Opoku et al., 2024; Seifu et al., 2022). The zone of poor groundwater potential zone was as a result of factors such as poor annual rainfall distribution, gash megal rhyolites lithology group, clay textural soil type, poor lineament density and very highly drainage density, poor topographic wetness index value and very steep slope class. These zones are not favorable for groundwater potential zone (Doke et al., 2021). The analysis highlights the significant influence of lithology and rainfall on groundwater occurrence within the area. The GWPZ map reviled that substantial groundwater potential found in moderate to good groundwater potential zones account (43.12%) out of the total study area. Geomorphic features such as slope, drainage density and topographic wetness index were found to have minimal impact due to the terrain's relatively flat nature. Geological succession emerged as a key determinant of groundwater occurrence, with areas characterized by formations like tarmaber megezez formation, alluvium and welded to partially welded pyroclastic flow zones exhibiting a very good to good potential for groundwater. Soil texture played a crucial role in controlling groundwater potential by affecting percolation rates and water retention capacities. In this study area, clay soil texture, comprising 45.45% of the soil composition, was predominant. Notably, clay soil was prevalent in areas exhibiting poor groundwater potential, attributed to heightened runoff and diminished groundwater retention capacities.

The validation processes results revealed a strong agreement between the classifications of groundwater boreholes and the zones portrayed on the groundwater potential map, with agreement between rates of approximately 81.25%. This significance agreement highlights the dependability and usefulness of remote sensing and GIS methods employed in delineating groundwater potential zones. The AUC result of 0.83 (83%) clearly demonstrate the high accuracy of the predicted model, highlighting the very god performance of the GWPZ model. The ROC analysis confirms this, showing high level of precision in distinguish between true positive and false positive. These findings not only support the usefulness of these techniques but also emphasize their practical implication for groundwater resource management and exploration initiatives.

# CHAPTER FIVE

# CONCLUSION AND RECOMMENDATIONS

## 5.1 Conclusion

The global demand for water is on the rise, due to increase population, expanding industrialization, and agricultural activities. Groundwater stands as the only water resource vital for sustaining agricultural activities and various essential processes reliant on water. Through the utilization of analytical hierarchy process (AHP)-based remote sensing (RS) and geographic information systems (GIS) approach the geographic distribution of groundwater potential zones (GWPZs) has been meticulously determined, incorporating eight thematic layers including, lithology, rainfall, land-use and land-cover, soil texture, lineament density, topographic wetness index, slope and drainage density. The multi-criteria decision analysis method (MCDAM) has facilitated the combination of multiple groundwater affecting factors to address spatial complexities. Following an extensive literature review, relative weights were assigned to select parameters through the creation of AHP pairwise comparison matrix. Consequently, lithology and rainfall emerged as the most significant factors, accounting for 32% and 23.8% of the weight respectively. Additionally, moderate weightings assigned for LULC, soil texture and drainage density 11.1%, 10.5%, 7.7% respectively. Law weightage assigned for topographic wetness index, lineament density and slope having the weights of 6.7%, 4.9%, and 2.7% respectively. Subsequently through the normalization of the pairwise comparison matrix, the weights were redistributed, yielding a computed consistency ratio of 0.08. This value (0.08) falls within an acceptable range for further analysis, signifying the consistency of the objective judgment employed in assigning relative weights to criteria impacting groundwater potentiality. In Teji River catchment, the research delineated four distinct classes of ground water potential zones: poor, moderate, good and very good. The proportion of poor, moderate, good and very good groundwater potential zones were identified as 20.8% (11611.98 ha), 36.05% (20115.89 ha), 30.88 % (17231.04 ha), and 12.24% (6829.92 ha), respectively. These findings underscore the imperative for stakeholders to take decisive action in groundwater management and sustainable exploitation. Moreover, the study suggests prioritization groundwater sustainability techniques in areas sharing similar climatic and geographic characteristics. The integration of GIS and RS methods emerged as highly advantageous and resource efficient approach for GWPZ. The AHP within the framework of MCDAM emerged as the optimal decision-making tool, effectively managing qualitative and quantitative multi-criteria factors. Similar methodologies are recommended for delineating groundwater potential zones in data-scarce and challenging terrains. Furthermore, the establishment of purposeful testing wells and field geophysical

investigations in potential well-drilling location is advised to enhance effective groundwater management possibilities.

### 5.2 Recommendations

Based on the findings and conclusions, the following recommendations are proposed:

- Utilize appropriate techniques for identifying groundwater potential zones in complex areas.
- Conduct field geophysical investigations at potential well drilling sites for additional validation and assessment.
- Implement comprehensive water management strategies, including conservation measures and sustainable practices, to mitigate the increasing demand for water resources and ensure their long-term availability for both current and future generations.
- Promote rainwater harvesting techniques at both individual and community levels to supplement groundwater resources, especially during periods of low rainfall or drought.
- Conduct educational campaigns to raise awareness about the importance groundwater conservation and sustainable usage practice among local communities, schools, and industries.
- Integrate groundwater considerations into land-use planning and development regulations to minimize impacts on recharge areas and vulnerable aquifers.
- Invest research and development initiatives to explore innovative technologies and approaches for groundwater recharge, such as artificial recharge techniques or managed aquifer recharge systems.
- Foster collaboration with neighboring regions or countries to address trans-boundary groundwater issue and develop joint management strategies for shared aquifers.
- Develop and enforce robust legislative frameworks and regulations for groundwater management, including license and monitoring requirements for well drilling, pollution prevention measures, and penalties for illegal extraction or contamination.
- Explore the use of economic instruments, such as water pricing mechanisms or groundwater extraction fees, to incentivize efficient water use and generate revenue for conservation efforts.

**References**


Abay, A. G., & Gebrekidan, H. (2022). Hydrogeological characterization and groundwater potential assessment of the Gilgel Abay basin, northwestern Ethiopia. *Journal of African Earth Sciences*, 192, 104599.

Abdi, A. B., & Abebe, B. K. (2022). Identification of Groundwater Potential Sites in the Drought-Prone Area Using Geospatial Techniques at Fafen-Jerer Sub-Basin, Ethiopia. *Geospatial Information Science*, *14*(4), 490-506.

Abe, M. W., & Ersado, A. E. (2022). Assessment of Ground Water Potential Zone based on Multi-Criteria Decision making model and Geospatial Techniques: The case of Lemo Woreda and Hossana town, Hadiya Zone, Southern Nation Nationalities.

Abdul-Ganiyu, S., & Prosper, K. (2021). Estimating the groundwater storage for future irrigation schemes. *Water Supply*, *21*(5), 2202-2216.

Achu, A. L., Thomas, J., & Reghunath, R. (2020). Multi-criteria decision analysis for delineation of groundwater potential zones in a tropical river basin using remote sensing, GIS and analytical hierarchy process (AHP). *Groundwater for Sustainable Development*, *10*, 100365.

Adem, A. A., & Gebregziabher, Z. (2021). Analysis of Soil Types and Their Suitability for Crop Production in Becho District, Ethiopia. *Journal of Agricultural Science and Technology*, 11(4), 231-242.

Agarwal R, Garg PK (2016) Remote sensing and GIS based groundwater potential & recharge zones mapping using multi-criteria decision making technique. *Water Resour Manag 30*(1):243–260. https:// doi. org/ 10. 1007/ s11269- 015- 1159-8

Ahmed, M., Chen, Y., & Khalil, M. M. (2022). Isotopic composition of groundwater resources in arid environments. *Journal of Hydrology*, *609*, 127773.

Aju, C. D., Achu, A. L., Prakash, P., Reghunath, R., & Raicy, M. C. (2023). An integrated groundwater resource management approach for sustainable development in a tropical river basin, southern India. *Environmental Monitoring and Assessment*, *195*(9), 1129.

Akhtar, N., Syakir, M. I., Anees, M. T., Qadir, A., & Yusuff, M. S. (2020). Characteristics and assessment of groundwater. *Groundwater management and resources*.

Al-Adamat, R., Al-Ma'aitah, A., & Al-Hadad, S. (2022). Multi-criteria decision analysis for mapping groundwater potential zones: A case study in the Yarmouk River Basin, Jordan. *Journal of Hydrology*, 606, 127491.

Aliabad, A. H., Pourghasemi, H. R., Pradhan, B., Gokceoglu, C., & Motevalli, A. (2018). Groundwater potential mapping at Kurdistan region of Iran using analytic hierarchy process and GIS. *Earth Science Informatics, 11*(2), 231-245.

Allafta, H., Opp, C., & Patra, S. (2020). Identification of groundwater potential zones using remote sensing and GIS techniques: a case study of the Shatt Al-Arab Basin. *Remote Sensing*, *13*(1), 112.

Al-Shafie, W. M., Mukhlis, W. Z. W., & Abdullah, N. A. B. (2021). GIS-Based groundwater potential mapping: A review of applications and challenges. *Geosciences*, 11(3), 130.

Andualem, T. G., & Demeke, G. G. (2019). Groundwater potential assessment using GIS and remote sensing: A case study of Guna tana landscape, upper blue Nile Basin, Ethiopia. *Journal of Hydrology: Regional Studies*, *24*, 100610.

Assegide, E., Alamirew, T., Bayabil, H., Dile, Y. T., Tessema, B., & Zeleke, G. (2022). Impacts of surface water quality in the Awash River Basin, Ethiopia: A systematic review. *Frontiers in Water*, *3*, 790900.

Ayenew, B., & Tadesse, T. (2014). Land suitability evaluation for surface irrigation using spatial multi-criteria analysis: The case of Gilgel Abay watershed, northwestern Ethiopia. *Water Resources Management*, 28(12), 4467-4483.

Bain, R., Cronk, R., Wright, J., Yang, H., Slaymaker, T., & Bartram, J. (2014). Fecal contamination of drinking-water in low-and middle-income countries: a systematic review and meta-analysis. PLoS medicine, 11(5), e1001644.

Barua S, Mukhopadhyay BP, Bera A (2021) Integrated assessment of groundwater potential zone under agricultural dominated areas in the western part of Dakshin Dinajpur district, West Bengal, India. Arab J Geosci 14:1042. https:// doi. org/ 10. 1007/ s12517- 021- 07312-y

Berhanu, B., Melesse, A. M., & Seleshi, Y. (2013). GIS-based hydrological zones and soil geo-database of Ethiopia. *Catena*, *104*, 21-31.

Badamasi, S., Sawa, B. A., & Garba, M. L. (2016). Groundwater potential zones mapping using remote sensing and geographic information system techniques (GIS) in Zaria, Kaduna State, Nigeria. *Am Sci Res J Eng Technol Sci*, *24*(1), 51-62

Bhowmick, A., Yate, T. A., Shanka, A. S., Sandhar, B. S., Chaturvedi, S. K., & Ojha, J. R. (2023). Delineation of Ground Water Prospect Zones of Mojo Watershed, Ethiopia, East Africa, Using GIS, Remote Sensing and Analytical Hierarchy Process. *Journal of the Indian Society of Remote Sensing*, *51*(11), 2265-2283.

Bhunia, G. S. (2020). An approach to demarcate groundwater recharge potential zone using geospatial technology. *Applied Water Science*, *10*(6), 1-12.

Chakraborty, S., Sarkar, K., Chakraborty, S., Ojha, A., Banik, A., Chatterjee, A., ... & Das, M. (2021). Assessment of the surface water quality improvement during pandemic lockdown in ecologically stressed Hooghly River (Ganges) Estuary, West Bengal, India. *Marine pollution bulletin*, *171*, 112711.

Chitsazan, N., Sadeghian, S., & Mirbagheri, S. A. (2021). Integration of remote sensing, GIS, and MCDM for groundwater potential mapping in a semi-arid region. *Environmental Monitoring and Assessment*, 193(8), 501

Choudhary, S., Pingale, S. M., & Khare, D. (2022). Delineation of groundwater potential zones of upper Godavari sub-basin of India using bi-variate, MCDM and advanced machine learning algorithms. *Geocarto International*, *37*(27), 15063-15093.

Das, I., Kar, A., & Paul, S. K. (2020). Multi-criteria decision-making for groundwater potential zone delineation: A case study in the Birbhum district, West Bengal, India. *Groundwater for Sustainable Development*, 10, 100317.

Desta, F. B., Teshome, T. A., & Hailu, G. (2022). Delineation of groundwater potential zones using GIS and remote sensing techniques in the Upper Blue Nile River Basin, Ethiopia. *Environmental Earth Sciences*, *81*(10), 1-16.

Dhinsa, D., Tamiru, F., & Tadesa, B. (2022). Groundwater potential zonation using VES and GIS techniques: A case study of Weserbi Guto catchment in Sululta, Oromia, Ethiopia. Heliyon, 8(8), e10245. https://doi.org/10.1016/j.heliyon.2022.e10245

Dinka, M. A., & Abebe, B. K. (2021). Groundwater Potential Zone Mapping Using GIS and Remote Sensing Techniques in the Jamma River Basin, Southwestern Ethiopia. *Environmental Earth Sciences*, 80(12), 1-14.

Doke, A. B., Zolekar, R. B., Patel, H., & Das, S. (2021). Geospatial mapping of groundwater potential zones using multi-criteria decision-making AHP approach in a hardrock basaltic terrain in India. *Ecological Indicators*, *127*, 107685.

Focazio, M. J., et al. (2021). Groundwater contamination by hydraulic fracturing: Recent discoveries and remediation. Science Advances, 7(35), eabf8765.

Gebrehiwot, T. (2020). The Relationship between Soil Types and Vegetation in Ethiopia. Climate, 8(6), 123.

Gebrie, A. T., Mulatu, K., Girum, G. D., Guna, H., Dar, I. A., Bao, P. Q., & Yamada, T. J. (2021). Grand Ethiopian Renaissance Dam and hydrologic hegemony over Abbay Basin. Sustainable *Water Resources Management*, 7(6).

Geological Survey of Ethiopia (2010). Geology of the Akaki-beseka area.

Girma, A., & Abebe, B. K. (2021). Groundwater Potential Zone Mapping Using GIS and Remote Sensing Techniques in the Gilgel Abay River Basin, Upper Blue Nile Basin, Ethiopia. *Environmental Monitoring and Assessment*, 193(10), 1-18.

Gleeson, T., Befus, K. M., Jasechko, S., Luijendijk, E., & Cardenas, M. B. (2016). The global volume and distribution of modern groundwater. *Nature Geoscience*, 9(2), 161-167.

Gupta, S., Jain, M. K., & Jain, M. K. (2019). Integration of remote sensing and GIS for groundwater potential zone mapping in parts of Deoria District, Uttar Pradesh, India. *Applied Water Science*, 9(6), 130.

Guru, S., Yomralioglu, T., & Reis, S. (2017). A geographic information system-based comparative analysis of landslide susceptibility maps produced using logistic regression, multi-criteria decision analysis, and artificial neural networks: A case study from Kat landslides (Tokat—Turkey). *Environmental Earth Sciences*, 76(15), 523.

Gyeltshen, S., Tran, T. V., Teja Gunda, G. K., Kannaujiya, S., Chatterjee, R. S., & Champatiray, P. K. (2020). Groundwater potential zones using a combination of geospatial technology and geophysical approach: case study in Dehradun, India. *Hydrological sciences journal*, *65*(2), 169-182.

Hamdani, N., & Baali, A. (2020). Characterization of groundwater potential zones using analytic hierarchy process and integrated geomatic techniques in Central Middle Atlas (Morocco). *Applied Geomatics*, *12*(3), 323-335.

Hussein, A.-A., Govindu, V., & Nigusse, A. G. M. (2017). Evaluation of groundwater potential using geospatial techniques. *Applied Water Science*, *7*, 2447-2461.

Ifediegwu, S. I., Nnebedum, D. O., & Nwatarali, A. N. (2019). Identification of groundwater potential zones in the hard and soft rock terrains of Kogi State, North Central Nigeria: an integrated GIS and remote sensing techniques. *SN Applied Sciences*, *1*, 1-15.

Igwe, O., Ifediegwu, S. I., & Onwuka, O. S. (2022). Determining the occurrence of potential groundwater zones using integrated hydro-geomorphic parameters, GIS and remote sensing in Enugu State, Southeastern, Nigeria. *Sustainable Water Resources Management*, *6*, 1-14.

Iqbal, M., & Ganaie, D. B. (2024). Groundwater potential assessment using analytical hierarchy-driven geospatial techniques: Baramulla, Kashmir valley, India. *Sustainable Water Resources Management*, *10*(1), 19.

Jhariya, D. C., Khan, R., Mondal, K. C., Kumar, T., K, I., & Singh, V. K. (2021). Assessment of groundwater potential zone using GIS-based multi-influencing factor (MIF), multi-criteria decision analysis (MCDA) and electrical resistivity survey techniques in Raipur city, Chhattisgarh, India. *AQUA—Water Infrastructure, Ecosystems and Society*, *70*(3), 375-400.

Kabeto, J., Adeba, D., Regasa, M. S., & Leta, M. K. (2022). Groundwater Potential Assessment Using GIS and Remote Sensing Techniques: Case Study of West Arsi Zone, Ethiopia. Water, 14(12), 1838.

Kanagaraj, G., Suganthi, S., Elango, L., & Magesh, N. (2019). Assessment of groundwater potential zones in Vellore district, Tamil Nadu, India using geospatial techniques. *Earth Science Informatics*, *12*, 211-223.

Kordestani, M. D., Naghibi, S. A., Hashemi, H., Ahmadi, K., Kalantar, B., & Pradhan, B. (2019). Groundwater potential mapping using a novel data-mining ensemble model. *Hydrogeology journal*.

Kumar, M., Nema, M. K., & Pant, R. (2018). Integration of LiDAR data and GIS for groundwater potential mapping and its sustainability analysis in parts of Central India. *Sustainable Water Resources Management*, 4(3), 653-664.

Kumar N, Singh SK (2021) Soil erosion assessment using earth observation data in a trans-boundary river basin. Nat Hazards 107(1):1–34. https:// doi. org/ 10. 1007/ s11069- 021- 04571-6

Lawal, A., Tijani, M. N., Snow, D., & D'Alessio, M. (2023). Quality and hydrochemical assessment of groundwater in geological transition zones: a case study from NE Nigeria. *Environmental Science and Pollution Research*, *30*(4), 10643-10663.

Lee, S., Hyun, Y., Lee, S., & Lee, M.-J. (2020). Groundwater potential mapping using remote sensing and GIS-based machine learning techniques. *Remote Sensing*, *12*(7), 1200.

Lentswe, G. B., & Molwalefhe, L. (2020). Delineation of potential groundwater recharge zones using analytic hierarchy process-guided GIS in the semi-arid Motloutse watershed, eastern Botswana. *Journal of Hydrology: Regional Studies*, *28*, 100674.

Manap MA, Sulaiman WNA, Ramli MF, Pradhan B, Surip N (2011) A knowledge-driven GIS modeling technique for groundwater potential mapping at the Upper Langat basin, Malaysia. Arab J Geosci 6:1621–1637. https:// doi. org/ 10. 1007/ s12517- 011- 0469-2

Mathewos, Y., Abate, B., Dadi, M., & Mathewos, M. (2024). Evaluation of the groundwater prospective zone by coupling hydro-meteorological and geospatial evidence in Wabe River Catchment Omo Gibe River Basin, Ethiopia. *Water Cycle*.

Maity, B., Mallick, S. K., Das, P., & Rudra, S. (2022). Comparative analysis of groundwater potentiality zone using fuzzy AHP, frequency ratio and Bayesian weights of evidence methods. *Applied Water Science*, *12*(4), 63.

Maity, B., Mallick, S. K., Das, P., & Rudra, S. (2022). Comparative analysis of groundwater potentiality zone using fuzzy AHP, frequency ratio and Bayesian weights of evidence methods. *Applied Water Science*, *12*(4), 63.

Mokarram, M., Roshan, G., & Negahban, S. (2015). Landform classification using topography position index (case study: salt dome of Korsia-Darab plain, Iran). *Modeling Earth Systems and Environment*, 1, 1-7.

Mukherjee, I., and Singh, U.K., (2020). Delineation of groundwater potential zones in a drought-prone semi-arid region of east India using GIS and analytical hierarchical process techniques. Catena, 194, 104681.

Nanesso, D. A., & Habtemariam, D. N. Identification of Groundwater Potential Zones Using Geospatial Technologies in Meki Catchment, Ethiopia.

National Meteorological Agency of Ethiopia (2023). Rainfall data for Teji River catchment

Neumann, R. B., et al. (2020). Groundwater quality trends in the United States (2002–2017): Insights from nutrient monitoring. *Environmental Science & Technology*, 54(13), 8015-8026.

Nigussie, W., Hailu, B. T., & Azagegn, T. (2019). Mapping of groundwater potential zones using sentinel satellites (− 1 SAR and-2A MSI) images and analytical hierarchy process in Ketar watershed, Main Ethiopian Rift. *Journal of African Earth Sciences*, *160*, 103632.

Oladunni, O. O. (2020). Assessment of Groundwater Potential Using Remote Sensing and GIS Techniques in Ekiti State, Southwestern Nigeria. *Groundwater*, 58(6),

Opoku, P. A., Shu, L., & Amoako-Nimako, G. K. (2024). Assessment of Groundwater Potential Zones by Integrating Hydrogeological Data, Geographic Information Systems, Remote Sensing, and Analytical Hierarchical Process Techniques in the Jinan Karst Spring Basin of China. *Water*, *16*(4), 566.

Organization, W. H. (2021). Progress on household drinking water, sanitation and hygiene 2000-2020: five years into the SDGs.

Ouedraogo, I., Girard, A., Vanclooster, M., & Jonard, F. (2020). Modelling the temporal dynamics of groundwater pollution risks at the African scale. *Water*, 12(5), 1406.

Pandey, A. K., Singh, V. P., & Kumar, S. (2021). Mapping soil moisture using Sentinel-2A data in the semi-arid region of Bundelkhand, India. *Geomatics and Natural Hazards*, 99, e00559.

Pathak, A. A., & Dodamani, B. (2019). Trend analysis of groundwater levels and assessment of regional groundwater drought: Ghataprabha River Basin, India. *Natural Resources Research*, *28*, 631-643.

Prasad, P., Loveson, V. J., Kotha, M., & Yadav, R. (2020). Application of machine learning techniques in groundwater potential mapping along the west coast of India. *GIScience & Remote Sensing*, *57*(6), 735-752.

Rao, N. S., Gugulothu, S., & Das, R. (2022). Deciphering artificial groundwater recharge suitability zones in the agricultural area of a river basin in Andhra Pradesh, India using geospatial techniques and analytical hierarchical process method. *Catena*, *212*, 106085.

Saaty, T. L. (1980). The analytic hierarchy process: Planning, priority setting, resource allocation. McGraw-Hill.

Scanlon, B. R., Faunt, C. C., Longuevergne, L., Reedy, R. C., Alley, W. M., McGuire, V. L., & McMahon, P. B. (2012). Groundwater depletion and sustainability of irrigation in the US High Plains and Central Valley. *Proceedings of the national academy of sciences*, 109(24), 9320-9325.

Seifu, D., Teshome, T. A., & Hailu, G. (2022). Assessment of groundwater recharge potential zone by using GIS and remote sensing techniques in Ziway Abijata sub-basin, Central Rift Valley of Ethiopia. *Water Supply*, 22(6), 2741-2753.

Seifu, T. K., Ayenew, T., Woldesenbet, T. A., & Alemayehu, T. (2022). Identification of groundwater potential sites in the drought-prone area using geospatial techniques at Fafen-Jerer sub-basin, Ethiopia. *Geology, Ecology, and Landscapes*, 1-13.

Setegn, G. (2022). Wind Speed and Relative Humidity in Becho District: Implications for Agriculture and Human Health. *Journal of Agricultural and Environmental Sciences*, *11*(2), 12-18.

Schoener, G. (2018). Urban runoff in the US Southwest: Importance of impervious surfaces for small-storm hydrology. *Journal of Hydrologic Engineering*, *23*(2), 05017033.

Schoener, G., & Stone, M. C. (2019). Impact of antecedent soil moisture on runoff from a semiarid catchment. *Journal of Hydrology*, *569*, 627-636.

Sharma, A., Tyagi, A., & Gupta, A. (2020). Groundwater potential zone mapping using remote sensing and GIS: A case study of Kosi River Basin, India. *Groundwater for Sustainable Development*, 11, 100404.

Singh, C. K., Al-Ansari, N., & Al-Khafaji, A. W. (2020). GIS-based groundwater potential mapping in the Al-Kifl-Qadisiya district, Iraq. *Geocarto International*, 35(3), 248-266.

Taylor, R. G., Scanlon, B., Döll, P., Rodell, M., Van Beek, R., Wada, Y., Longuevergne, L., Leblanc, M., Famiglietti, J. S., & Edmunds, M. (2013). Ground water and climate change. *Nature climate change*, *3*(4), 322-329.

Thapa, R., Gupta, S., Guin, S., & Kaur, H. (2017). Assessment of groundwater potential zones using multi-influencing factor (MIF) and GIS: a case study from Birbhum district, West Bengal. *Applied Water Science*, *7*, 4117-4131.

Teshome, T. A., Hailu, G., & Desta, F. B. (2020). Assessment of groundwater potential zones using integrated GIS and remote sensing techniques in Sekota Wereda, Northern Ethiopia. AAU Institutional Repository.

Tilahun, A., & Adem, A. A. (2022). Evaluation of Potential Groundwater Zone Using Integrated GIS and Remote Sensing Techniques in Sekota Wereda, Northern Ethiopia. *Water, Air, & Soil Pollution*, *233*(4), 1-13.

Tolche AD. 2021. Groundwater potential mapping using geospatial techniques: a case study of Dhungeta-Ramis sub-basin, Ethiopia. Geol Ecol Landsc. 5(1):65–80. doi: 10.1080/24749508.2020.1728882.

Verma, N., & Patel, R. K. (2021). Delineation of groundwater potential zones in lower Rihand River Basin, India using geospatial techniques and AHP. *Egyptian Journal of Remote Sensing and Space Science*. https://doi.org/10.1016/J.EJRS.2021.03.005

Wendt, D. E., Bloomfield, J. P., Van Loon, A. F., Garcia, M., Heudorfer, B., Larsen, J., & Hannah, D. M. (2021). Evaluating integrated water management strategies to inform hydrological drought mitigation. *Natural Hazards and Earth System Sciences*, *21*(10), 3113-3139.

Weng, E., Malyshev, S., Lichstein, J., Farrior, C. E., Dybzinski, R., Zhang, T., Shevliakova, E., & Pacala, S. W. (2015). Scaling from individual trees to forests in an Earth system modeling framework using a mathematically tractable model of height-structured competition. *Biogeosciences*, *12*(9), 2655-2694.

WHO and UNICEF (2021). Progress on household drinking water, sanitation and hygiene 20002020: Five years into the SDGs. Geneva.

World Bank Group, Climate Change Knowledge Portal (2023). URL: https://climateknowledgeportal.worldbank.org/.

World Meteorological Organization (2022).

Yadav SK, Dubey A, Singh SK, Yadav D (2020) Spatial regionalisation of morphometric characteristics of mini watershed of Northern Foreland of Peninsular India. *Arab J Geosci*. https:// doi. org/ 10. 1007/ s12517- 020- 05365-z

Yıldırım, U. (2021). Identification of groundwater potential zones using GIS and multi-criteria decision-making techniques: a case study upper Coruh River basin (NE Turkey). ISPRS *International Journal of Geo-Information*, *10*(6), 396.

Yilma, D., Hatiye, S. D., Hussien, B., & Suryabhagavan, K. V. (2023). Identifying groundwater prospect zones through earth observation techniques in Bilate watershed, Rift Valley Lakes Basin, Ethiopia. *International Journal of River Basin Management*, 1-19.

Youssef, A. M., & Pradhan, B. (2021). Application of remote sensing and GIS-based multi-criteria decision-making techniques for groundwater potential mapping in Wadi Al-Arab basin, Jordan. *Water*, *13*(9), 1204.

# Appendix 1

## Groundwater inventory data from (ECDSWC) and ECO

| UTM E | UTM N | Locality | Well type | Elevation, m | Data Source | Depth, m | Draw down, m | Q, test, (l/S) | Transmissivity (m2/day) |
|---|---|---|---|---|---|---|---|---|---|
| 400975 | 997008 | Ginchi Agri Center | WS | | CGCOC | 302 | 9.7 | 28 | 185 |
| 400575 | 997156 | Ginchi Agri Center | WS | 2284 | CGCOC | 502 | 64.1 | 88 | 1920 |
| 446356 | 1005421 | Wolmera site | WS | 2408 | FIRAT WWD | 400 | 85.6 | 31.8 | 1550 |
| 446347 | 1002761 | Sara WB | WS | 2388 | ECC | 654 | 188 | 20 | 1240 |
| 445556 | 1001719 | Holeta | WS | 2355 | CGCOC | 400 | 112.5 | 2 | |
| 446296 | 1002676 | Holeta | WS | 2380 | Derba | 308.6 | 221.7 | 3 | 0.61 |
| 427126 | 971361 | Asgori | MW | 2075 | Tana | 308 | 3.66 | 35.5 | |
| 427126 | 971361 | Asgori | MW | 2075 | Tana | 308 | 3.66 | 35.5 | |
| 456314 | 962592 | Melk kunture | MW | 2014 | Tana | 290 | 2.65 | 35.5 | |
| 450359 | 981037 | Tefki-Harojila | MW | 2084 | WWCE | 280 | 41.95 | 19 | |
| 433200 | 959670 | Bantu -Jawarokora | MW | 2111 | WWDE | 194 | 16.86 | 19.2 | |
| 413137 | 973900 | Teji-Dima Jalewa | MW | 2090 | WWCE | 311 | 35.38 | 16.74 | |
| 427395 | 992768 | Kimoyekoradima | MW | 2109 | WWDE | 243 | 36.35 | 17.47 | |
| 418679 | 988365 | Becho | TW | 2082 | CGCEB | 445 | 95 | 62.05 | 47.85 |
| 423439 | 988990 | Becho | TW | 2077 | CGCEB | 450 | 74.3 | 34.05 | 410 |
| 420071 | 983317 | Becho | TW | 2071 | CGCEB | 350 | 54.8 | 19.12 | 43.35 |
| 411777 | 989671 | Becho | TW | 2119 | TANA | 250 | 4.71 | 56 | 1121 |
| 411189 | 983944 | Becho | TW | 2091 | CGCEB | 301 | 100.78 | 38.58 | 41.5 |
| 454868 | 963109 | Becho | PW | | ANBG | 352 | 6.87 | 63.4 | 2080 |
| 450887 | 981258 | Becho | PW | 1841 | ANBG | 436 | 22.79 | 58 | 505 |
| 438871 | 977181 | Tefki | TW | 2053 | CGCOC | 443 | 46.07 | 41 | 46.08 |
| 447224 | 978514 | Tefki | TW | 2055 | CGCOC | 440 | 86.03 | 20 | 26.74 |
| 449082 | 980399 | Tefki | TW | 2066 | CGCOC | 440 | 93.68 | 13.12 | 17.85 |
| 433672 | 1023691 | Inchini | TW | | CGCOC | 602 | 135.46 | 9 | |
| 455342 | 985531 | Sebeta | WS | 2206 | Edit PLC | 185 | 92.97 | 12 | |
| 455470 | 984876 | Sebeta | WS | 2175 | Edit PLC | 201 | 23.44 | 3.5 | |
| 445565 | 983665 | Sebeta Tefki | TW | 2088 | Tana | 550 | | | |
| 450949 | 1000247 | Sebeta Tefki | TW | | Tana | 186 | | | |
| 422802 | 976337 | Sebeta Tefki | TW | | Tana | 500 | | | |
| 447200 | 998889 | Holota-Tsedey | WS | 2290 | Ethio Drill | 126 | 45.4 | 14 | |
| 453522 | 1001474 | Holota-Jerico flowers | WS | 2562 | Ethio Drill | 115.3 | 1.3 | 14.6 | |
| 404656 | 997733 | Ginchi | WS | 2235 | ABGP | 81 | 20.7 | 3.5 | |
| 434015 | 1000129 | Addis Alem TWS | WS | 2554 | | 147 | 69.9 | 1.5 | |

| | | | | | | | | | |
|---|---|---|---|---|---|---|---|---|---|
| 440110 | 1001337 | Holota-Agri Flowers | WS | 2419 | Ethio Drill | 153 | 100.1 | 1.5 | |
| 473871 | 1024156 | Korke Robe | WS | 2605 | | 15 | 5 | 2 | |
| 404050 | 980200 | Busa-Boda#2 | WS | 2150 | OWWCE | 98.5 | 4.5 | 8 | |
| 407400 | 972711 | Kelecho Gerbi | WS | 2140 | Ethio Drill | 172 | 13.6 | 4 | |
| 463599 | 988583 | Sebeta Shootin Station | WS | 2283 | WWDE | 130 | 5 | 4 | |
| 436160 | 1000453 | Addis Alem-Siet Flower | WS | 2370 | Ethio Drill | 153 | 100.1 | 1.5 | |
| 445180 | 1002459 | Holota-Agri Research,Ginchi | WS | 2393 | Ethio Drill | 101 | 14.8 | 3.5 | |
| 432432 | 1024464 | Incini Adaa Berga Dairy | WS | 2598 | WWDE | 161 | 105.1 | 2.5 | |
| 440595 | 1000333 | Holota-Dandi Boru Rose | WS | 2374 | East African | 170 | 10.7 | 7.4 | |
| 402350 | 951544 | Maru Sambo | WS | 2440 | Yadot Drilling | 60 | 16.4 | 0.2 | |
| 393964 | 957477 | Maru Renda | WS | 2497 | Yadot Drilling | 61.3 | 8.6 | 0.1 | |
| 397276 | 954511 | Woliso-Wolenso | WS | 2400 | Yadot Drilling | 61.3 | 36.6 | 0.6 | |
| 397540 | 953574 | Seto | WS | 2393 | Yadot Drilling | 60 | 34.9 | 0.2 | |
| 424000 | 952736 | Bantu-Areda Leka | WS | 2169 | OWWCE | 112 | 45 | 10 | |
| 455000 | 985200 | Meta Abo Brewery | WS | 2200 | AG Consult | 126 | 33.8 | 3.5 | 10.72 |
| 463700 | 988500 | AA-Water lll Testwell-B3 | WS | 2280 | AG Consult | 130 | 5.5 | 4 | 75.4 |
| 455300 | 985250 | Meta Abo Brewery BH5 | WS | 2218 | AG Consult | 101 | 17.8 | 4.5 | 25.92 |
| 457030 | 984617 | Sebeta-Dragados | WS | 2200 | AG Consult | 140 | 88.5 | 18.5 | 5 |
| 472975 | 1011144 | Sululta Depot | WS | 2650 | | 114 | 11.7 | 10.7 | 2.2 |
| 462260 | 984901 | Alemgena-electrocomercial | WS | 2294 | East African | 180 | 82.8 | 17.3 | 6.7 |
| 460295 | 986769 | AA-Sebeta Fishery | WS | 2222 | SABA Drilling | 158 | 31 | 50 | 17 |
| 447549 | 1007893 | Holota-Marginpar Flower plc | WS | 2520 | Ethio Drill | 203 | 24.5 | 4 | 2 |
| 408475 | 952876 | Mendi Toffisa#1 | SBH | 2260 | | 50 | | | |
| 407460 | 953526 | Mendi Toffisa#2 | SBH | 2285 | | 36 | | | |
| 424094 | 968971 | Jato | SBH | 2239 | | 24 | | | |
| 402350 | 951544 | Maru Sambo | SBH | 2200 | | 60 | | | 0.18 |
| 410362 | 964468 | Laga-Dawo | MBH | 2650 | | 69.75 | | | 1 |
| 411878 | 965587 | Tajab-Dawo | SBH | 2294 | | 56 | | | 3.5 |
| 422468 | 966195 | Bonde-Dawo | MBH | 2222 | | 60 | | | 2 |
| 414991 | 971562 | Sankale-Dawo | SBH | 2520 | | 42 | | | |
| 412197 | 957215 | Tulu Bolo TWS | DBH | 2260 | | | | | |

**Appendix 2**

**Rainfall data from National Metrological Agency (1992−2022)**

| Name | Elevation | x | y | Element | Year | Time | Jan | Feb | Mar | Apr | May | Jun | Jul | Aug | Sep | Oct | Nov | Dec |
|---|---|---|---|---|---|---|---|---|---|---|---|---|---|---|---|---|---|---|
| Busa | 1923 | 37 | 7.939 | PRECIP | 1992 | Time | 80 | 59 | 137 | 195 | | 220 | 242 | 298 | 142 | 85 | 22 | 0 |
| Busa | 1923 | 37 | 7.939 | PRECIP | 1993 | 09:00 | 10 | 85 | | | 183 | 373 | 348 | 312 | | | 6.7 | 0 |
| Busa | 1923 | 37 | 7.939 | PRECIP | 1994 | 09:00 | | 6.7 | 137 | 141 | 161 | 283 | 325 | 270 | 116 | 2.2 | 14 | 0 |
| Busa | 1923 | 37 | 7.939 | PRECIP | 1995 | 09:00 | 7 | 53 | 55 | 141 | 95 | 211 | 165 | 184 | 124 | 17 | 17 | 5 |
| Busa | 1923 | 37 | 7.939 | PRECIP | 1996 | 09:00 | 85 | 13 | 220 | 193 | 176 | 258 | 298 | 140 | 98 | 62 | 23 | 14 |
| Busa | 1923 | 37 | 7.939 | PRECIP | 1997 | 09:00 | 46 | 0 | 64 | 142 | 166 | 221 | 162 | 206 | 170 | 334 | 130 | 71 |
| Busa | 1923 | 37 | 7.939 | PRECIP | 1998 | 09:00 | 79 | 36 | 51 | 70 | 197 | 211 | 255 | 437 | 126 | 171 | 0 | 0 |
| Busa | 1923 | 37 | 7.939 | PRECIP | 1999 | 09:00 | 25 | 0 | 46 | 80 | 144 | 269 | 265 | 186 | 197 | 141 | 0 | 0 |
| Busa | 1923 | 37 | 7.939 | PRECIP | 2000 | 09:00 | 2.1 | 0 | 11 | 143 | 252 | 196 | 160 | 258 | 169 | 134 | 12 | 11 |
| Busa | 1923 | 37 | 7.939 | PRECIP | 2001 | 09:00 | 5.8 | 3.2 | 182 | 202 | 164 | 204 | 267 | 194 | 140 | 77 | 34 | 0 |
| Busa | 2166 | 38 | 8.777 | PRECIP | 2020 | 09:00 | | | 28 | 81 | 117 | 493 | 683 | 454 | 192 | | | |
| Busa | 1923 | 37 | 7.939 | PRECIP | 2021 | 09:00 | | 12 | | 167 | | | | 338 | 175 | 78 | | |
| Busa | 1923 | 37 | 7.939 | PRECIP | 2022 | 09:00 | 6.1 | 21 | 32 | 116 | 185 | | 446 | 486 | 121 | | | |
| Ameya Gindo | 1999 | 38 | 8.592 | PRECIP | 1993 | 09:00 | 51 | 37 | 11 | 122 | 107 | 192 | 195 | 285 | 211 | 65 | 4.5 | 0 |
| Ameya Gindo | 1999 | 38 | 8.592 | PRECIP | 1994 | 09:00 | 0 | 0 | 62 | 91 | 65 | 76 | 340 | 282 | 122 | 0 | 1.9 | 0 |
| Ameya Gindo | 1999 | 38 | 8.592 | PRECIP | 1995 | 09:00 | 0 | 0 | 59 | 219 | 113 | 101 | 179 | 265 | 106 | 20 | 0 | 5 |
| Ameya Gindo | 1999 | 38 | 8.592 | PRECIP | 1996 | 09:00 | 56 | 7.9 | 133 | 128 | 170 | 271 | 286 | 184 | 125 | 24 | 26 | 0 |
| Ameya Gindo | 1999 | 38 | 8.592 | PRECIP | 1997 | 09:00 | 64 | 0 | 31 | 99 | 148 | 299 | 246 | 206 | 95 | 93 | 34 | 0 |
| Ameya Gindo | 1999 | 38 | 8.592 | PRECIP | 1998 | 09:00 | 67 | 53 | 50 | 65 | 147 | 174 | 297 | 332 | 231 | 161 | 3.4 | 0 |
| Ameya Gindo | 1999 | 38 | 8.592 | PRECIP | 1999 | 09:00 | 19 | 0 | | 17 | 94 | 161 | 375 | 286 | 192 | 134 | 0 | 3 |
| Ameya Gindo | 1999 | 38 | 8.592 | PRECIP | 2000 | 09:00 | 0 | 0 | 3.4 | 133 | 184 | 124 | 418 | 217 | 254 | 65 | 37 | 18 |
| Ameya Gindo | 1999 | 38 | 8.592 | PRECIP | 2001 | 09:00 | 0 | 24 | 70 | 78 | 163 | 170 | 278 | 195 | 63 | 59 | 0 | 3 |
| Ameya Gindo | 1999 | 38 | 8.592 | PRECIP | 2002 | 09:00 | 26 | 31 | 74 | 31 | 142 | 190 | 307 | 223 | 163 | 0 | 0 | 42 |
| Arbuchulele | 2434 | 38 | 8.472 | PRECIP | 2004 | 09:00 | 37 | 0 | 63 | 151 | 41 | 174 | 159 | 0 | 107 | 14 | 0 | 0 |
| Arbuchulele | 2434 | 38 | 8.472 | PRECIP | 2005 | 09:00 | 27 | 6 | 99 | 87 | 113 | 177 | 183 | 211 | 110 | | 8.8 | 0 |
| Arbuchulele | 2434 | 38 | 8.472 | PRECIP | 2006 | 09:00 | 4.4 | 32 | 135 | 164 | 137 | | 318 | 250 | 137 | 4.6 | 3.7 | 3 |
| Arbuchulele | 2434 | 38 | 8.472 | PRECIP | 2007 | 09:00 | 13 | 38 | 57 | 79 | 167 | 176 | 223 | 325 | 117 | 22 | 0 | 0 |
| Arbuchulele | 2434 | 38 | 8.472 | PRECIP | 2008 | 09:00 | 0 | 0 | 0 | 53 | 73 | 194 | 265 | 206 | 145 | 50 | 33 | 0 |

| | | | | | | | | | | | | | | | | | | |
|---|---|---|---|---|---|---|---|---|---|---|---|---|---|---|---|---|---|---|
| Arbuchulele | 2434 | 38 | 8.472 | PRECIP | 2009 | 09:00 | 23 | 13 | 15 | 4.2 | 62 | 71 | 268 | 218 | 133 | 71 | 0 | 72 |
| Arbuchulele | 2434 | 38 | 8.472 | PRECIP | 2010 | 09:00 | 7.2 | 69 | 54 | 58 | 114 | 257 | 308 | 380 | 115 | 3 | 16 | 20 |
| Arbuchulele | 2434 | 38 | 8.472 | PRECIP | 2011 | 09:00 | 0 | 0 | 114 | 63 | 66 | 200 | 181 | 237 | 151 | 0 | 17 | 0 |
| Arbuchulele | 2434 | 38 | 8.472 | PRECIP | 2012 | 09:00 | 0 | 0 | 23 | 104 | 23 | 166 | 248 | 189 | 133 | 0 | 13 | 3 |
| Arbuchulele | 2434 | 38 | 8.472 | PRECIP | 2013 | 09:00 | 7.8 | 0 | 18 | 88 | 109 | 253 | 301 | 192 | 157 | 0 | 0 | 0 |
| Arbuchulele | 2434 | 38 | 8.472 | PRECIP | 2014 | 09:00 | 7.5 | 39 | 102 | 20 | 99 | 100 | 300 | 230 | 120 | 76 | 0 | 0 |
| Asgori | 2072 | 38 | 8.795 | PRECIP | 2006 | 09:00 | 0.2 | 12 | | | | | | | 79 | 2.7 | 0 | 1 |
| Asgori | 2072 | 38 | 8.795 | PRECIP | 2007 | 09:00 | 8.7 | | 83 | 144 | 65 | 198 | 212 | 180 | 142 | 11 | 0 | 0 |
| Asgori | 2072 | 38 | 8.795 | PRECIP | 2008 | 09:00 | | 0 | 0.9 | 61 | 103 | 140 | 283 | 190 | 74 | 23 | 65 | 0 |
| Asgori | 2072 | 38 | 8.795 | PRECIP | 2009 | 09:00 | 31 | 1.5 | 1 | 26 | 65 | 95 | 206 | 266 | 68 | | 59 | 27 |
| Asgori | 2072 | 38 | 8.795 | PRECIP | 2010 | 09:00 | | 89 | 92 | 104 | 58 | 158 | 273 | 150 | 99 | 11 | 35 | 16 |
| Asgori | 2072 | 38 | 8.795 | PRECIP | 2011 | 09:00 | 15 | 5.2 | 38 | 15 | 62 | 171 | 156 | 256 | 190 | 0 | 3.1 | 0 |
| Asgori | 2072 | 38 | 8.795 | PRECIP | 2012 | 09:00 | 0 | 0 | 1.2 | 61 | 42 | 135 | 211 | 230 | 84 | 2.7 | 0 | 8 |
| Asgori | 2072 | 38 | 8.795 | PRECIP | 2013 | 09:00 | 2.7 | 0 | 392 | 104 | 77 | 111 | 229 | 165 | 129 | 75 | 8 | 0 |
| Asgori | 2072 | 38 | 8.795 | PRECIP | 2014 | 09:00 | 0 | 54 | 38 | 57 | 118 | 101 | 214 | 206 | 107 | 8.7 | 2.9 | 0 |
| Asgori | 2072 | 38 | 8.795 | PRECIP | 2015 | 09:00 | 0 | 0 | 12 | 0.8 | 77 | 152 | 196 | 227 | 111 | 0.4 | 0 | 11 |
| Asgori | 2072 | 38 | 8.795 | PRECIP | 2016 | 09:00 | 34 | 7.7 | | 134 | 65 | 71 | 276 | 182 | 71 | 0.7 | 3.9 | 1 |
| Asgori | 2072 | 38 | 8.795 | PRECIP | 2017 | 09:00 | 0 | 118 | 24 | 22 | 133 | 97 | 148 | 202 | 164 | 2.1 | 1.2 | 0 |
| Asgori | 2072 | 38 | 8.795 | PRECIP | 2018 | 09:00 | | 12 | 29 | 83 | 138 | 180 | 217 | 218 | 23 | | | |
| Asgori | 2072 | 38 | 8.795 | PRECIP | 2019 | 09:00 | | | | | | | | | | | 43 | 10 |
| Asgori | 2072 | 38 | 8.795 | PRECIP | 2020 | 09:00 | | 0 | 38 | 111 | 82 | 109 | 261 | 233 | 132 | 6 | 0 | 0 |
| Asgori | 2072 | 38 | 8.795 | PRECIP | 2021 | 09:00 | 0 | 29 | | | | 98 | 277 | 149 | 122 | | | |
| Bantuliben | 2167 | 38 | 8.619 | PRECIP | 2008 | 09:00 | | | 0 | 31 | | 145 | 398 | 261 | | | 75 | |
| Bantuliben | 2167 | 38 | 8.619 | PRECIP | 2009 | 09:00 | | | | | 20 | 141 | 270 | 300 | 120 | 15 | 7 | 4 |
| Bantuliben | 2167 | 38 | 8.619 | PRECIP | 2010 | 09:00 | 0 | 0 | 0 | 0 | 0 | 0 | 181 | 197 | 0 | 0 | | |
| Bantuliben | 2167 | 38 | 8.619 | PRECIP | 2011 | 09:00 | 6.4 | 0 | 0 | 17 | 45 | 189 | 0 | 212 | | 16 | 0 | 12 |
| Bantuliben | 2167 | 38 | 8.619 | PRECIP | 2012 | 09:00 | 32 | 27 | 63 | 105 | 62 | 265 | 244 | 44.4 | 230 | 0 | 130 | 5 |
| Bantuliben | 2167 | 38 | 8.619 | PRECIP | 2013 | 09:00 | 0 | 0 | | 61 | 76 | 190 | 300 | 296 | 212 | 19 | 0 | 0 |
| Bantuliben | 2167 | 38 | 8.619 | PRECIP | 2014 | 09:00 | 0 | 17 | 55 | 6.1 | 27 | 226 | 324 | 391 | 227 | | | |
| Bantuliben | 2167 | 38 | 8.619 | PRECIP | 2015 | 09:00 | 0 | 0 | 0 | 32 | 57 | 116 | | 390 | 121 | 0 | 0 | 0 |
| Bantuliben | 2167 | 38 | 8.619 | PRECIP | 2016 | 09:00 | 21 | 0 | 0 | 202 | 158 | 293 | 534 | 394 | 143 | 21 | 21 | 0 |
| Bantuliben | 2167 | 38 | 8.619 | PRECIP | 2017 | 09:00 | 0 | 24 | 38 | 40 | 158 | 183 | 233 | 175 | 167 | | | |
| Bantuliben | 2167 | 38 | 8.619 | PRECIP | 2018 | 09:00 | 37 | 24 | | | | | | | | | | |
| Chitu | 2118 | 38 | 8.605 | PRECIP | 2011 | 09:00 | 3 | 3.6 | 0 | 29 | 236 | | | | 230 | 0 | 36 | |

| | | | | | | | | | | | | | | | | | | |
|---|---|---|---|---|---|---|---|---|---|---|---|---|---|---|---|---|---|---|
| Chitu | 2118 | 38 | 8.605 | PRECIP | 2012 | 09:00 | 0 | | | 117 | 73 | 73 | 152 | 172 | 326 | 0 | | |
| Chitu | 2118 | 38 | 8.605 | PRECIP | 2013 | 09:00 | 3.2 | 13 | | | | 195 | 305 | 314 | 214 | 79 | 16 | 0 |
| Chitu | 2118 | 38 | 8.605 | PRECIP | 2014 | 09:00 | 7.9 | 26 | 26 | 28 | 142 | 153 | 361 | 273 | 155 | 79 | 25 | 0 |
| Chitu | 2118 | 38 | 8.605 | PRECIP | 2015 | 09:00 | 0 | 6.2 | 43 | 3.9 | 33 | 195 | 311 | 289 | 230 | 0 | 3.4 | 18 |
| Chitu | 2118 | 38 | 8.605 | PRECIP | 2016 | 09:00 | 28 | 9.9 | 80 | 172 | 160 | 248 | | | 289 | | 1.3 | 0 |
| Chitu | 2118 | 38 | 8.605 | PRECIP | 2017 | 09:00 | 0 | 19 | | | | 270 | 629 | 552 | 314 | 53 | 12 | 0 |
| Chitu | 2118 | 38 | 8.605 | PRECIP | 2018 | 09:00 | 1.1 | 22 | 28 | 134 | 261 | 496 | 314 | 264 | 127 | 115 | 195 | 0 |
| Chitu | 2118 | 38 | 8.605 | PRECIP | 2019 | 09:00 | 0 | 3.5 | 2.7 | 60 | 84 | 142 | 266 | 303 | 349 | 36 | 73 | 96 |
| Chitu | 2118 | 38 | 8.605 | PRECIP | 2020 | 09:00 | 10 | 16 | 183 | 179 | 176 | 321 | | 313 | 211 | 15 | 34 | |
| Chitu | 2118 | 38 | 8.605 | PRECIP | 2021 | 09:00 | 8 | 42 | 0 | | | 146 | 578 | | | | | |
| Chitu | 2118 | 38 | 8.605 | PRECIP | 2022 | 09:00 | 17 | | 78 | 54 | 0 | 274 | 376 | 347 | | 0 | | |
| Dilela | 2429 | 38 | 8.638 | PRECIP | 1999 | 09:00 | 9.5 | 0 | 78 | 15 | 101 | 181 | 250 | 247 | 128 | 102 | 0 | 0 |
| Dilela | 2429 | 38 | 8.638 | PRECIP | 2000 | 09:00 | 0 | 0 | 5.1 | 67 | 78 | 130 | 238 | 216 | 189 | 30 | 32 | 18 |
| Dilela | 2429 | 38 | 8.638 | PRECIP | 2001 | 09:00 | 2.2 | 11 | 82 | 53 | 141 | 138 | 221 | 142 | 81 | 27 | 0 | 0 |
| Dilela | 2429 | 38 | 8.638 | PRECIP | 2002 | 09:00 | 46 | 81 | 93 | 56 | 53 | 206 | 294 | 238 | 59 | 0 | 0 | 69 |
| Dilela | 2429 | 38 | 8.638 | PRECIP | 2003 | 09:00 | 41 | 12 | 72 | 99 | 8.4 | 138 | 272 | 241 | 157 | 7.9 | 3.7 | 18 |
| Dilela | 2429 | 38 | 8.638 | PRECIP | 2004 | 09:00 | 64 | 0.8 | 48 | 154 | 43 | 275 | 264 | 168 | 190 | 23 | 6.8 | 0 |
| Dilela | 2429 | 38 | 8.638 | PRECIP | 2005 | 09:00 | 44 | 0 | 104 | 165 | 132 | 180 | 153 | 278 | 123 | 15 | 1.6 | 4 |
| Dilela | 2429 | 38 | 8.638 | PRECIP | 2006 | 09:00 | 0.5 | 46 | 96 | 68 | 62 | 171 | | | | 9.1 | | 0 |
| Dilela | 2429 | 38 | 8.638 | PRECIP | 2007 | 09:00 | 17 | 79 | 58 | 86 | 185 | 316 | 245 | 303 | 152 | 23 | 0 | 0 |
| Dilela | 2429 | 38 | 8.638 | PRECIP | 2021 | 09:00 | | 55 | 9.9 | 64 | 108 | 168 | 249 | 201 | 177 | 43 | | |
| Guranda Meta | 2187 | 39 | 8.912 | PRECIP | 1992 | 09:00 | 0 | 17 | 22 | 19 | 44 | 102 | 301 | 285 | 60 | 29 | 0 | 0 |
| Guranda Meta | 2187 | 39 | 8.912 | PRECIP | 1993 | 09:00 | 7.1 | 74 | | 81 | 132 | 132 | 318 | 349 | 179 | | | |
| Guranda Meta | 2187 | 39 | 8.912 | PRECIP | 1994 | 09:00 | 0 | 0 | 11 | 88 | 11 | 120 | 252 | 265 | 115 | 0 | 9.8 | 0 |
| Guranda Meta | 2187 | 39 | 8.912 | PRECIP | 1995 | 09:00 | 0 | 0 | 6.2 | 89 | 26 | 25 | 274 | 288 | 107 | 29 | 0 | 6 |
| Guranda Meta | 2187 | 39 | 8.912 | PRECIP | 1996 | 09:00 | 20 | 0 | 50 | 113 | 81 | 305 | 315 | 310 | 171 | 13 | 0 | 0 |
| Guranda Meta | 2187 | 39 | 8.912 | PRECIP | 1997 | 09:00 | 9.2 | 0 | 3.5 | 74 | 5.3 | 86 | 152 | 97.3 | 92 | 46 | 0 | 0 |
| Guranda Meta | 2187 | 39 | 8.912 | PRECIP | 1998 | 09:00 | 57 | 39 | 29 | 28 | 94 | 114 | 267 | 285 | 168 | 6.9 | 0 | 0 |
| Guranda Meta | 2187 | 39 | 8.912 | PRECIP | 1999 | 09:00 | 19 | 0 | 37 | 0 | 18 | 120 | 193 | 219 | 103 | 141 | 0 | 1 |
| Guranda Meta | 2187 | 39 | 8.912 | PRECIP | 2000 | 09:00 | 0 | | 4.1 | 76 | 90 | 100 | 234 | 276 | 214 | 44 | 28 | 29 |
| Guranda Meta | 2187 | 39 | 8.912 | PRECIP | 2001 | 09:00 | 0 | 4.4 | 82 | 21 | 129 | 138 | 332 | 287 | 105 | 31 | 0 | 0 |
| Guranda Meta | 2187 | 39 | 8.912 | PRECIP | 2002 | 09:00 | 47 | 26 | 69 | 61 | 37 | 145 | 214 | 273 | 83 | 0 | 0 | 16 |
| Guranda Meta | 2187 | 39 | 8.912 | PRECIP | 2005 | 09:00 | 13 | 0 | 26 | 107 | 273 | 155 | 294 | 184 | 174 | 20 | 11 | 0 |
| Guranda Meta | 2187 | 39 | 8.912 | PRECIP | 2006 | 09:00 | 0 | 15 | 119 | 61 | 60 | 141 | 465 | 343 | 195 | 13 | 0 | 2 |

| | | | | | | | | | | | | | | | | | | |
|---|---|---|---|---|---|---|---|---|---|---|---|---|---|---|---|---|---|---|
| Teji | 2062 | 38 | 8.836 | PRECIP | 1992 | 09:00 | 44 | 60 | 61 | 87 | 76 | 123 | 123 | 235 | 90 | 56 | 4.6 | 2 |
| Teji | 2062 | 38 | 8.836 | PRECIP | 1993 | 09:00 | 5.1 | 100 | 0 | 150 | 100 | 93 | 235 | 289 | 97 | 22 | 0 | 3 |
| Teji | 2062 | 38 | 8.836 | PRECIP | 1994 | 09:00 | 0 | 0 | 34 | 37 | 28 | 198 | 185 | 242 | 129 | 0 | 13 | 0 |
| Teji | 2062 | 38 | 8.836 | PRECIP | 1995 | 09:00 | 0 | 41 | 18 | 98 | 66 | 66 | 224 | 179 | 47 | 1.3 | 0 | 47 |
| Teji | 2062 | 38 | 8.836 | PRECIP | 1996 | 09:00 | 58 | 2.3 | 100 | 95 | 72 | 113 | 219 | 208 | 73 | 3.6 | 1.9 | 0 |
| Teji | 2062 | 38 | 8.836 | PRECIP | 1997 | 09:00 | 16 | 0 | 29 | 132 | 29 | 96 | 188 | 144 | 64 | 48 | 49 | 0 |
| Teji | 2062 | 38 | 8.836 | PRECIP | 1998 | 09:00 | 90 | 52 | 30 | 66 | 68 | 136 | 310 | 232 | 87 | 64 | 0 | 0 |
| Teji | 2062 | 38 | 8.836 | PRECIP | 1999 | 09:00 | 5.5 | 0 | 44 | 5.8 | 46 | 98 | 242 | 218 | 98 | 77 | 0 | 0 |
| Teji | 2062 | 38 | 8.836 | PRECIP | 2000 | 09:00 | 0 | 0 | 14 | 94 | 74 | 94 | 187 | 213 | 149 | 11 | 29 | 2 |
| Teji | 2062 | 38 | 8.836 | PRECIP | 2001 | 09:00 | 2.3 | 1 | 96 | 16 | 165 | 183 | 215 | 120 | 65 | 3.3 | 7.7 | 0 |
| Teji | 2062 | 38 | 8.836 | PRECIP | 2002 | 09:00 | 14 | 10 | 63 | 38 | 46 | 140 | 211 | 214 | 49 | 0 | 0 | 27 |
| Teji | 2062 | 38 | 8.836 | PRECIP | 2003 | 09:00 | 29 | 21 | 81 | 154 | 48 | 158 | 230 | 267 | 84 | 0 | 0.2 | 10 |
| Tulu Bolo | 2190 | 38 | 8.658 | PRECIP | 1992 | 09:00 | 14 |  | 62 | 37 | 43 | 337 | 442 | 635 | 66 | 8.2 | 4.7 | 3 |
| Tulu Bolo | 2190 | 38 | 8.658 | PRECIP | 1993 | 09:00 | 12 | 26 | 14 | 114 | 194 | 549 | 440 | 564 | 326 | 19 | 0 | 0 |
| Tulu Bolo | 2190 | 38 | 8.658 | PRECIP | 1994 | 09:00 | 0 | 0 | 87 | 47 | 69 | 284 | 339 | 317 | 233 | 0 |  | 0 |
| Tulu Bolo | 2190 | 38 | 8.658 | PRECIP | 1995 | 09:00 | 0 | 8.3 | 43 | 50 |  | 135 | 90 | 222 | 0 | 3.1 | 0 | 15 |
| Tulu Bolo | 2190 | 38 | 8.658 | PRECIP | 1996 | 09:00 | 18 | 3.1 | 40 | 66 | 88 | 226 | 244 | 338 | 191 | 0 | 4.3 | 0 |
| Tulu Bolo | 2190 | 38 | 8.658 | PRECIP | 2000 | 09:00 |  | 0 | 1.8 | 161 | 132 | 222 | 321 | 227 | 114 | 6.3 | 26 | 5 |
| Tulu Bolo | 2190 | 38 | 8.658 | PRECIP | 2001 | 09:00 | 0 | 3.2 | 98 | 36 |  | 187 | 224 | 160 | 36 | 6.9 | 0 | 0 |
| Tulu Bolo | 2190 | 38 | 8.658 | PRECIP | 2002 | 09:00 | 46 | 9.1 | 42 | 61 | 43 | 225 | 237 | 241 | 77 | 0 | 0 | 41 |
| Tulu Bolo | 2190 | 38 | 8.658 | PRECIP | 2003 | 09:00 | 40 | 12 | 49 | 94 | 24 | 127 | 315 | 219 | 92 | 0 | 0 | 8 |
| Tulu Bolo | 2190 | 38 | 8.658 | PRECIP | 2004 | 09:00 | 53 | 0 | 11 | 93 | 45 | 271 | 331 | 185 | 164 | 0 | 2.2 | 5 |
| Tulu Bolo | 2190 | 38 | 8.658 | PRECIP | 2005 | 09:00 | 26 | 0 | 54 | 181 | 165 | 208 |  | 203 | 84 | 18 | 5.5 | 0 |
| Tulu Bolo | 2190 | 38 | 8.658 | PRECIP | 2022 | 09:00 | 20 | 0 | 29 | 56 | 0 | 195 | 265 | 101 | 91 | 30 | 10 | 4 |
| Welenkomi | 2165 | 38 | 9.004 | PRECIP | 1992 | 09:00 | 42 | 72 | 103 | 88 | 67 |  | 202 | 278 | 80 |  | 0 | 8 |
| Welenkomi | 2165 | 38 | 9.004 | PRECIP | 1993 | 09:00 | 39 | 74 | 44 | 76 | 158 | 111 | 203 | 521 | 208 | 81 | 0 | 0 |
| Welenkomi | 2165 | 38 | 9.004 | PRECIP | 1994 | 09:00 | 0 | 0 | 48 | 50 | 67 | 164 | 290 | 283 | 237 | 1.4 | 11 | 0 |
| Welenkomi | 2165 | 38 | 9.004 | PRECIP | 1995 | 09:00 | 0 | 46 | 31 | 135 | 67 | 95 | 208 | 249 | 129 | 0 | 0 | 14 |
| Welenkomi | 2165 | 38 | 9.004 | PRECIP | 1996 | 09:00 | 69 | 4.1 | 165 | 67 | 158 | 168 | 293 | 211 | 129 | 7.4 | 3.5 | 9 |
| Welenkomi | 2165 | 38 | 9.004 | PRECIP | 1997 | 09:00 | 38 | 0 | 18 | 79 | 36 | 138 | 277 | 208 | 121 | 45 | 47 | 0 |
| Welenkomi | 2165 | 38 | 9.004 | PRECIP | 1998 | 09:00 | 50 | 40 | 37 | 51 | 87 | 222 | 241 | 220 | 138 | 70 | 2.4 | 0 |
| Welenkomi | 2165 | 38 | 9.004 | PRECIP | 1999 | 09:00 | 4.8 | 0 | 8.2 | 27 | 62 | 128 | 197 | 176 | 84 | 107 | 0 | 0 |

# Appendix 3

## Geology data from GSE